2019

Effects of substrate stiffness, cadherin junction and shear flow on tensional homeostasis in cells and cell clusters

BOSTON UNIVERSITY

COLLEGE OF ENGINEERING

Dissertation

EFFECTS OF SUBSTRATE STIFFNESS, CADHERIN JUNCTION

AND SHEAR FLOW ON TENSIONAL HOMEOSTASIS IN

CELLS AND CELL CLUSTERS

by

HAN XU

B.S., Case Western Reserve University, 2014

Submitted in partial fulfillment of the

requirements for the degree of

Doctor of Philosophy

2019

Approved by

First Reader   _____
Dimitrije Stamenović, Ph.D.
Professor of Biomedical Engineering
Professor of Materials Science and Engineering

First Reader   _____
Michael L. Smith, Ph.D.
Associate Professor of Biomedical Engineering
Associate Professor of Materials Science and Engineering

Third Reader   _____
Joe Tien, Ph.D.
Associate Professor of Biomedical Engineering
Associate Professor of Materials Science and Engineering

Fourth Reader   _____
Michael Albro, Ph.D.
Assistant Professor of Mechanical Engineering
Assistant Professor of Materials Science and Engineering
Assistant Professor of Biomedical Engineering

Fifth Reader   _____
Joana Figueiredo, Ph.D.
Institute of Molecular Pathology and Immunology
University of Porto

ACKNOWLEDGMENTS

EFFECTS OF SUBSTRATE STIFFNESS, CADHERIN JUNCTION

AND SHEAR FLOW ON TENSIONAL HOMEOSTASIS IN

CELLS AND CELL CLUSTERS

HAN XU

Boston University College of Engineering, 2019

Major Professors: Dimitrije Stamenović, Ph.D., Professor of Biomedical Engineering, Professor of Materials Science and Engineering

and

Michael L. Smith, Ph.D., Associate Professor of Biomedical Engineering, Associate Professor of Materials Science and Engineering

ABSTRACT

Cytoskeletal tension plays an important role in numerous biological functions of adherent cells, including mechanosensing of the cell's microenvironment, mechanotransduction, cell spreading and migration, cell shape stability, and in stem cell lineage. It is believed that for normal biological functions the cell must maintain its cytoskeletal tension stable, at a preferred set-point level, under external perturbations. This is known as *tensional homeostasis*. Any breakdown of tensional homeostasis is closely associated with disease progression, including cancer, atherosclerosis, and thrombosis. The exact mechanism and the relevant environmental conditions for the maintenance of tensional homeostasis are not yet fully understood. This thesis investigates the impacts of substrate stiffness, availability of functional cadherin junctions and steady shear stress on tensional homeostasis of cells and cell clusters.

We define tensional homeostasis as the ability of cells to maintain a consistent

level of tension with low temporal traction field fluctuations. Traction forces of isolated cells, multicellular clusters, and monolayer are measured using micropattern traction microscopy. Temporal fluctuations of the traction field are calculated from time-lapsed traction measurements. Results demonstrated that substrate stiffness, cadherin cell-cell junctions and shear stress all impact tensional homeostasis. In particular, we found that stiffer substrates promoted tensional homeostasis in endothelial cells, but were detrimental to tensional homeostasis in vascular smooth muscle cells. We also found that E-cadherins were essential for tensional homeostasis of gastric cancer cells and that extracellular and intracellular mutations of E-cadherin had domain-specific effects on tensional homeostasis. Finally, laminar flow-induced shear stress led to increased traction field fluctuations in endothelial cell monolayers, contrary to reports of physiological shear promoting vascular homeostasis. A possible reason for this discrepancy might be the limitation of our approach which could not account for mechanical balance of traction forces in the monolayers.

Through the exploration of these environmental factors, we also found that tensional homeostasis was a length scale-dependent and cell type-dependent phenomenon. These insights suggest that future studies need to take a more comprehensive approach and aim to make observations of different cell types on multiple length scales, in order decipher the mechanism of tensional homeostasis and its role in (patho)physiology.

TABLE OF CONTENTS

LIST OF TABLES

LIST OF FIGURES

xiii

LIST OF ABBREVIATIONS

AGS……………………………………………..……..Gastric adenocarcinoma

BAEC…………………………………………………..Bovine aortic endothelial cell

BVSMC…………………………….................……Bovine vascular smooth muscle cell

E-cad………………………..………………………………………..E-cadherin

EC………………………………………………………………Endothelial cell

ECM………………………………………………….…………..Extracellular matrix

FA…………………………………………………………..………Focal adhesion

Fn………………………………………………………………….Fibronectin

HDGC…………………………………………....Hereditary diffuse gastric cancer

MTM……………………………………....…………Micropattern traction microscopy

PAA……………………………………………………………… Polyacrylamide

PDMS…………………………………………………………..Polydimethylsiloxane

SMC………………………………………………………………Smooth muscle cell

Vtn…………………………………………………………..……Vitronectin

GLOSSARY OF MATH SYMBOLS

σ	Standard deviation
a	Radius of the dot pattern
CV	Coefficient of variation
F	Force vector
F	Force magnitude
$\langle F \rangle$	Time-averaged force magnitude
F_{im}	Vector sum of all focal adhesion forces (i.e. the imbalanced force)
M_{xy}, M_{yx}	First order moment of x- and y- component force in y- and x- directions
p	Level of significance in statistical tests
r	Correlation coefficient of a force pair
R	Coefficient of global correlation of all forces
T	Sum of all traction force magnitudes
$\langle T \rangle$	Time-averaged sum of traction magnitudes
u	Displacement vector
ν	Poisson's ratio

Chapter 1: INTRODUCTION

Adherent cells are equipped with the acto-myosin machinery that can generate tensile forces within the actin cytoskeleton. This cytoskeletal tension plays an important role in a number of biological functions of cells including mechanosensing of the cell's microenvironment, mechanotransduction, cell spreading and migration, maintenance of cell shape stability, and stem cell lineage (Civelekoglu-Scholey & Scholey, 2010; Renkawitz & Sixt, 2010). It is believed that for normal biological functions the cell must maintain its cytoskeletal tension stable, at a preferred set-point level, under external perturbations. This is known as *tensional homeostasis* (Brown, Prajapati, McGrouther, Yannas, & Eastwood, 1998). Any breakdown of tensional homeostasis is closely associated with disease progression including cancer, atherosclerosis, and thrombosis (Chien, 2007; Paszek et al., 2005; Provenzano & Keely, 2011).

The exact mechanism of how cells maintain tensional homeostasis is not yet fully understood. It has been hypothesized that individual cells rely on their own internal feedback system to maintain tensional homeostasis, independent of external factors. This has been supported by experimental data obtain almost exclusively on fibroblasts (Brown et al., 1998; Webster, Ng, & Fletcher, 2014). Our recent study challenged this view by showing that tensional homeostasis is cell-type dependent (Zollinger et al., 2018). Some cell types, such as fibroblasts and vascular smooth muscle cells, can achieve tensional homeostasis in isolation, whereas other cell types, such as endothelial cells and epithelial cells, can achieve tensional homeostasis only if they form multicellular clusters.

When we think of external factors that may impact tensional homeostasis, the first

thought is often associated with dynamic perturbations in the vasculature, such as periodic stretching of the endothelium due to the pulsatile nature of blood pressure and blood flow-induced dynamic shear stress. Similar dynamic conditions exist in the pulmonary parenchyma and in the guts. While dynamic perturbations from the mechanical environment are important for understanding tensional homeostasis, static conditions in the cell's microenvironment could also impact tensional homeostasis. For example, stent implants can disrupt continuity of the endothelial monolayer interrupting thereby force transmission between endothelial cells at the wound edge and thus causing break down in tensional homeostasis, which is closely associated with ensuing inflammation and thrombosis (Zimmer & Nickenig, 2010). Stiffening of the extracellular matrix due to tumor formation may stimulate contractility of epithelial cells which, in turn, may lead to disruption of cell-cell contacts and thus of force transmission between cells, which is also detrimental to tensional homeostasis (Paszek et al., 2005). Consequently, tumor growth will be uninterrupted in the absence of the constraining effect of cell-cell interaction. Steady, unidirectional shear flow experienced by the peripheral blood vessel is believed to promote tensional homeostasis in the endothelium and thus is considered to be atheroprotective (Chien, 2007; Jay D. Humphrey, 2008a). In this thesis, we studied the impact of several non-dynamic perturbations, including substrate stiffness, steady shear flow and cell-cell adhesions on tensional homeostasis of different cell types. Thus, our *working hypothesis* is that *cells require specific non-dynamic environmental conditions in order to maintain tensional homeostasis*.

For the purpose of this study, we define tensional homeostasis as the ability of

cells to maintain a consistent level of tension with low temporal fluctuations. We use micropattern traction microscopy (MTM) to measure temporal variability of cell-substrate traction forces in isolated cells and in multicellular clusters (Polio, Rothenberg, Stamenović, & Smith, 2012). As a metric of temporal fluctuations of the traction field, we use the coefficient of variation (CV) which shows the extent of traction forces/field variability in relation to the time-average of those fluctuations. This variability can be caused by variability of individual focal adhesion traction forces and the temporal correlation between focal adhesion forces. If there exists a positive correlation between forces within a cell, this correlation results in a higher CV of the traction field compared to the situation where all forces act randomly and independent of each other. Our specific aims are as follows.

1.1 Aim 1: To investigate the impact of substrate stiffness on tensional homeostasis at the single focal adhesion (FA) level and at the whole cell level.

Rationale: Substrate stiffness is a property of the microenvironment that directly affects the stress and strain experienced by the cell. There is ample evidence that substrate stiffness affects cell's contractility and thereby tension generation in the cell (Doyle, Carvajal, Jin, Matsumoto, & Yamada, 2015; Huynh et al., 2011; Izquierdo-Álvarez et al., 2019; Krishnan et al., 2011; Polte, Eichler, Wang, & Ingber, 2004; Sazonova et al., 2015; Urbano, Furia, Basehore, & Clyne, 2017; Zhou, Lee, Weng, Fu, & García, 2017). Thus, altering substrate stiffness may impact the cell ability to achieve tensional homeostasis. Plotnikov and colleagues observed changes in traction force

dynamics on the FA level due to changes in substrate stiffness(Plotnikov, Pasapera, Sabass, & Waterman, 2012). However, no evidence how traction field dynamics on the whole cell level is affected by substrate stiffness. In this aim, we investigate and compare how changes in substrate stiffness affect traction force dynamics at the FA level and at the whole cell level.

Approach: We use MTM to measure temporal fluctuations of traction forces in isolated endothelial cells and in isolated vascular smooth muscle cells which are cultured on substrates of stiffness ranging from 3.6 to 30 kPa. For each cell type and for each substrate stiffness, we compute *CV* of traction forces of individual FA forces and of the whole traction field. From these data, we are able to determine how substrate stiffness may affect tensional homeostasis in different cell types and whether tensional homeostasis is achieved at the FA level or it requires cooperation of all FAs within a cell.

1.2   Aim 2: To investigate the impact of cell-cell adhesion via cadherin on tensional homeostasis of isolated gastric carcinoma cells and of multicellular clusters of those cells.

Rationale: Previous studies suggested that for achieving tensional homeostasis endothelial cells might require cell-cell contact (Canović, Zollinger, Tam, Smith, & Stamenović, 2016). It was found that endothelial cells cannot maintain low temporal fluctuation of the traction field in isolation and that temporal fluctuations of the traction field of a multicellular cluster are attenuated with increasing number of cells in the cluster. While there are a number of transmembrane proteins that are present at cell-cell junctions, cadherin has a major role in intercellular force transmission. Moreover,

cadherin-integrin crosstalk regulates cytoskeletal tension, which further emphasizes the importance of cadherin in tensional homeostasis (Levenberg, Katz, Yamada, & Geiger, 1998; Nelson & Chen, 2003; Ryan, Foty, Kohn, & Steinberg, 2001). Importantly, the subtype of cadherin and the level of expressions tend to differ based on the cell type.

Approach: We use MTM to measure temporal fluctuations of traction forces in isolated human gastric carcinoma cells that either express no E-cadherin (native condition), wild-type E-cadherin, or E-cadherin with a site-specific point mutations, as well as in clusters of those cells. The comparison between *CV*s of the two across the cell lines provides insight into E-cadherin's role in epithelial cell tensional homeostasis.

1.3   Aim 3: To investigate the impact of steady shear flow on endothelial cell tensional homeostasis.

Rationale: Fluid shear stress is a known regulator of endothelial cell behavior (Chien, 2007; Conway et al., 2013; Shiu et al., 2004; Steward, Tambe, Hardin, Krishnan, & Fredberg, 2015; Ting et al., 2012). It has been shown that endothelial cells reorient their contractile cytoskeletal stress fibers to align with direction of laminar shear flow. This alignment is believed to aid achievement and/or maintenance of tensional homeostasis, since stress fibers are major force-generating structures in the cells (Krishnan et al., 2012). Past studies disagree on the effect of shear force on tension levels in endothelial cell monolayers (Conway et al., 2013; Shiu et al., 2004; Steward et al., 2015; Ting et al., 2012). Some studies show an increase in tension following application of shear, while others show the opposite. Furthermore, temporal variability of cytoskeletal tension after extended periods of application of steady shear flow has not

been examined. By exposing both monolayers and isolated endothelial cells to flow-induced shear stress, we investigate the effect of this stress on tensional homeostasis.

Approach: Monolayers and single endothelial cells are exposed to laminar shear flow with shear stress ranging from 1 to 12 dyn/cm^2 in a custom designed flow chamber which allows traction force measurements using MTM during shear flow application. Traction forces are measured over 2 h under static condition and 2 h under flow conditions. If shear flow is beneficial for tensional homeostasis, we would expect *CV* of the traction field to decrease with increasing shear flow.

1.4   Summary

In summary, the overreaching goal of this thesis is to investigate non-dynamic environmental factors that may affect the cell's ability to achieve tensional homeostasis. While we do recognize that dynamic external perturbations (e.g., applied periodic stretch or pulsatile shear flow) may be a compelling physiological problem, we believe that our investigation is a step in the right direction since there are virtually no quantitative studies about the effect of external disturbances (neither static nor dynamics) on tensional homeostasis in multicellular forms. We hope that results of our investigation will provide new insight into mechanism that determine tensional homeostasis in cells and multicellular clusters in response to alterations in substrate stiffness, unidirectional laminar shear flow, and cadherin junction. Ultimately, we expect that this new knowledge will help in the development of new preventive and therapeutic measures in diseases such as cancer and atherosclerosis.

1.5   Thesis Outline

Following Introduction, in Chapter 2 we provide a brief history of the development of the idea of homeostasis in physiology, and a critical review of the literature on the subject of tensional homeostasis in cells. In Chapter 3, we describe the methods, materials and tools that we used in our investigation. In Chapters 4 through 6, we provide results obtained for each Specific Aim flowed by discussion of those results. For each aim, more specific background information as well as an introduction to the topic is given at the opening of the chapter. Results and discussions are presented in a manner similar to the typical academic paper format. Chapter 4 describes findings related to tensional homeostasis of isolated smooth muscle and endothelial cell cultured on substrates of different stiffness. Chapter 5 describes the effect of healthy and mutated E-cadherin on tensional homeostasis in epithelial cells. Chapter 6 describes the effect of steady laminar shear flow of different magnitudes on tensional homeostasis of endothelial monolayer and isolated endothelial. Finally, Chapter 7 offers an overarching summary of the project findings, their significance and where these results may lead in future studies.

Chapter 2: BACKGROUND

2.1   The Concept of Tensional Homeostasis

In the late 1800s, French physiologist Claude Bernard promulgated the idea of the consistency in the internal environment, or the *milieu intérieur* (Bernard, Dastre, Vulpian, & Bert, 1878). This phrase refers to the interstitial fluid and its physiological capacity to ensure protective stability for the tissues and organs of multicellular organisms in response to disturbances from the environment. Bernard's work laid the groundwork for the development of one of the fundamental principles of physiology called *homeostasis*, the term coined by American physiologist Walter B. Cannon.   According to Cannon, *homeostasis* describes the "fairly constant or steady state, maintained in many aspects of the bodily economy even when they are beset by conditions tending to disturb them" (Cannon, 1929).

The term homeostasis is used to describe the state of equilibrium of many physiological quantities. Amongst them, the most familiar are perhaps the core body temperature (37ºC) and blood pressure (90–120/60–80 mmHg). The nature of physiology is dynamic; our bodies undergo a variety of internal changes constantly in response to environmental changes. This makes the identification of any physiological quantity in homeostasis more complex. Ideally, one must have a method of measuring such a quantity repeatedly over time.

In living cells, mechanical stress plays an important role in regulating and controlling various cellular functions including spreading, migration, contractility, invasion, and mechanotransduction. Consequently, homeostasis in living cells level is

often associated with the cell's ability to maintain its internal cytoskeletal prestress (or tension) stable in the presence of disturbances from the cellular microenvironment. In 1994, investigators from the Robert A. Brown's group from the University College London carried out biomechanical experiments in living fibroblasts seeded in a collagen gel scaffold. These investigators observed that the contractions generated by fibroblasts increase gradually following seeding and eventually reach stable equilibrium (Eastwood, McGrouther, & Brown, 1994). In a subsequent study, they found that fibroblasts in a collagen gel actively respond to external unloading of tension by increasing contraction and respond to loading of tension by relaxing their tensional states (Brown et al., 1998) (Fig. 1). This observation prompted them to use the term *tensional homeostasis*, which the investigators defined as the cells' tendency to adjust their cytoskeletal tension in order to maintain a constant endogenous matrix tension in the gel.

Tensional homeostasis is essential for the normal physiological function of many types of tissues in the body. Breakdown of tensional homeostasis is closely associated with the onset and progression of a disease. Two prominent examples of this are related to (patho)physiology of the endothelium and the epithelium. For vascular endothelial cells, maintenance of tensional homeostasis downregulates pro-inflammatory signaling and thus is atheroprotective (Chien, 2007). Such conditions exist in straight portions of blood vessels where the blood flow is laminar. However near branching points and in curved regions of the blood vessels, the complex or disturbed flow pattern leads to breakdown of tensional homeostasis and results in sustained pro-inflammatory signaling (Chien, 2007). In the epithelium, breakdown of tensional homeostasis has been linked to

pathology of epithelial cancer (Butcher, Alliston, & Weaver, 2009; Paszek et al., 2005; Provenzano & Keely, 2011), which accounts for about 80-90% of all cancers, including breast cancer and gastric cancer. It has been argued that cancer cells overexpress Rho-kinase, which in turn stimulates the cells' contractile machinery. Increase in cell contractility leads to disruption of cell-cell adhesions and therefore disruption in intercellular stress transmission, which causes breakdown in tensional homeostasis (Butcher et al., 2009; Paszek et al., 2005).

While the importance of tensional homeostasis for normal physiological function of cells and tissues has been well documented, the mechanisms by which cells achieve and maintain tensional homeostasis remain largely unknown. Most past studies of tensional homeostasis have been qualitative and based on circumstantial evidence. For example, Mizutani and colleagues demonstrated that cellular stiffness returned to a set point level after stretching or relaxing single fibroblasts (Mizutani, Haga, & Kawabata, 2004). To the extent that the cell stiffness is closely associated with cytoskeletal tension (Wang et al., 2001), the investigators interpreted their observation as an indication that isolated living cells were capable of maintaining tensional homeostasis. Simultaneous measurements of cellular traction forces and the projected area of focal adhesions (FAs) in fibroblasts revealed a linear relationship between the force and the FA area (Balaban et al., 2001; Goffin et al., 2006; Tan et al., 2003). This, in turn, implies that cells were capable of maintaining constant the stress acting on the FAs, regardless of their size and the magnitude of the contractile force, which was interpreted as an evidence of tensional homeostasis at the subcellular level (Jay D. Humphrey, 2008a). Taken together, these

results lead to a hypothesis that tensional homeostasis exists across a wide range of length scales and time scales (Jay D. Humphrey, 2008a). However, with the progression of single cell manipulation and traction measurement techniques, new evidence emerged that challenged the idea that tensional homeostasis is length scale-independent. Results obtained by the Fletcher's group indicated that single fibroblasts do not appear to have a preferred, "set-point" homeostatic tension; instead these cells minimize changes in forces due to strain. The investigators termed this phenomenon "tensional buffering" (Webster et al., 2014). Recent findings of our group revealed that isolated endothelial cells exhibit large, erratic temporal fluctuations of their traction field (Canović et al., 2016; Krishnan et al., 2012). However, when the endothelial cells formed multicellular clusters, temporal fluctuation become attenuated with increasing cluster size (Canović et al., 2016) (Fig. 2), suggesting that cell clustering promotes tensional homeostasis.

These discoveries call for a change in the way we study tensional homeostasis. First of all, the definition of tensional homeostasis is an evolving concept since its conception. While Brown et al.'s definition is conceptually easy to understand, we need a more quantitative definition to refer to when studying it. Our group proposed a new definition of tensional homeostasis as *the ability of cells to maintain a consistent level of tension with low temporal fluctuations* (Canović et al., 2016). Although this definition does not specify a threshold below which tensional homeostasis is achieved, it does permit quantitative comparison to determine how different factors, such as multicellularity, cell type, substrate stiffness, shear flow, or stretch impact tensional homeostasis.

Tensional homeostasis appears to be essential for effective barrier function. Interestingly, traction fluctuations in monolayers of endothelial cells were recently shown to be predictive of gap formation and loss of barrier function (Valent, van Nieuw Amerongen, van Hinsbergh, & Hordijk, 2016). In fact, in normal conditions, endothelial cells exist in monolayers, where cell-cell bonds create a multicellular structure that functions as a mechanical barrier and is fundamental for endothelial function (Yuan & Rigor, 2010). Thus, there is a growing interest in measuring the dynamics of temporal and spatial variability of intracellular tension and also in how molecules pivotal for cell-cell adhesion may impact this process.
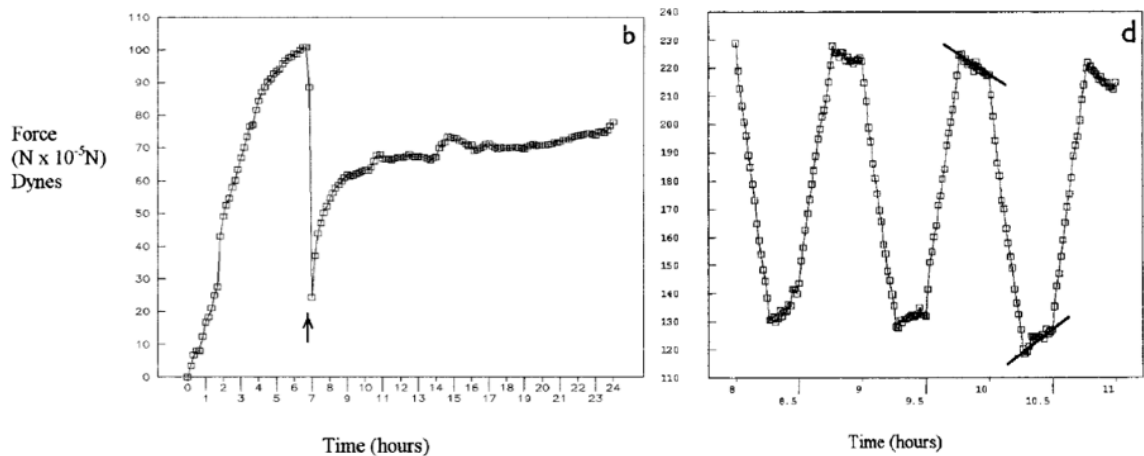
Figure 1: Fibroblasts seeded in a collagen gel responds to external mechanical loading and unloading by adjusting their tension. The left panel shows the force measured following an unloading (arrow). The right panel shows cyclic loading and unloading with resting periods between them. During the resting periods, tendencies of the tension being brought towards a middle level is seen (solid line marks the slope of the data) (Adapted from Brown et al., 1998).
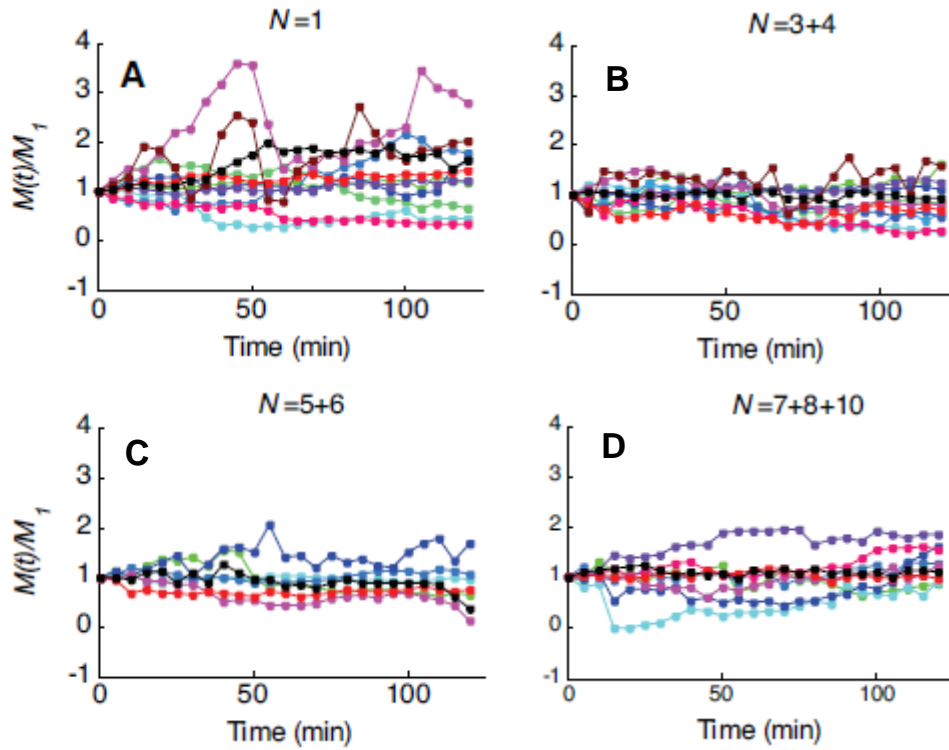
Figure 2: Time-lapse plots of the net contractile moment. Net contractile moment (*M(t)*), which is a scaler metric of the traction field, normalized by its initial value (*M₁*) exhibits a greater variability for single cells (A) than for 3- and 4-cell clusters (B), 5- and 6-cell clusters (C) and 7-, 8- and 10-cell clusters (D). Each color represents a different cell/cluster (Adapted from Canović, 2016).

2.2   Length and Time Scales of Tensional Homeostasis

It has been widely accepted that maintenance of tensional homeostasis is controlled across multiple length scales: at the individual cell level (Jay D. Humphrey, 2008a, 2008b; Mizutani et al., 2004; Provenzano & Keely, 2011) and in larger, multicellular forms (Bazzoni & Dejana, 2004; Brown et al., 1998; Guillot & Lecuit, 2013; Macara, Guyer, Richardson, Huo, & Ahmed, 2014). Studies carried out on isolated fibroblasts support the idea that individual cells can control tensional homeostasis (Mizutani et al., 2004). These cells have shown the ability to maintain steady prestress following an externally applied mechanical disturbance. Since fibroblasts do not form monolayers *in vivo*, cell-cell cooperation to maintain tensional homeostasis is probably not needed. However, the situation is quite different with cells that form monolayers *in vivo*, such as endothelial and epithelial cells, where tensional homeostasis may be achieved only in multicellular clusters (Canović et al., 2016). *It remains to be determined how, and indeed whether, tension is stabilized across multiple length scales, from focal adhesions to multicellular assemblies, and thus tensional homeostasis is itself a phenomenon that requires investigation across broad scales of both length and time.*

Cellular prestress generated through the actomyosin contractile machinery is balanced across integrins adherent to the extracellular matrix (ECM), as well as through cadherins adherens junctions. This balance between tension applied to cadherins and integrins is confounded by the surprising finding that epithelial cells can exert tension to E-cadherin even in the absence of coupling to neighboring cells (Borghi et al., 2012). This finding may indicate that tensional homeostasis in cell types that require adherens

junctions for normal physiological function may require multicellularity. Past studies

have shown that there is a cross-talk between cadherin and integrins that can affect cell

mechanical behaviors (e.g., motility), as both molecules are coupled to the actin

cytoskeleton (Mui, Chen, & Assoian, 2016; Schwartz & DeSimone, 2008; Weber,

Bjerke, & DeSimone, 2011). According to these studies, this crosstalk also affects tension

generation (Mui et al., 2016; Nelson, Pirone, Tan, & Chen, 2004), which could serve as a

possible explanation for the cell ability to exert tension on E-cadherins even in the

absence of cell-cell adhesions. Importantly, this crosstalk appears to be regulated by

substrate stiffness; with stiffer substrate favoring cell-ECM force transmission and softer

substrates cell-cell force transmission (Collins, Denisin, Pruitt, & Nelson, 2017; Polio,

Stasiak, Krishnan, & Parameswaran, 2018; Tsai & Kam, 2009), suggesting that the

ability of cell clusters to achieve tensional homeostasis may be substrate stiffness-

dependent.

   While stiffness sensing is a relatively widely-studied topic in mechanobiology,

there is a gap between its impact across cellular length scales and the way it is being

examined and reported. First of all, effects of stiffness span multiple length scales, but

most studies tend to look at one length scale at a time. At the FA level, the intracellular

structures and signaling pathways are connected to the ECM. Thus, these FAs not only

demonstrate traction force dynamics that are affected by substrate stiffness, but FAs are

also essential for the cell's ability to sense this stiffness in the first place. Maturation of

FAs is enhanced on stiffer substrates compared to soft ones, which makes them more

stable on stiff surfaces (Doyle et al., 2015). Traction force profiles are also different on

stiff versus soft substrates, as showed by Plotnikov *et al.* (2012). These investigators found that more FAs exhibit fluctuating or "tugging" forces on soft substrates, and that this type of tugging FA force was essential for durotaxis. On the cellular level, response to stiffness is better established. This response includes increased cell spreading area (Jalali, Tafazzoli-Shadpour, Haghighipour, Omidvar, & Safshekan, 2015; Plotnikov et al., 2012; Polte et al., 2004; Sazonova et al., 2015, 2011), more pronounced stress fiber formation and cytoskeletal protein content (Birukova et al., 2013; Byfield, Reen, Shentu, Levitan, & Gooch, 2009; Sazonova et al., 2011), and increased cytoskeletal tension with increased substrate stiffness (Doyle et al., 2015; Huynh et al., 2011; Izquierdo-Álvarez et al., 2019; Krishnan et al., 2011; Polte et al., 2004; Sazonova et al., 2015; Urbano et al., 2017; Zhou et al., 2017). Furthermore, there is evidence that multicellular smooth muscle cell clusters respond to substrate stiffness differently from single cells, suggesting the effect of stiffness mechanosensing continues to be nuanced on larger length scales (Sazonova et al., 2011). All these findings suggest that observations made on one length scale only tell a partial story. Therefore, it is important to cross length scales in the same study to determine whether subcellular dynamics lead to global cellular responses.

Snapshots of traction at only a single point in time are also limited in the information they can provide. For example, tugging behavior of FAs on softer substrates was observed by measuring individual FA forces every 5 s over a 2 min window of observation (Plotnikov et al., 2012). In previous studies by our group, we have observed temporal fluctuation of endothelial cells over two hours by measuring traction forces every 5 min (Canović et al., 2016). We sought to determine whether these cellular level

temporal fluctuations can be affected by substrate stiffness as well. Finally, different cell types are acclimated to different stiffness environments *in vivo,* and these cell types and tissues also have dissimilar mechanical functionalities, such as the maintenance of vascular tone by vascular smooth muscle cells and the barrier function of endothelial cells. Hence, cell type-dependent differences in stiffness sensing is a distinct possibility. While stiffness-related studies have used different types of cells, from fibroblasts to vascular cells, it is rare to find comparisons across those cell types within the same study. Our recent study of tensional homeostasis revealed a difference in the way vascular smooth muscle cells and endothelial cells maintain stable cytoskeletal tension (Zollinger et al., 2018), which led us to believe that there may be differences in their tensional responses to substrate stiffness as well.

In our studies of tensional homeostasis, we have used MTM to measure cell-substrate traction in cells and clusters. Since traction forces arise as a result of cytoskeletal contractile forces, measurements of traction forces provide insight into cytoskeletal prestress. In the MTM technique, cells/clusters are cultured on a soft, elastic polyacrylamide (PAA) gel substrates microprinted with a regular array of fibronectin dots. Since cells can only form FAs at the dots, by observing dot displacements caused by cell contractile apparatus, we can compute FA traction forces from the dot displacements and known elastic properties of the substrate (Polio et al., 2012; 2014). By quantitating traction forces temporal fluctuations over an extended time period (1-2 h), we have been able to compare how these fluctuations differ between FAs, cells and clusters.

The above approach has been useful for studying tensional homeostasis in a quantitative manner in the absence of external disturbances. While this is a biologically important discovery, it is relative narrow in scope since tensional homeostasis is primarily associated with the ability of cells and tissues to restore stable and preferred level of cytoskeletal tension in response to external disturbances. For example, in the endothelium, the cells are continuously exposed to blood-flow induced shear stress and to periodic stretch of the vessel walls due to the pulsatile nature of blood pressure. How these mechanical disturbances affect tensional homeostasis has not yet been fully explained. While it has been argued that unidirectional laminar flow that exists in the straight portion of blood vessels is beneficial for endothelial homeostasis since it does not produce pro-inflammatory signaling (Chien, 2007), it has not yet been quantitatively measured how shear flow impacts traction field variability and homeostasis in monolayers of endothelial cells.

In this thesis, we intended to fill same of the gaps in our understanding of tensional homeostasis. First, we investigated the impact of substrate stiffness on cell's ability to achieve tensional homeostasis at the whole cell level, at the FA level, and in different cell types. Second, we investigated the role of cadherins in tensional homeostasis. For that purpose, we used gastric carcinoma epithelial cells with different types of mutations of their cadherin adhesions. Finally, we investigated the impact of laminar shear flow of different magnitudes on tensional homeostasis of isolated endothelial cells and on monolayers of endothelial cells.

Chapter 3: MATERIALS AND METHODS

3.1   Cell Culture

All cell types used in this study are cultured in a sterile incubator set at 37ºC and 5% CO_2 content.

3.1.1   *Bovine Aortic Endothelial Cells (BAECs)*

BAECs (Cell Application) were cultured in Dulbecco's Modified Eagle Medium (DMEM) with 1 g/L glucose (Corning) supplemented with 10% bovine calf serum (Sigma Aldrich) and 1% antibiotic–antimycotic solution (100x; Sigma Aldrich). BAECs were used between passage 3-13 for experiments.

3.1.2   *Bovine Vascular Smooth Muscle Cells (BVSMCs)*

BVSMCs (Cell Application) were cultured in DMEM with 1 g/L glucose (Corning) supplemented with 10% bovine calf serum (Sigma Aldrich) and 1% antibiotic– antimycotic solution (100x; Sigma Aldrich). BVSMCs were used between passage 3-15 for experiments.

3.1.3   *Human Gastric Adenocarcinoma (AGS) Cells*

All AGS cells were transfected and prepared by Dr. Joana Figueiredo at University of Porto, under the advisement of Dr. Joana Paredes and Dr. Raquel Seruca. AGS cells were stably transfected with a vector encoding wile-type (WT) E-cadherin (E-cad), E-cad bearing a point mutation or an empty vector (Mock). Using Lipofectamine 2000 (Invitrogen), according to the manufacture procedure. Transfected AGS cells were cultured in Roswell Park Memorial Institute (RPMI) medium supplemented with 10%

fetal bovine serum (Hyclone) and 1% penicillin–streptomycin (10,000 U/mL; Gibco) and maintained under antibiotic resistance to blasticidin (5 lg/mL; Gibco, Invitrogen). Cells were grown up to 90% confluency before passaging.

3.1.4   Cell Seeding for Micropattern Traction Microscopy (MTM)

All cell types were seeded 18-24 h onto the protein patterned PAA gel substrates before MTM experiments, in order to allow for attachment and FA maturation. Media was changed 1 h before all experiments. Seeding density for single cell experiments were between 30,000 to 50,000 cells per gel (25 μm diameter, round gel), and for multicellular cluster experiments between 50,000 to 100,000 cells per gel.

3.2   Protein Isolation and Labeling

3.2.1   Fibronectin Isolation

Fibronectin (Fn) was isolated from pooled human blood plasma (Valley Biomedical). The procedure was described previously (Smith et al., 2007). Briefly, the isolation and purification process involves two columns: size exclusion column containing Sepharose 4B (sigma) and affinity column containing Gelatin Sepharose (GE Healthcare). The columns were gravity packed and conditioned with phosphate buffered saline (PBS) (Sigma Aldrich) and 2mM of ethylenediaminetetraacetic acid (EDTA) (Sigma Aldrich). Plasma is passed through the size exclusion column first, collecting the filtered plasma. Then the filtered plasma is run through the affinity column and the run-through is discarded since Fn binds with gelatin in the affinity column. Finally, the

affinity column is rinsed with 1M NaCl, 0.5 M urea and 6 M urea in PBS to remove Fn from the beads. Concentration of Fn is tested with a NanoDrop (ThermoFisher). Solvent (PBS) is replaced with DI water using a PD-10 desalting column (GE Healthcare) before storing at −20ºC.

3.2.2   Protein Labeling

A variety of proteins were used as substrates for experiments, including Fn, vitronectin (VTN) (MTI GlobalStem) and collagen VI (Col VI) (abcam). Proteins were labeled with AlexaFluor 488 succinimidyl ester (ThermoFisher) at 30-70 molar excess. Labeling was done according to protocol provided by ThermoFisher, which requires 1 h incubation at room temperature. Fn was labeled in solution of PBS. Excess free dye was removed using a PD-10 column before confirming final concentration of the labeled Fn. Since VTN was only used in combination with Fn, it was not labeled separately. For Col VI, due to the limited amount of protein, the free dye was not filtered after labeling.

3.3   Micro-contact Patterning

Micro-contact patterning is used to place the desired protein pattern onto a glass coverslip. Detailed method is described in Polio *et al.* (2012). Briefly, a polydimethylsiloxane (PDMS) elastomer stamp is molded from silicon wafer created from soft photolithography. The PDMS stamp is then plasma treated and a solution of fluorescently labeled protein (e.g., Fn) is placed on top of the stamp at room temperature. During the incubation, the fluorescent protein "ink" adsorbs onto the stamp. The dried stamp is then inverted onto a cleaned and plasma treated glass coverslip to transfer the

protein onto the coverslip. The protein patterned coverslip is then used to transfer the pattern onto a polyacrylamide gel.

The pattern designed for traction microscopy is an array of 2 μm diameter dots with 6 μm center-to-center separation.
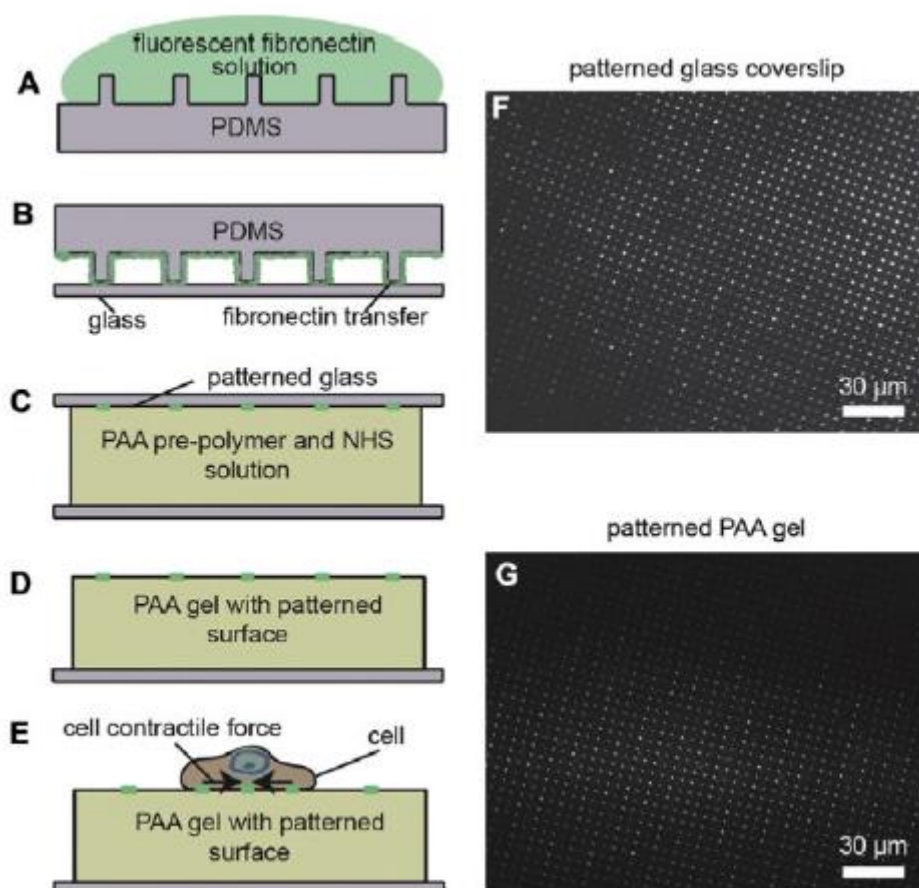
Figure 3: Diagram of micro-contact patterning procedure. Fluorescently labeled

fibronectin (Fn) in PBS is adsorbed onto the plasma-treated, hydrophilic stamp (A). After

the stamp is allowed to dry, the Fn is stamped onto the plasma-treated coverslip (B). The

patterned coverslip is then placed onto a PAA gel pre-polymer solution (C) to allow the

pattern to be transferred and covalent bonded with the PAA polymer after polymerization

(D). The pattern allows cell attachment on the Fn-patterned gel (E). Fluorescent

microscopic images are shown using a ×40 water objective of a microcontact-printed

pattern on glass (F) and a pattern after transfer onto the PAA gel (G). Scale bars = 30 μm

(Adapted from Polio et al., 2012).

3.4   Polyacrylamide (PAA) Gel Synthesis

PAA gels were made in a sterile biosafety cabinet. The elastic modulus (E) of

PAA gels can be tuned by changing the acrylamide and bis-acrylamide ratio in the

precursor solution. Using the same recipes previously established in our lab (Polio,

2012), PAA gels for this project were made with acrylamide and bis-acrylamide contents

shown in Table.1. Acrylic acid N-hydroxysuccinimide (NHS) ester (Sigma) was added to

the gel solution at 0.002% (w/w) to covalently bond the patterned protein onto the top of

the gel as it polymerized. PAA gels are allowed to polymerize for 45min at room

temperature and then stored in 4ºC in saline solution until ready to use.

Table 1: Polyacrylamide Gel Recipes

Acrylamide (m/v)	Bis-acrylamide (m/v)	Elastic Modulus (kPa)
10%	0.07%	3.6
10%	0.13%	6.7
10%	0.26%	13.6
8%	0.35%	30

3.5   Micropattern Traction Microscopy

3.5.1   Experimental Procedure

A micropatterned gel was seeded with cells according to the seeding procedures

described in Section 3.1.4. Experiments took place in an environmental chamber that

maintains 37ºC, 70% humidity and 5% CO_2. Fluorescent protein pattern and cells were

imaged with an Olympus IX881 microscope and a Hamamatsu Orca R2 camera. An image was taken every 5 min for 1-2 h, depending on the experiment.

3.5.2 *Image Processing and Traction Calculations*

Images of the cells and the fluorescent Fn dot array were analyzed using custom MATLAB (MathWorks) scripts, as previously described previously (Polio et al., 2012). The program finds the displacement vector (**u**) of the geometrical center of Fn dots and calculates the corresponding traction force vectors (**F**) according to the following formula $\mathbf{F} = \pi E a \mathbf{u} / (1 + \nu - \nu^2)$, where $a = 1$ μm is the radius of the dot markers and $\nu = 0.445$ is the Poisson's ratio of the PAA gel substrate (Maloney, Walton, Bruce, & Van Vliet, 2008).

Traction forces under 0.3 nN were removed, because below that magnitude the measured force is indistinguishable from background noise. This threshold was chosen based on background displacements measurements (Polio et al., 2012), and modified to fit the softest substrate used in experiments (3.6kPa).

Forces of a cell/cluster was balanced using a MATLAB program as described previously (Canović et al., 2014).

3.5.3 *Focal Adhesion Tracking*

We track individual FAs through the 1-2 h experiment by matching the location of measured FA from one frame to the next. As long as the force associated with the FA is above threshold (0.3 nN) the FA is considered mechanically engaged. To obtain the

lifetime of an engaged FA, MATLAB counted the number of continuous frames where the magnitude of a given FA force was above threshold. If the force disappeared or dropped below the threshold, we assumed that particular FA had disassociated. Given the 1-2 h duration of the experiments and the sampling rate of every 5 min, our shortest and longest lifetime were ≤5 min and 60-120 min, respectively.

3.5.4   *Assessment of Variability/Metric for Homeostasis*

The state of tensional homeostasis is assessed by the temporal variability of traction. We used a coefficient of variation (*CV*) as a metric of temporal variability. The coefficient of variation shows the extent of variability of a given quantity relative to its mean. It is defined as the ratio of the standard deviation to the mean. According to our definition of tensional homeostasis, the lower the *CV*, the more homeostatic is FA/cell/cluster is. Theoretically, *CV* approaches zero when tensional homeostasis is achieved.

For an individual FA force, we obtain the corresponding *CV* of force time lapses as

$$CV_F = \frac{\sigma(F)}{\langle F \rangle},$$
(1)

where $\sigma(F)$ is the standard deviation and $\langle F \rangle$ is the time-average of the magnitude of the FA traction force vector *F(t)*.

In the case of the traction field of a cell or a multicellular cluster, we first computed a scaler metric for the strength of the traction field. We use the sum of

magnitudes of all FA force vectors within the cell (T). At a given time (t), those metrics

are given as follows

$$T(t) = \sum_{i=1}^{N(t)} F_i(t),$$ (2)

where $F(t) = \|\mathbf{F}(t)\|$. The corresponding CV is then calculated as follows

$$CV_T = \frac{\sigma(T)}{\langle T \rangle}$$ (3)

where $= \sigma(T)$ is the standard deviation and $\langle T \rangle$ is the time-average of $T(t)$.

3.6   Assessment of Correlation between FA forces

Correlation between FA forces describes extent to which the individual forces

increase/decrease in sync with each other. It have been shown that CV_T depends on the

correlation between traction forces (Li, Barbone, Smith, & Stamenović, 2019). A

positive/negative correlation between forces leads to higher/lower values of CV_T. Using

the algorithm of Li *et al.* (2019), we carried out a correlation of measured traction forces

described below. To see the method for tracking FA forces individually, please reference

section 3.5.3.

For each pair of forces (F_j, F_k) within a cell, we calculated the corresponding

correlation coefficient, $r(F_j, F_k)$, as follows

$$r(F_j, F_k) = \frac{\sum_{i=1}^{N_\tau} [F_j(t_i) - \langle F_j \rangle][F_k(t_i) - \langle F_k \rangle]}{N_\tau \sigma(F_j)\sigma(F_k)},$$ (4)

where $\sigma(F_j)$ and $\sigma(F_k)$ are standard deviations of F_j and F_k, respectively, $j,k = 1.2,...N$,

where N is the total number of FA forces within a cell, and N_τ is the number of 5-min

observation time intervals ($N_\tau = 13$ for 1 h observations and $N_\tau = 25$ for 2 h observations).

We used such obtained correlation coefficients to create a symmetric correlation

matrix whose elements are $r(F_j,F_k)$. According to Eq. (4), the diagonal elements of the

matrix all have the value of unity. We then summed all the elements in this matrix, and

subtracted the sum of all diagonal elements (which is equal to N) in order to obtain a

coefficient of global correlation of all forces in the cell (R) as follows

$$R = \sum_{j,k=1}^{N} r(F_j, F_k) - N . \tag{5}$$

If $R = 0$, then there was no global correlation between forces in a cell; if $R < 0$, then there

was a negative global correlation; and if $R > 0$, then there was a positive global

correlation.

Since the number of FAs vary between cells, we normalized R from Eq. 5 by $N(N$

$- 1)$ and obtained the normalized global correlation coefficient (R_{norm}). Note that R_{norm} is

the average Pearson's correlation coefficient of each pair of forces. Thus, if $0 < R_{norm} \leq$

1, all forces in the cluster exhibit a predominantly positive correlation, and if $-1 \leq R_{norm}$

< 0, the forces in the cluster exhibit a predominantly negative correlation.

Additionally, we calculate the contribution of force correlation to CV_T, which is

the difference between theoretical CV_T when all the force pairs are not correlated and the

experimentally measured CV_T. We randomized fluctuations of measured FA forces by

reordering, in a random fashion, their 5-min interval fluctuations using MATLAB; e.g., a natural 5-min fluctuations array $F(t_1)$, $F(t_2)$, $F(t_3)$,…. $F(t_{25})$, became a random 5-min fluctuations array $F(t_7)$, $F(t_{19})$, $F(t_3)$,… etc. This procedure did not alter values of CV_F and $\langle F \rangle$, while at the same time it reduced temporal correlation between FA forces that existed before reordering. In each cell/cluster, experimentally measured forces were replaced by the corresponding randomized forces and CV_T was computed as above (Eqs. 2 and 3).

3.7   Statistical Analysis

Through Kolmogorov-Smirnov normality test, we obtained that some of the data groups do not follow a normal distribution. Taken the non-normal distribution into account, in the results sections we graph median values of the data groups instead of the mean. The error bars represent median absolute deviations, unless otherwise stated. To test the difference between median values of two data groups, the Mann-Whitney U test is performed. Significance is defined as $p < 0.05$. Additionally, non-parametric Kruskal-Wallis test is done on groups of three or more. Significance is still defined at $p < 0.05$. Finally, for testing if two distributions are the same, without specifically comparing median values, 2-sample Kolmogorov-Smirnov test was used and significance is defined as $p < 0.05$.

The particular types of test performed in any given graph will be described in the captions of the figures.

Chapter 4: THE EFFECT OF SUBSTRATE STIFFNESS ON TRACTION

DYNAMICS AND TENSIONAL HOMEOSTASIS[1]

This chapter deals with Specific Aim 1: **To investigate the impact of substrate stiffness on tensional homeostasis at the single focal adhesion level and at the whole cell level.**

4.1   Background

Stiffness mechanosensing is a major topic in mechanobiology. Cells receive mechanical cues from their environment that instructs their behaviors. Substrate stiffness determines the stress and strain they experience through FAs. Substrate stiffness is also altered in a number of pathologies, such as aging of the vasculature and in the tumor microenvironment. Cells are able to sense and respond to these stiffness changes and their reaction to this change either furthers the progression of the disease, or corrects the path back to normal physiology. Importantly, for our considerations, substrate stiffness also has an established effect on cell contractility, which in turn suggests that it may have an impact on tensional homeostasis of the cells.

Substrate stiffness is known to increase contractility in a number of cell types (Doyle et al., 2015; Huynh et al., 2011; Izquierdo-Álvarez et al., 2019; Krishnan et al., 2011; Polte et al., 2004; Sazonova et al., 2015; Urbano et al., 2017; Zhou et al., 2017). However, the effect of stiffness on temporal fluctuations of traction forces is less known. Plotnikov et al. (2012) reported that more fluctuating or "tugging" FA forces were found in fibroblasts on softer substrates, indicating that fluctuation may increase with

---

[1] The content of this chapter has been submitted for publication in *Cellular and Molecular Bioengineering*.

decreasing stiffness. However, it is unclear whether similar effects occur on cell or on multicellular levels.

We hypothesize that substrate stiffness will alter both the set point cytoskeletal tension and the temporal variability in tension. Previous results showed that higher mean tension of the traction field corresponded to lower variability of the traction field (Canović et al., 2016). Thus, it is possible that stiffer substrates will lower traction field variability by enhancing its mean tension, thus promoting tensional homeostasis. However, there are also other factors at play, including increased spread area and more matured FAs on stiffer substrates. These are also expected to play a role in influencing tensional homeostasis.

4.2   Experimental Design

BVSMCs and BAECs are seeded on Fn patterned PAA gels with different values of the elastic modulus. PAA gels have tunable stiffness by changing the ratio of acrylamide and bis-acrylamide in the precursor solution (see Table 1 in Chapter 3). Traction forces of BVSMC and BAEC single cells were measured using MTM at 5 min intervals, over for 2 h.

33
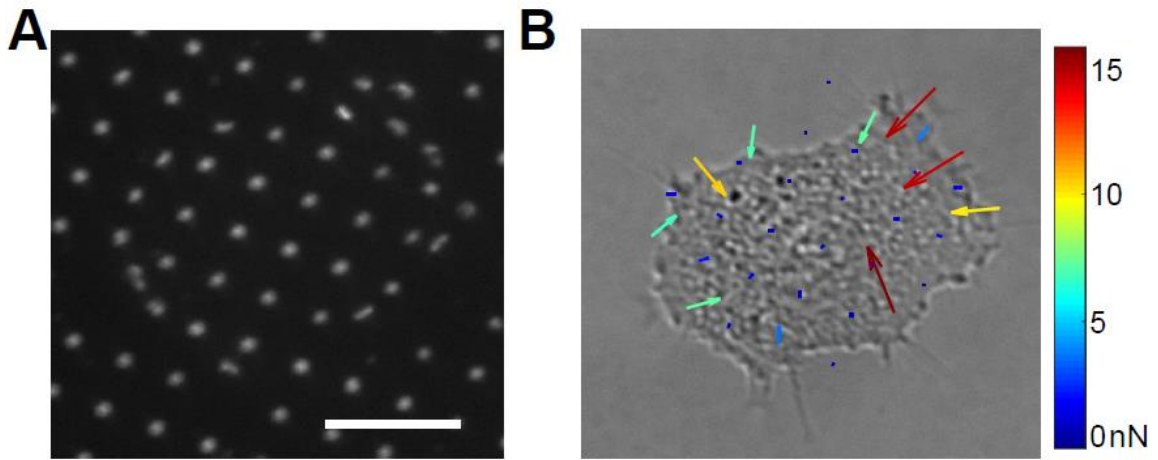
Figure 4: Micropattern traction microscopy (MTM) is used to measure traction forces at the cell-substrate interface. In MTM, fibronectin dots form a predetermined array on the gel, which is then displaced by tractions generated by the cells (A). Displacement is recorded by MATLAB program and traction forces are calculated from measured displacements and known gel elastic properties as described in Section 3.5.2 (B). An example of MTM on a bovine vascular smooth muscle cell (BVSMC) on cultured on 13.6 kPa stiffness polyacrylamide (PAA) gel patterned with fibronectin dots is shown here. (Scale bar: 15 μm)
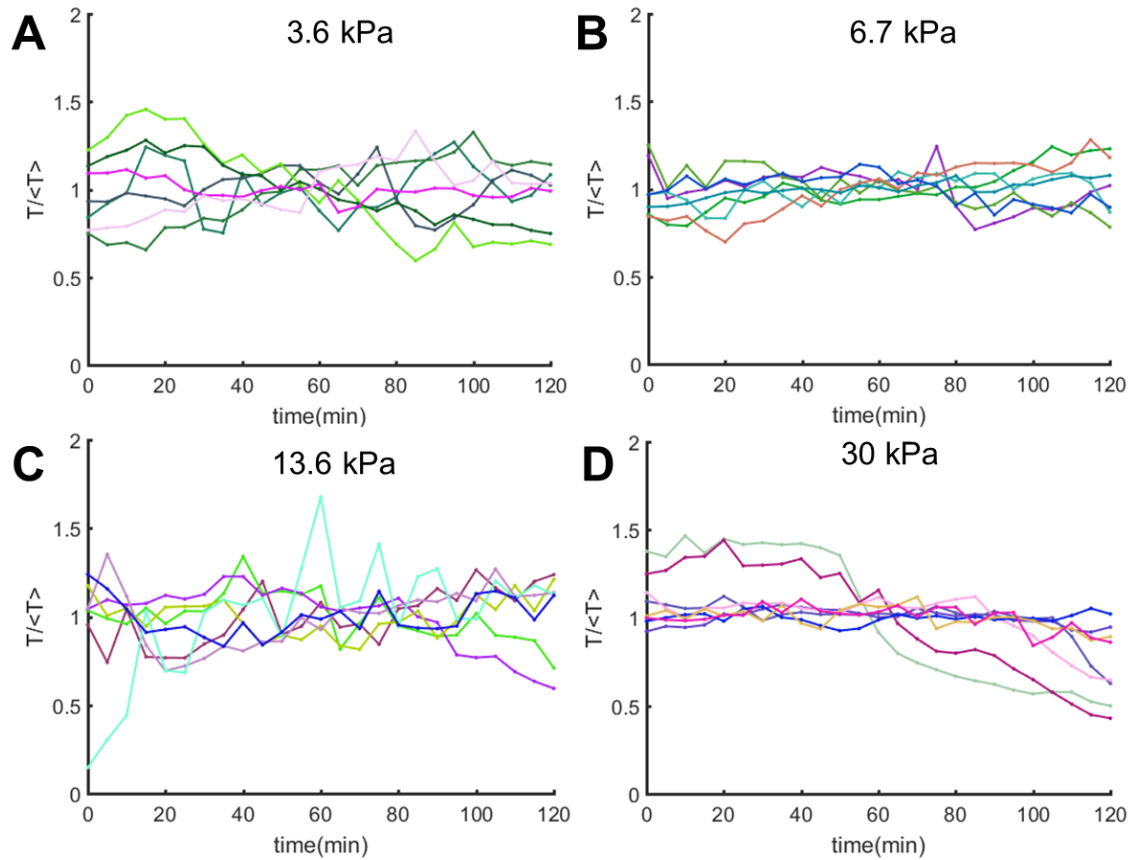
Figure 5: Time lapses of the normalized sum of traction force magnitudes ($T/\langle T \rangle$) of single bovine vascular smooth muscle cells (BVSMCs) on substrates with stiffness ranging from 3.6 to 30 kPa. Time-lapse shows results from 2 h of experiments with 5 min sampling rate. Each color represents a different single cell.
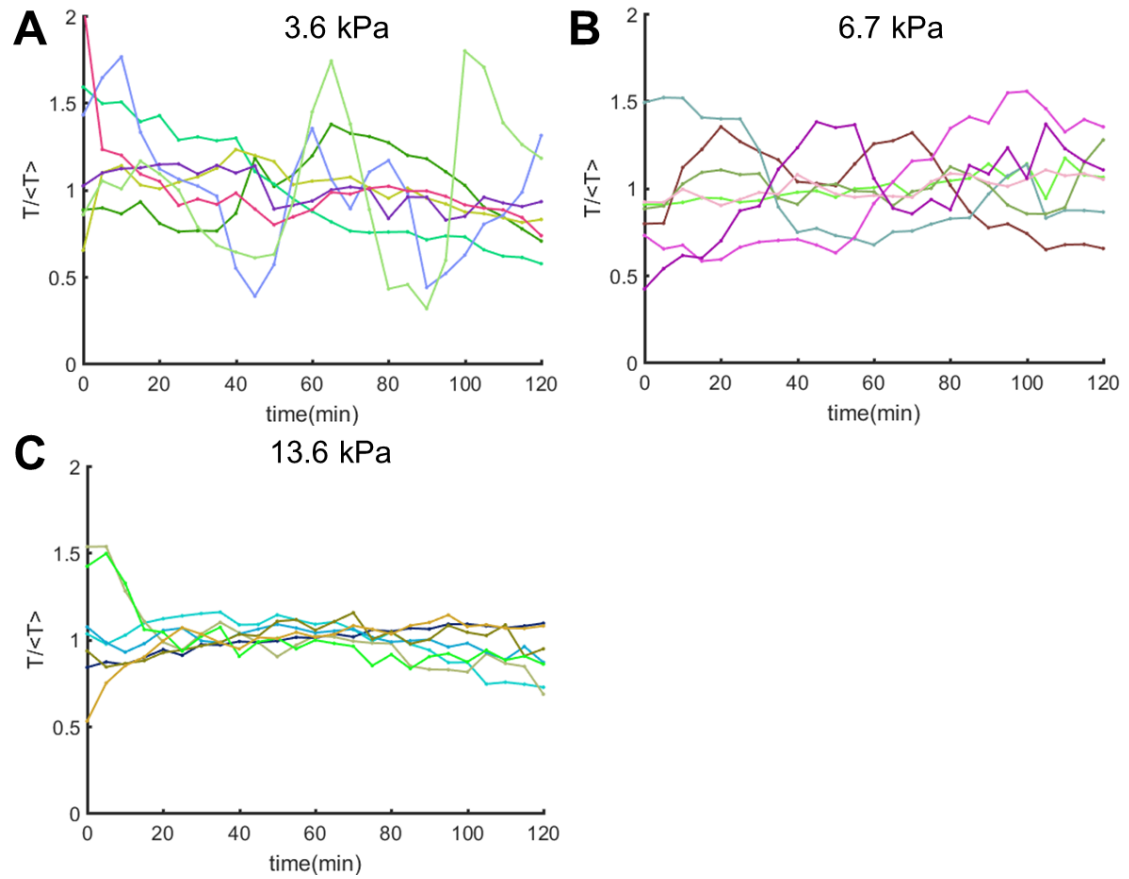
Figure 6: Time-lapses of the normalized sum of traction force magnitudes ($T/\langle T \rangle$) of single bovine aortic endothelial cells (BAECs) on substrates with stiffness ranging from 3.6 to 13 kPa. Time-lapse shows results from 2 h of experiments with 5 min sampling rate. Each color represents a different single cell.

4.3   Results

We observed that traction forces formed centripetal patterns; forces of greater

magnitude were located near the cell boundary, whereas traction forces of lower

magnitude were located away from the cell boundary (Fig. 4). This pattern of traction

remained consistent on all the substrates of different stiffnesses for both cell types (data

not shown). These findings were consistent with data from the literature (Balaban et al.,

2001; Butler, Tolić-Nørrelykke, Fabry, & Fredberg, 2002; Dembo & Wang, 1999). Time-

lapse of $T/\langle T \rangle$ of representative BVSMCs and BAECs on substrates of different stiffness

are shown in Fig. 5 and Fig. 6, respectively.

4.2.1   Effects of substrate stiffness on traction dynamics of BVSMCs

Smooth muscle cells showed increased numbers of FAs and traction forces with

increasing substrate stiffness (Fig. 7A,B). Cells that were cultured on 30 kPa stiff gels

had FA forces that were significantly higher than those on softer PAA gels. The

maximum FA force on a given substrate increased with increasing substrate stiffness

(Fig. 7B). We also found that BVSMCs had more mechanically engaged FAs on stiffer

substrates and a significantly higher number of engaged FAs on 30 kPa stiff gels

compared to substrates of lower stiffness (Fig. 7B). The fraction of surviving FAs

decreased rapidly with increasing observation time (Fig. 7C). The rate of decrease was

affected by the substrate stiffness, but not in a systematic way. The 30 kPa stiff gel had

more longer-lived FAs, with 45.26% of FAs surviving for the entire 120 min, whereas

13.6 kPa stiff gel had more shorter-lived FAs, with the lowest percentage (24.5%) of FAs

surviving for the duration of our observation window (i.e., 120min). Gels of 3.6 kPa and

6.7 kPa stiffness showed similar distributions of FA lifetime, with 33.16% and 36.31% of FAs surviving for 2 h, respectively (Fig. 7C).

It has been reported that in BAECs FA forces of larger magnitude exhibit smaller values of CV_F than FA forces of smaller magnitudes (Canović et al., 2016). Here we observed a similar trend in BVSMCs on substrates of different stiffnesses (Fig. 8A). Moreover, on each substrate, FA forces of the highest magnitude had nearly the same low value of CV_F (Fig. 8A). For example, the highest forces on 3.6 kPa stiff substrate were around 10 nN and had a similar average CV_F as the highest forces on the 30 kPa stiff gel, which was around 80 nN (Fig. 8A). Furthermore, we plotted CV_F with respect to dot displacement on each surface (Fig. 8B). Despite the increasingly higher ranges of FA forces shown on stiffer surfaces, the dot displacements, which represent substrate deformation caused by cellular traction forces, showed the same range. The CV_F of BVSMCs on various stiffness surfaces also showed the same dependency to dot displacements (Fig. 8B).

The differences in force range and lifetime distribution on surfaces of different stiffness were also reflected at the whole-cell level. In BVSMCs, the average sum of the magnitudes of traction forces, $\langle T \rangle$, increased with increased substrate stiffness (Fig. 9A). On the other hand, cells exhibited a significant increase of CV_T only from 6.7 to 13.6 kPa stiff gels, and changes of CV_T for other examined substrate stiffnesses were not statistically significant (Fig. 9B).
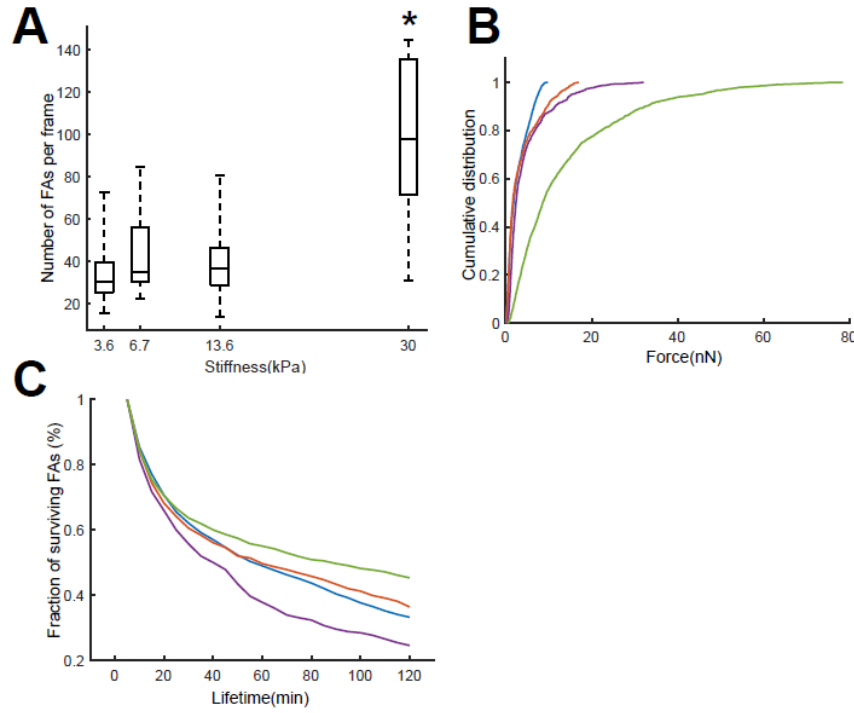
Figure 7: BVSMCs have significantly more engaged focal adhesions (FAs) on stiffer surface compare to softer ones. Stiffer surfaces also have stronger FA forces and induced different distributions of FA lifetime. The average numbers of engaged FAs over 2 h (25 frames) are plotted against substrate stiffness (A). The average number of FAs of each group in increasing stiffness order are: 35, 45, 40 and 96. FA number of 30 kPa group is significantly different from the other stiffness. There are significant differences in distributions of FA force magnitudes (B) and lifetimes (C) between all the groups. Significance is defined by $p < 0.05$ in 2-sample Kolmogorov-Smirnov test (*). (blue: 3.6 kPa; orange: 6.7 kPa; purple: 13.6 kPa; green: 30 kPa) ($n = 43, 13, 14, 15$ cells and 2663, 1030, 1155, 2333 FA forces tracked for 3.6 kPa, 6.7 kPa, 13.6 kPa and 30 kPa substrates, respectively; numbers of independent experiments for each group in increasing stiffness order are 2, 3, 3 and 4.)
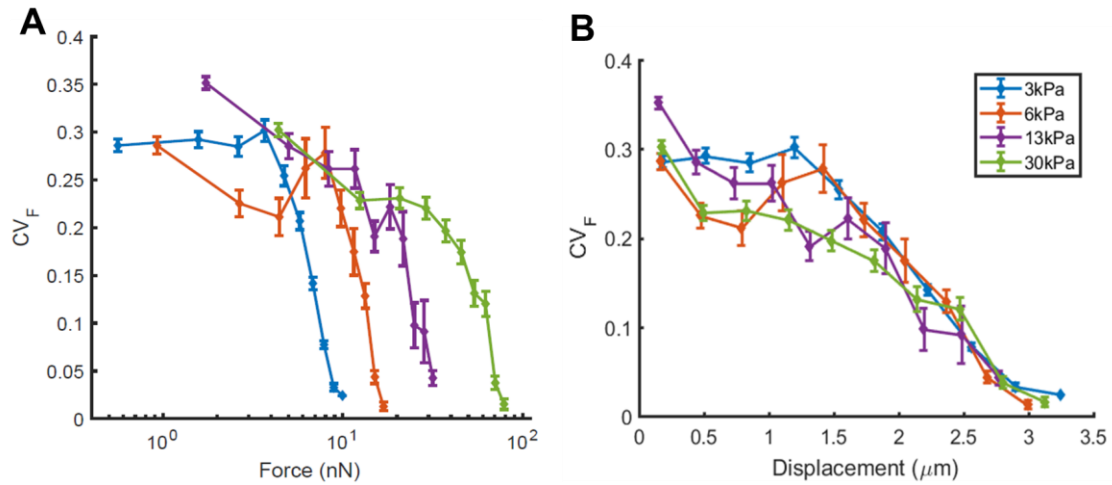
Figure 8: On all surfaces, BVSMC FA forces of greater magnitude are less variable.

FA forces on all 4 different stiffness surfaces are grouped into 10 equal sized bins each by force magnitude. The average CV_F of each bin is plotted with respect to their force magnitudes (A) and dot displacements (B). BVSMCs show higher FA force ranges on stiffer surfaces, while the dot displacements remain in the similar range. Additionally, the level of fluctuation showed a similar relationship with displacement on all stiffness surfaces. Error bars represent standard error. (blue: 3.6 kPa; orange: 6.7 kPa; purple: 13.6 kPa; green: 30 kPa)
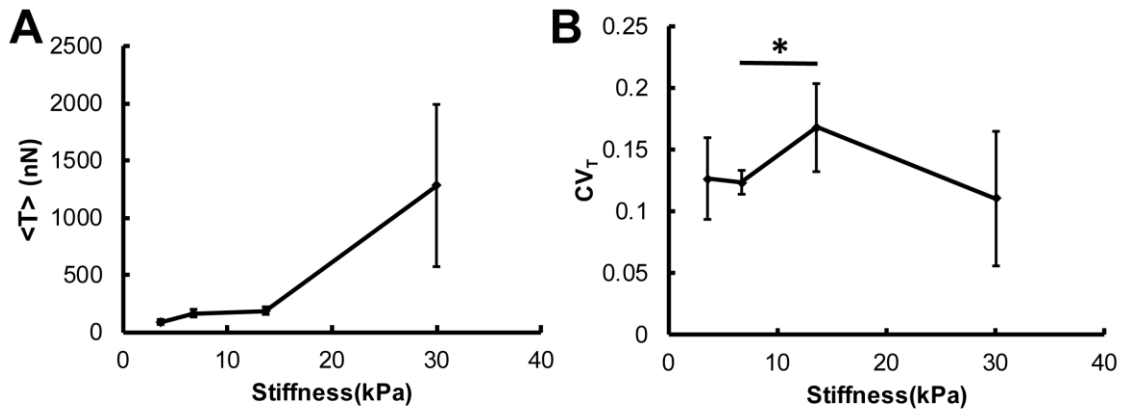
Figure 9: The mean strength of the traction field in **BVSMCs increases with stiffer surfaces, but the traction field are less stable on surfaces stiffer than 6.7kPa.** Time-averaged of the strength of the traction field ($\langle T \rangle$) systematically increases with increasing substrates stiffness (A), whereas the coefficient of temporal variation of the strength of the traction field (CV_T), does not change systematically with increasing substrate stiffness (B). Error bars represent median absolute deviations. All groups have significantly different sums of traction from each other (not marked in graph) (* Mann-Whitney U test, $p < 0.05$). ($n = 43$, 13, 14 and 15 cells in increasing order of stiffness)

4.2.2   Effects of substrate stiffness on traction dynamics of BAECs

We next evaluated the impact of substrate stiffness on BAECs to determine whether the substrate stiffness-dependent characteristics observed in BVSMCs are universal or cell-type specific. Endothelial cells also exhibited more engaged FAs on stiffer substrates, but the significant change happened on 13.6 kPa gel and the increase was not as steep as in BVSMCs (Fig. 7A vs. Fig. 10A). Another trend consistent with BVSMCs was the increasing magnitude of FA forces with increasing stiffness (Fig. 7B vs. Fig. 10B). The fraction of surviving FAs also decreased rapidly with increasing observation time in BAECs (Fig. 10C). However, the lifetime distribution of FA forces was much less dependent on substrate stiffness than it was for BVSMCs (see Fig. 7C vs. Fig. 10C).

Higher FA traction forces in BAECs were associated with lower CV_F overall (Fig. 11A). However, different from the BVMSCs, the highest FA forces on stiffer substrates had higher values of CV_F, suggesting that FA force regulatory mechanisms break down or do not function in BAECs under the very highest mechanical loads (Fig. 11A). Additionally, BAECs showed similar ranges of displacements on 3.6 kPa and 6.7 kPa surfaces, while showing a smaller range of displacement on the 13.6 kPa surface. CV_F followed the same trend with increasing displacement on the two lower stiffness surfaces as well, while on 13.6 kPa surface CV_F decreased faster with increasing stiffness compared to the other two surfaces (Fig. 11B).

On the whole-cell length scale, BAECs did not respond to increasing of substrate stiffness the same way BVSMCs did. While stiffer substrates induced increased $\langle T \rangle$ (Fig.

9A), the increase was only significant between 3.6 and 6.7 kPa stiff gels., whereas 13.6 kPa stiff gel exhibited a similar level of $\langle T \rangle$ as 6.7 kPa stiff gel (Fig. 12A). Furthermore, CV_T of BAECs systematically decreased with increasing substrate stiffness (Fig. 12B), which was different from the behavior observed in BVSMCs (Fig. 9B).
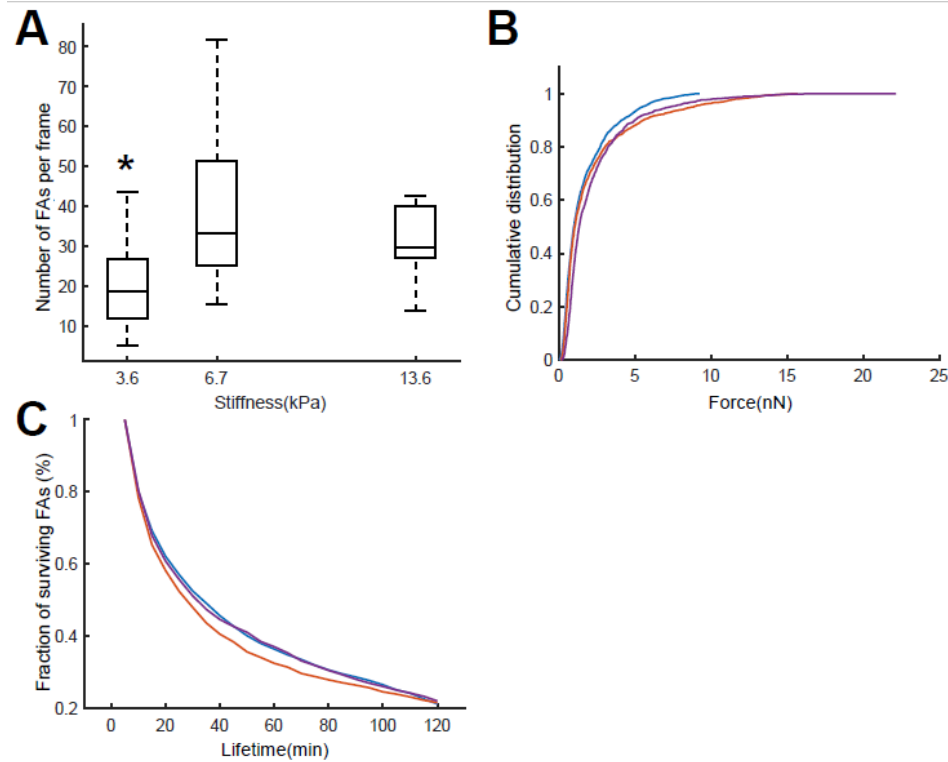
Figure 10: BAECs have more engaged FAs and higher FA forces on stiffer surfaces, but the difference is FA lifetime distribution is minimal. The average numbers of engaged FAs over 2 h (25 frames) are plotted against substrate stiffness (A). The average number of FAs of each group in increasing stiffness order are as follows: 20, 39 and 32. FA number of 3.6 kPa group is significantly different from the other two stiffness. (* 2-sample Kolmogorov-Smirnov test, $p < 0.05$). Cumulative distribution of FA force magnitudes (B) are all significantly different from each other, but FA lifetime distributions (C) only showed significant difference between 6.7 kPa and 13.6 kPa. (blue: 3.6 kPa; orange: 6.7 kPa; purple: 13.6 kPa) (n = 49, 20, 16 cells and 2134, 1789, 1099 FA forces tracked for 3.6 kPa, 6.7 kPa and 30 kPa substrates respectively; numbers of independent experiments are 7, 3 and 2 in increasing order of stiffness).
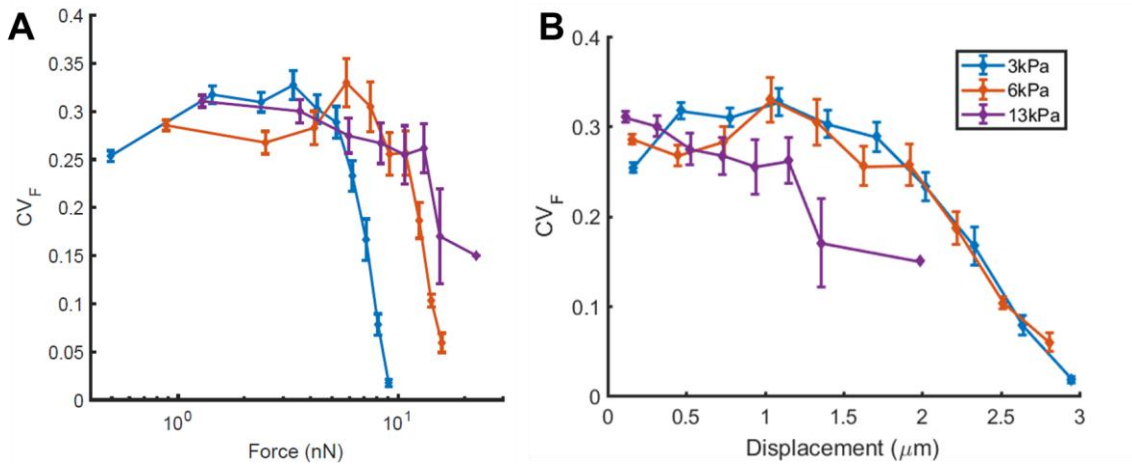
Figure 11: Traction FA forces of greater magnitude in BAECs are less variable, and stiffer substrates cause higher variability in larger forces. FA forces are sorted into 10 bins by magnitude. Average CV_F of each bin is plotted against the force magnitudes (A) and dot displacements (B) of that bin. BAECs showed higher ranges of FA forces on stiffer surfaces, and similar displacement ranges between 3.6 kPa and 6.7 kPa substrates. Fluctuations levels for FA forces on those two surfaces also appeared similar. Error bars represent standard error. (blue: 3.6 kPa; orange: 6.7 kPa; purple: 13.6 kPa)
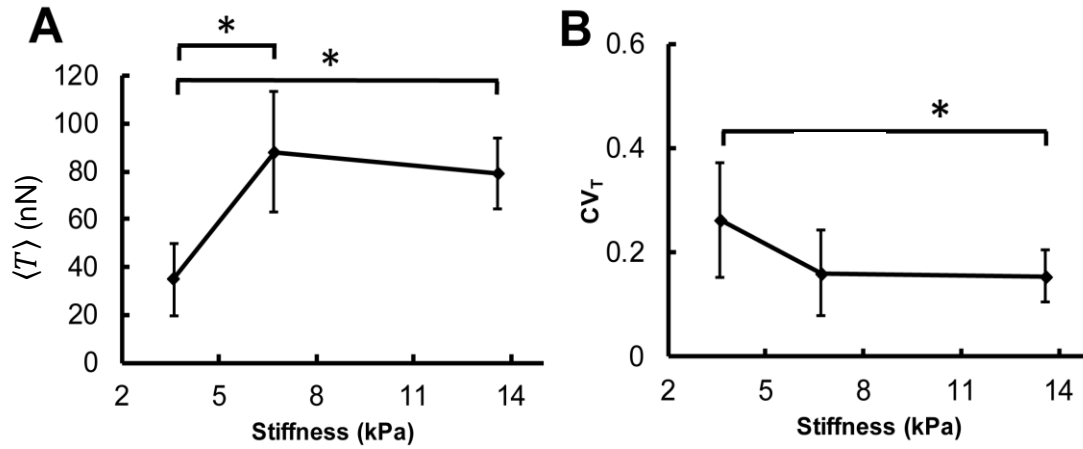
Figure 12: Time-averaged sum of traction forces ($\langle T \rangle$) in BAECs does not exhibit a systematic increase with increasing substrate stiffness, but its temporal fluctuations decrease with increasing stiffness. $\langle T \rangle$ is significantly greater on the 6.7 kPa and 13.6 kPa stiff substrates than on the 3.6 kPa stiff substrate (A), whereas the coefficient of temporal variation of the traction field (CV_T) systematically decreases with increasing substrate stiffness (B). Error bars represent median absolute deviation. (* Mann-Whitney U test, $p < 0.05$). (n = 49, 20 and 16 cells in increasing order of stiffness)

4.4   Discussions

Substrate stiffness is well established in its capacity to regulate numerous cell functions, including contractility. In fact, the two form a feedback loop between the cytoskeleton and the substrate. Cells require cytoskeletal contractions to generate traction forces in order to probe substrate stiffness, and the substrate stiffness affects the contractility of the cell. Since traction forces arise in response to internal stress generation by the cell's contractile machinery, variability of the traction field provides a direct insight into tensional homeostasis. However, exactly how stiffness regulates traction force generation has not been thoroughly explored across length scales. In this study, we examined the effects of substrate stiffness on tensional homeostasis by measuring cellular traction force dynamics at the FA level and at the whole cell level in BVSMCs and BAECs. Our results revealed that with increasing substrate stiffness temporal fluctuations of the traction field attenuated in BAECs and not in BVSMCs. This, in turn, suggests that the effect of substrate stiffness on tensional homeostasis is cell type-dependent. Specifically, stiffer substrates promote tensional homeostasis in BAECs and are detrimental to tensional homeostasis in BVSMCs. Substrate stiffness also had an effect on fluctuation on the FA level. We found that the response of individual FA force dynamics to substrate stiffness could be different even if cellular level changes seemed similar. Taken together, these results are novel findings.

We investigated the effect of substrate stiffness on traction dynamics and on tensional homeostasis on two length scales at the same time – the individual FA level and the whole cell level. At the FA level, tensional homeostasis can be interpreted as the

stability of the force magnitude generated by a single FA. Substrate stiffness has known impact on FAs. It can influence FAs in a number of aspects, including their number, size, lifetime, magnitude of traction force, spatial distribution, and lifetime of the FA structure. Some of these factors are more well-studied than others. In our study, we found that the average CV_F was highest on 13.6 kPa stiff substrates for both BAECs and BVSMCs (data not shown). For BVSMCs, our comparison groups included 30 kPa stiff substrates, where the average CV_F was lower than on 13.6 kPa stiff gels, which was consistent with the observations of Plotnikov et al (2012). However, we did not observe higher FA force fluctuations on substrates with stiffnesses lower than 8.6 kPa in either BVSMCs or BAECs. We posit that these differences should not be overlooked, as general conclusions regarding stiffness sensing may be specific for a given cell type and not generally applicable across other cells. For example, physiological conditions that lead to increased vascular stiffness, such as the normal aging process, may cause instability in endothelial contractile dynamics as FA forces increase towards this upper region of forces that are highly variable (Fig. 11, 13.6 kPa group). These data also necessitate future consideration of both FA force and lifetime when considering FA mechanics, as we show that both factors can impact FA force fluctuations at least in some cell types.

Additionally, on the FA scale, we found that the fluctuations of FA forces exhibit a consistent relationship with substrate displacement on different stiffnesses (Fig. 8B and 11B). It has been long debated whether the governing factor of cells' responses to stiffness is strain or stress. Past studies have shown contradicting results, with some demonstrating that cells maintain constant traction stress (Freyman, Yannas, Yokoo, &

Gibson, 2002) and others showing that they maintain constant strain on the substrate (Ghibaudo et al., 2008; Saez, Buguin, Silberzan, & Ladoux, 2005; Trichet et al., 2012). Yip and colleagues proposed that cells maintain constant strain on softer surfaces and switches to keeping a consistent level of stress on stiffer surfaces (Yip et al., 2013). Their observations showed a cut-off stiffness of around 20 kPa for fibroblasts. Our observation showed that BVSMCs maintained the same levels of substrate displacement on stiffnesses ranging from 3.6 kPa to 30 kPa, and BAECs maintained constant displacement on 3.6 kPa and 6.7 kPa surfaces. BAECs started to show lower ranges of displacements on 13.6 kPa surfaces, possibly due to limits of acto-myosin force generation. Moreover, we found that when cells showed a consistent level of displacement on varying surfaces, the FA traction fluctuations also showed a similar relationship with displacement. This suggested that the mechanism of traction fluctuation could have been governed by substrate deformation on those stiffnesses as well.

As we move up in length scale, cell level dynamics are calculated by first grouping the FA forces by cell and finding their collective profile over time. The question of how the FA traction dynamics contribute to the overall traction field dynamics and tensional homeostasis at the whole cell level on different substrate stiffness remains unanswered. To address this problem, we analyzed both cellular traction field fluctuations and FA traction force fluctuations. Our results showed that variability of the traction field, CV_T, was affected by factors other than variability of FA forces, CV_F. These data support the claim that studies of individual FAs in a single cell type may be insufficient for generating a mechanistic understanding of cellular tensional homeostasis

at a given stiffness. The following are our considerations for several contributing factors.

4.4.1   Mechanistic Considerations

Li et al. (2019) recently carried out a theoretical study where they identified several factors that may explain differences between CV_T and CV_F behaviors. One major factor affecting CV_T is the number of FAs. Based on the central limit theorem, which assumes that force fluctuations are independent (i.e., uncorrelated over the observation time), one would predict that CV_T would decrease with increasing number of FAs following an inverse squarer-root dependence. We found, however, that FA forces were correlated and that this correlation is affected by substrate stiffness (Fig. 13). The temporal correlation between FA forces may be explained by the tendency of all traction force vectors within a cell to be at mechanical equilibrium at all times. Consequently, perturbation that alters magnitude and/or direction of one force vector must be accompanied by simultaneous readjustment of all other force vectors in order to maintain equilibrium. As a result of positively correlated FA forces, CV_T should have higher values than in the case of uncorrelated forces and should attenuate with an increasing number of FAs at a rate which is slower than the inverse square-root dependence (Li et al., 2019). Additionally, stability of FAs also influences CV_T. If FAs were stable over the entire observation time, their forces would have higher mean magnitude and smaller temporal fluctuations than forces of unstable FAs. Consequently, traction forces corresponding to stable FAs would have lower values of CV_F than traction forces of unstable FAs (Li et al., 2019).

In the context of the above considerations, we may explain some of our findings.

For example, BVSMCs had a smaller number of FAs per cell on 13.6 kPa stiff substrates than on 30 kPa stiff substrates, while FA numbers were similar on 13.6 and 6.7 kPa substrates. This would suggest that CV_T at 13.6 kPa would be equal to the CV_T at 6.7 kPa, but greater than CV_T at 30 kPa. Furthermore, stability of FAs was smallest on 13.6 kPa stiff substrates, suggesting that the corresponding CV_T would be greater than for cells on either 6.7 or 30 kPa stiff substrates. Finally, the correlation coefficient at 13.6 kPa stiff substrate is somewhat higher than at 6.7 kPa stiff substrates and considerably smaller than at 30 kPa stiff substrate. Thus, CV_T at 13.6 kPa would be greater than at 6.7 kPa and smaller than at 30 kPa. Despite these predictions, experimental data showed that CV_T at 13.6 kPa was significantly greater than at 6.7 kPa and virtually equal to CV_T at 30 kPa (Fig. 13). This, in turn, suggests that cells on 6.7 and 13.6 kPa stiff substrates have CV_T that is mainly determined by stability of FAs, whereas on 30 kPa stiff substrates, CV_T is determined by both the correlation between forces and the number of FAs.

Our correlation analysis reveals that BAECs exhibit higher values of the normalized correlation coefficients than BVSMCs for different values of substrate stiffness (Fig. 13). This is consistent with the observed values of CV_T which in BAECs are roughly above 0.2 (Fig. 12B) and in BVSMCs roughly below 0.2 (Fig. 9B). Interestingly, BAECs could achieve lower values of CV_T when they are organized in multicellular clusters, more so the bigger the cluster size is (Canović et al., 2016), partly due to a decrease in correlation between traction forces (Li et al., 2019). Since BAECs *in vivo* form confluent monolayers, then it is reasonable to expect that it could be easier for cells to achieve a reduction in temporal variability of their traction field, and therefore the

state of tensional homeostasis, at a multicellular level than at a single cell level.

Finally, FA force dynamics are likely fundamentally dependent on the integrin profile used to engage the substrate. Cell type-dependent differences in the integrin profile available to adhere to our Fn dot patterns will likely have a direct impact on FA force fluctuations, and this hypothesis lends itself to future investigations that use substrates of different ECM compositions. This is further supported by past studies that found the types of ECM protein substrate influenced whole cell level response to stiffness. Sazonova et al. (2015) observed that SMCs increased spread area on stiffer Fn substrate and decreased spread area on stiffer laminin substrate. Gershlak et al. (2013) found that the spread area and contractility of mesenchymal stem cells were both impacted by the components and ratio of heart ECM protein substrates. It would be worthwhile to extend the study down to FA level responses.
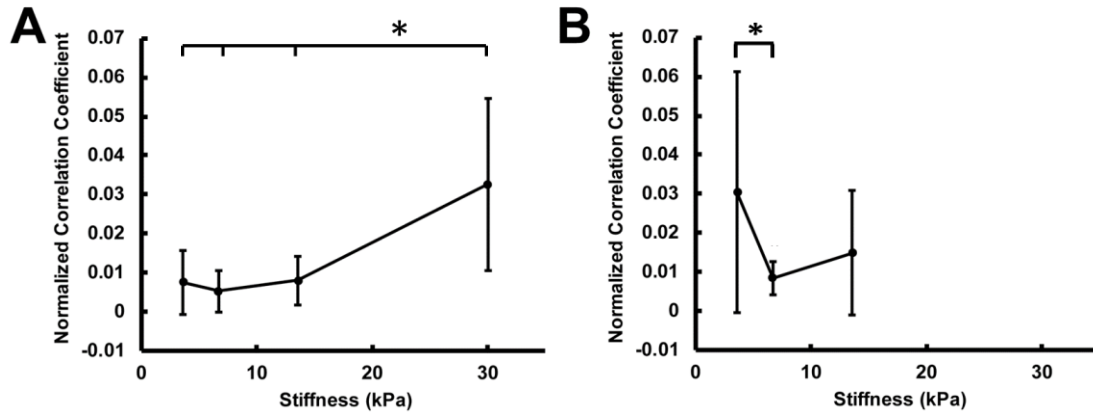
Figure 13: Correlation between FA forces for both BVSMCs and BAECs are affected by substrate stiffness. Normalized Pearson correlation coefficients of cells are plotted against substrate stiffness (A: BVSMCs; B: BAE Cs). The correlation coefficient of BAECs cultured on the 6.7 kPa stiff substrate is significantly different from the correlation coefficient BAECs cultured on the 3.6 kPa stiff substrate; the correlation coefficient of BVSMCs cultured on the 30 kPa stiff substrate is significantly different from the correlation coefficient of BVSMCs cultured on 3.6, 6.7, and 13.6 kPa stiff substrates. (* 2-sample Kolmogorov-Smirnov test, $p < 0.05$).

4.4.2   Limitations

Several limitations of our approach are noteworthy. First, in tracking individual

FAs, we were in fact tracking FA forces. By our definition, if the force applied at an FA

dropped below the 0.3 nN experimental threshold (Polio et al., 2012), we considered that

particular FA was inactive. However, it is possible for the FA structure, or the adhesive

plaque of proteins on the intracellular side of the FA, to remain at least momentarily

without a measurable force to the substrate. This could have skewed the measured

lifetime of FAs. Second, the Fn dot pattern used in MTM spatially restricted where FAs

can form. Nevertheless, this had little effect on the observed traction force distribution

according their magnitude (i.e., large forces near the edges and small forces in the

interior), since similar distribution was observed previously, where traction forces were

measured on soft substrates with continuous coating of ECM proteins and where FA

formation was not constrained (Balaban et al., 2001; Butler et al., 2002; Dembo & Wang,

1999). Third, naturally formed FAs acquire elongated shapes (Stricker, Aratyn-Schaus,

Oakes, & Gardel, 2011; Zimerman, Volberg, & Geiger, 2004) and, based on the

observations of Plotnikov and colleagues, the peak of traction can either be at the

midpoint of their length or closer to the cell edge (distal) end of the FA (Plotnikov et al.,

2012). The position of the peak was also correlated with the tugging behavior of the FA

force, where the closer the peak was to the distal end of the FA, the higher the ratios of

tugging forces were found (Plotnikov et al., 2012). However, we assume that the peak of

the FA traction force is always located at the geometric center of each Fn dot when

calculating traction. Finally, as a scalar metric of the strength of the traction field we

used the sum of magnitudes of traction force vectors (*T*). This metric did not take into account differences in cell shapes nor the vector nature of force. In that regard, a more appropriate metric would be the traction moment (i.e., the first moment of the traction field) that we used in our previous studies (Canović et al., 2016; Zollinger et al., 2018). We carried out data analysis using the traction moment metric and found no qualitative difference in the data behavior when we used the strength of the traction field metric.

4.4.3 Summary

In conclusion, this aim provided insights on the effects of substrate stiffness on the traction dynamics and tensional homeostasis of BAECs and BVSMCs from both the FA level and the whole cell level. Our results demonstrated that substrate stiffness affected FAs' number, stability, force magnitude, fluctuations, and correlation between FA forces. Together, all these factors contributed to cell type-dependent changes in cellular traction dynamics, and resulted in less homeostatic BVSMC cell tension on stiffer substrates and the opposite in BAECs. Future studies of stiffness-dependent biomechanics of cells should focus on holistic metrics of FA behavior that are assessed from a single FA to whole cell dynamics. Furthermore, it is conceivable that these attributes of FAs also play a major role in multicellular ensembles of cells that are critically important to study due to the addition of cell-cell adhesion molecules in their mechanical stability. Likewise, our study suggests that the types and distribution of integrins, which vary from cell type to cell type, may have a major impact on stiffness-dependent biomechanics. This understanding across length scales is necessary to fully understand how matrix stiffness impacts tensional homeostasis in healthy conditions and,

more importantly, in pathological conditions such as cancer or vascular aging where environmental stiffness is altered.

Chapter 5: THE ROLE OF CADHERIN IN TENSIONAL HOMEOSTASIS

This chapter deals with Specific Aim 2: **To investigate the impact of cell-cell adhesion via cadherin on tensional homeostasis of isolated gastric carcinoma cells and of multicellular clusters of those cells**.

5.1   Background

Cells rarely act in isolation in the body. Cell-cell adhesion molecules mechanically couples neighboring cells, so that the action of individual cells translate into tissue-level behaviors. When cells form of a multicellular cluster, it creates both mechanical and biochemical conditions for changes in cellular tension. From a mechanical point of view, the presence of cell-cell contacts changes the cells' state of force balance. In the absence of cell-cell contacts, mechanical equilibrium demands that cell-substrate traction forces must be balanced at every instant. If cells form confluent clusters, cell-substrate traction forces are also balanced at the cluster level, but not necessarily at the individual cell level. The reason is that cytoskeletal tension within a cell is partly transmitted to the substrate and partly to the adjacent cells. Thus, mechanical equilibrium of a single cell within a cluster demands that cell-substrate traction forces and cell-cell traction forces acting on the cell are balanced at every instant (Trepat et al., 2009). Because traction forces in a cluster are not balanced at the individual cell level, there exists a residual tension build up in the cluster from the cluster boundary, where cluster forces are greater, to the cluster interior, where the cluster forces are smaller. The unbalanced portion of traction forces is transferred from the boundary cells towers the interior cells causing the tension buildup within cells. This buildup increases

with increasing number of cells in the cluster until it eventually plateaus (Tam, Smith, & Stamenović, 2017; Trepat et al., 2009). This, in turn, becomes detrimental for tensional homeostasis, since the tension buildup is associated with increasing temporal fluctuations of the cytoskeletal tension (Tam et al., 2017). On the other hand, multicellular clusters tend to have larger spread area than single cells, which means they could form more FAs on the substrate, and an increasing number of FAs would lead to reduction of tensional fluctuations for the reason explained in the previous chapter. Thus, there are two competing influences on tensional homeostasis in confluent multicellular forms.

In addition to the mechanical aspects of force transmission via cell-cell junctions, biochemical signals can also be a factor in multicellular clusters. The force transduction between cells in a cluster relies on transmembrane proteins that couple neighboring cells at cell-cell junctions. Cadherin is a family of Ca^{2+} ion-dependent transmembrane protein that has been shown to bear force at adherens junctions (Chen, Tan, & Tien, 2004; Gomez, McLachlan, & Yap, 2011). The force-sensitivity of cadherin junctions and downstream signaling are linked to cytoskeleton organization and basic cell function such as cell spreading and proliferation (Caveda et al., 1996; Chen et al., 2004). There are also mounting evidence of cross-talk between cadherin junctions and FAs (Levenberg et al., 1998; Nelson et al., 2004; Ryan et al., 2001). For these reasons, we consider cadherin a prime candidate for impacting tensional homeostasis.

Our recently study revealed that tensional homeostasis is a cell-type dependent phenomenon. Certain cell types, like fibroblasts and BVSMCs, exhibited no significantly different levels of traction field temporal fluctuations in single cells and in clusters,

whereas other cell types, like BAECs, exhibited significantly lower traction field fluctuations in multicellular clusters than in single cells (Zollinger et al., 2018). Based on those observations, we hypothesized that cadherin adherens junctions played a role in achieving tensional homeostasis in cells that exists in monolayers *in vivo* and form barrier functions that are dependent on the integrity of cell-cell junctions. To test this hypothesis, we used gastric adenocarcinoma (AGS) cells transfected with WT E-cadherin and Mock vectors as models for healthy epithelial cells and epithelial cells with no E-cadherin expression respectively. The results showed that E-cadherin expression stabilized cell traction in both clusters and single cells, suggesting that E-cadherins are important for achieving tensional homeostasis (Zollinger et al., 2018). Following in the direction indicated by this new evidence, we look further into the molecule E-cadherin by examining AGS cells with mutated E-cad.

5.1.1   E-cadherin

For epithelial cells, their predominant cadherin subtype is E-cadherin (E-cad). Cell-cell contacts via E-cad are linked to actin cytoskeleton and are also subjected to and respond to forces between cells. Thus, they are thought to contribute to homeostasis between cells and their microenvironment (Provenzano & Keely, 2011). Here we examine the role of E-cad in tensional homeostasis of gastric carcinoma epithelial (AGS) cells in the presence/absence of E-cad, or whose E-cad junctions are mutated.

E-cad is the calcium-dependent cell-cell adhesion protein on epithelial cells. It is generally considered the prototype of all cadherins because of its early identification and its thorough characterization, both in normal and in pathological conditions (Roy & Berx,

2008). The mature E-cad molecule consists of a single transmembrane domain, a cytoplasmic domain and an extracellular domain that contains five so-called extracellular cadherin repeats (EC1 to EC5). Unlike the other cadherin repeats, EC5 contains conserved cysteines that form disulfide bridges which affects formation of cell-cell contact (Ozawa, Hoschützky, Herrenknecht, & Kemler, 1990). For this reason, EC5 is also sometimes referred to as the membrane proximal extracellular domain (MPED) (Nollet, Kools, & van Roy, 2000; Roy & Berx, 2008). The cytoplasmic domain of E-cad can be further divided into two subdomains: juxtamembrane domain and β-catenin binding domain (Roy & Berx, 2008). Juxtamembrane domain binds with p120-catenin at the plasma membrane, which stabilizes the E-cad complex and prevents entry of E-cad into degradative endocytic pathways (Davis, Ireton, & Reynolds, 2003; Ireton et al., 2002). E-cad anchors F-actin indirectly through the β-catenin binding domain, or the intracellular domain. Through connection with β-catenin/αE-catenin, the E-cad complex is coupled with the force generating actomyosin network in the epithelial cell (Hartsock & Nelson, 2008).

Normal function and expression of E-cad is critical for epithelial tissue homeostasis. Loss of E-cad contributes to cancer metastasis (Stemmler, 2008). One of the most studied case of cancer involving E-cad alterations is the hereditary diffusive gastric cancer (HDGC), where CDH1 germline gene mutation or deletion results in E-cad inactivation (Figueiredo et al., 2013). In the context of this chapter, HDGC-related E-cad mutants are used to model the pathology of epithelial tensional homeostasis in gastric

cancer. We use AGS cells as a model because E-cad is known to be significantly downregulated in gastric cancer (Carneiro et al., 2012; Chan, 2006)

5.1.2 *AGS Cell Lines*

Our collaborators from the Seruca lab, from the Institute of Molecular Pathology and Immunology of the University of Porto, Portugal, kindly provided AGS cells transfected with either wild-type E-cad (WT-Ecad), a hereditary diffusive gastric cancer (HDGC) related E-cad mutant, or a mock vector. The E-cad mutants come in two types: extracellular mutant A634V and intracellular mutant V832M (Figueiredo et al., 2013) (Fig. 14).
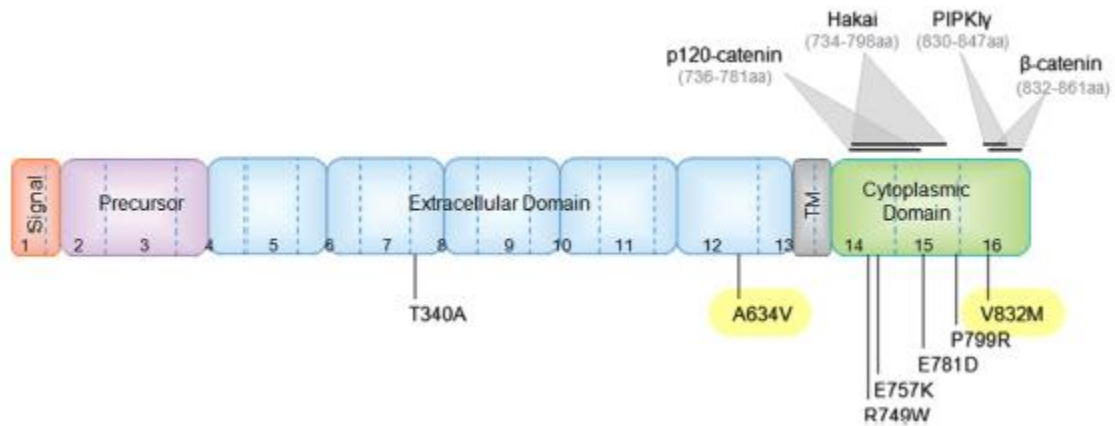
Figure 14: Illustration of the locations of E-cad missense mutations. The yellow-highlighted mutations are used in the experiments described in this chapter. Diagram also shows the biding regions of E-cad binding partners in the cytoplasmic domain (Figueiredo et al., 2013)

5.2   Experimental Design

AGS cells were plated onto a micropatterned PAA gel. Patterned dots were comprised of a protein mix of fibronectin and vitronectin (MTI GlobalStem), where each were present at 0.125 mg/mL. This combination was shown to be more suitable for adhesion of these cells than a single protein (data not shown). Both protein concentrations used were well above previously described concentrations of ~0.05 mg/mL needed for saturating levels of protein (Kalaskar, Downes, Murray, Edgar, & Williams, 2013). The pattern was made up of 2 μm dots at 6 μm center-to-center separation.

Because of their cancerous phenotype, AGS cells express no endogenous E-cad (Carneiro et al., 2012; Chan, 2006). AGS cell lines transfected with wild-type (WT) E-cad, E-cad with point mutations (extracellular and intracellular) or an empty vector (Mock), where the cells do not express E-cad, are seeded on patterns of mixed Fn and vitronectin (Vtn). To demonstrate the transfection, immunofluorescent staining was done on AGS cells transfected with Mock and WT E-cad vectors (Fig. 15). The staining showed no native E-cad expression in Mock transfected cells and that transfected WT E-cad is located at the cell-cell junctions at high concentration as expected (Fig. 15) (Zollinger et al., 2018). Cells and grid are imaged for traction measurements every 5 min for 1 h. Due to the volume of experiments under this aim, we chose 1 h as the time frame instead of 2 h. We found no difference in behavior between the first and second hour of experiment with any cells in our previous experiments. Tractions of both single cells and clusters are measured using MTM.

Cluster is defined as any cell structure that contains more than one cells. For a

cluster to be included in the data set, there must be no new cell joining or leaving (including mitosis and/or death) the cluster during the period of imaging. Additionally, the entire cluster must be contained within the field of view, and the cluster must remain a solid shape (no empty holes in the middle of the cluster).
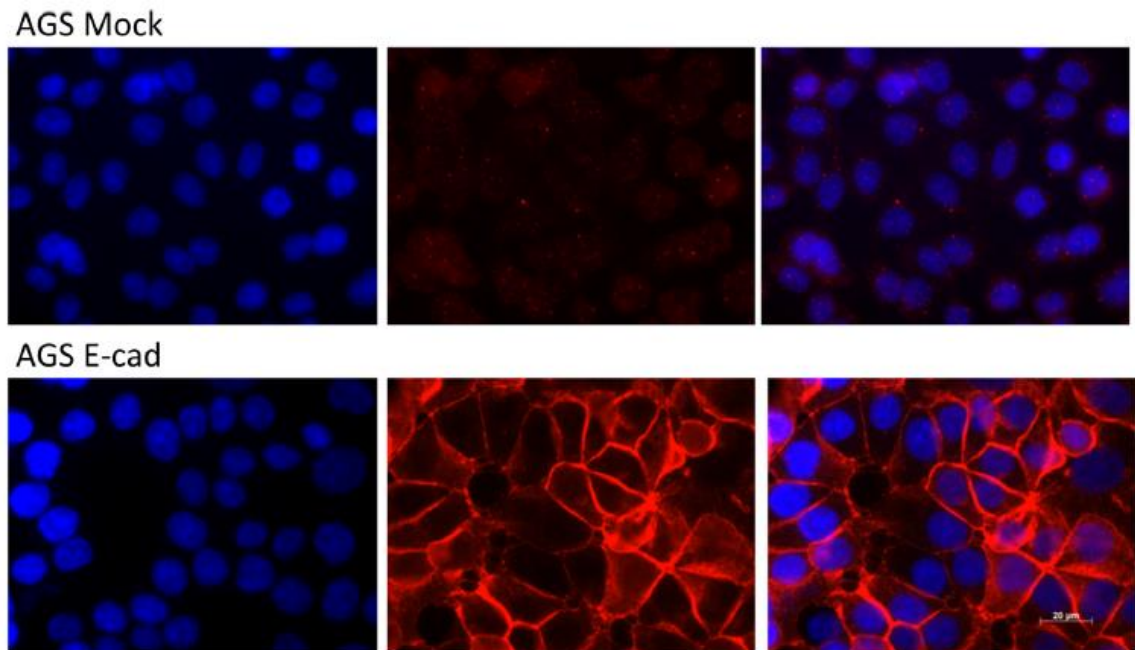
Figure 15: Immunofluorescent stains of nuclei (blue) and E-cad(red) in AGS Mock and AGS WT E-cad cells. The AGS Mock cells display negligible levels of E-cad, while the AGS WT E-cad cells show high levels of E-cad localized to the cell membrane at cell-cell junctions as expected. (Courtesy of Joana Figueiredo, Ph.D.) (Zollinger et al., 2018)

5.3   Results

We measured traction forces for single cells and clusters for all AGS cell lines (Fig. 16). The sum of traction force magnitudes (T) are quantified and fluctuation of T normalized to its time-average ($\langle T \rangle$) is also calculated for all cell lines for both single cells and clusters (Fig. 17).

AGS cells transfected with different E-cad variants or the empty mock vector generated different levels of $\langle T \rangle$ on their substrate (Fig. 18). The $\langle T \rangle$ of extracellular mutant transfected cells is significantly higher than that of the WT E-cad transfected cells. The Mock cells had significantly lower $\langle T \rangle$ compared to all the other three groups of single cells. The traction field profile agrees with Seruca group's finding comparing the adhesiveness of AGS cell lines on different protein substrates. They found that extracellular mutants were the most adhesive on Fn and Vtn substrate (Unpublished data). As expected, $\langle T \rangle$ of clusters is significantly higher than $\langle T \rangle$ of individual single cells. Due to the different number of cells in the clusters, a fair comparison cannot be directly drawn across the cluster groups of the cell lines. Instead, we calculated the $\langle T \rangle$ per cell in a cluster. Mock cell clusters displayed significantly lower $\langle T \rangle$ per cell compared to the three other groups; and the intracellular mutant clusters showed significantly higher $\langle T \rangle$ per cell compared to WT E-cad transfected cells (Fig. 18).

Comparing CV_T of single cells and that of clusters is one way of assessing whether cell-cell contact is a requirement for tensional homeostasis. The clusters of each cell line range from containing 2-14 cells. We observed that isolated WT E-cad, intracellular mutant and mock vector transfected cells all showed significantly higher CV_T

compared to clusters (Fig. 19). This is qualitatively consistent with the previous observations in endothelial cells (Canović et al., 2016). However, AGS cells transfected with extracellular mutants do not exhibit the same behavior, but instead showed similar level of fluctuations in both single cells and in clusters.

Different variant of E-cad clearly had an effect on the traction level and tensional homeostasis of AGS cells, even though tractions on the substrate are measured through integrin-substrate interactions. Comparing the WT E-cad cells and the Mock cells, the latter had significantly higher CV_T in isolated cells and in clusters. In cells transfected with mutated E-cad, the effects of the mutation on tensional homeostasis is dependent on the location of the mutation. Intracellular mutant transfected cells exhibit significantly lower CV_T in clusters compared to isolated cells similar to WT E-cad and Mock cells. Extracellular mutant transfected cells, however, showed similar values of CV_T in clusters and in isolated cells. This suggests that the extracellular mutation of E-cad may have negatively affected the way tensional homeostasis is achieved in clusters. Additionally, intracellular mutant transfected cells showed significantly higher fluctuation in isolated cells compared to all the other groups (Fig. 19). This suggests that while intracellular mutation did not affect tensional homeostasis in clusters, it did cause disturbance in homeostasis in isolated cells.

The correlation analysis on the AGS cells revealed that cells with mutated E-cad generally showed higher correlation of FA forces in single cells. WT E-cad and Mock vector transfected cells exhibited correlation coefficient of around zero, which means that FA traction forces were not correlated. There was statistically significant difference

between the correlation coefficients of single extracellular mutant cells and single Mock

cells. All clusters exhibited positive correlation between forces. WT E-cad transfected

clusters showed significantly higher correlation compared to intracellular mutant clusters

(Fig. 20). The distribution of the correlation coefficient for all the groups (signified by the

error bars) are quite large, suggesting a more diverse sample range than the other metrics

we examined. It is also worth noting that in all cell lines except the intracellular mutants,

the correlation between forces was greater in single cells than in clusters. Since CV_T was

higher in single cells compared to clusters, this suggests that the correlation between

forces was not a major determinant of CV_T in theses cell lines. Compared to BAECs and

BVSMCs we examined in Aim 1 (Chapter 4, Fig. 12), this fact about the AGS cell lines

was different from our expectations.
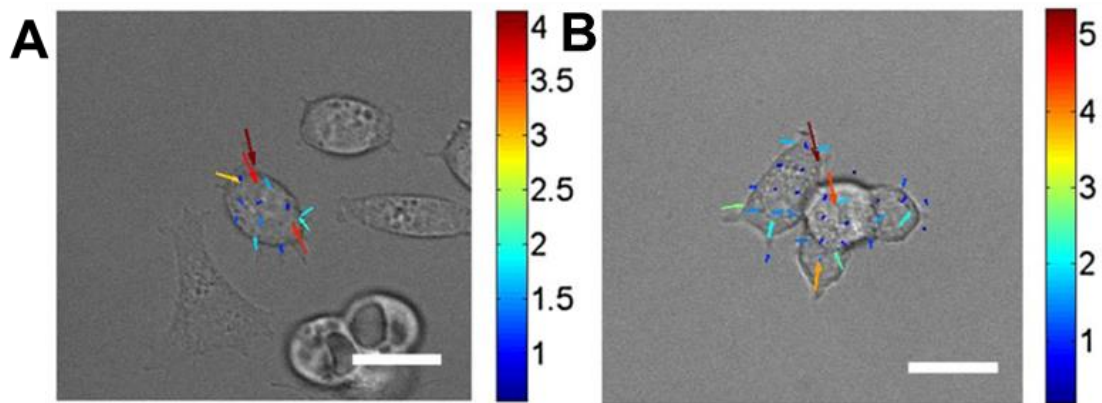
Figure 16: Representative image of AGS WT E-cad single cells are shown with MATLAB calculated traction vectors. Single (A) and 4-cell cluster (B) are shown here. Scale bar represent 20 μm. Color bar corresponds to the magnitudes of traction force vectors in nN.
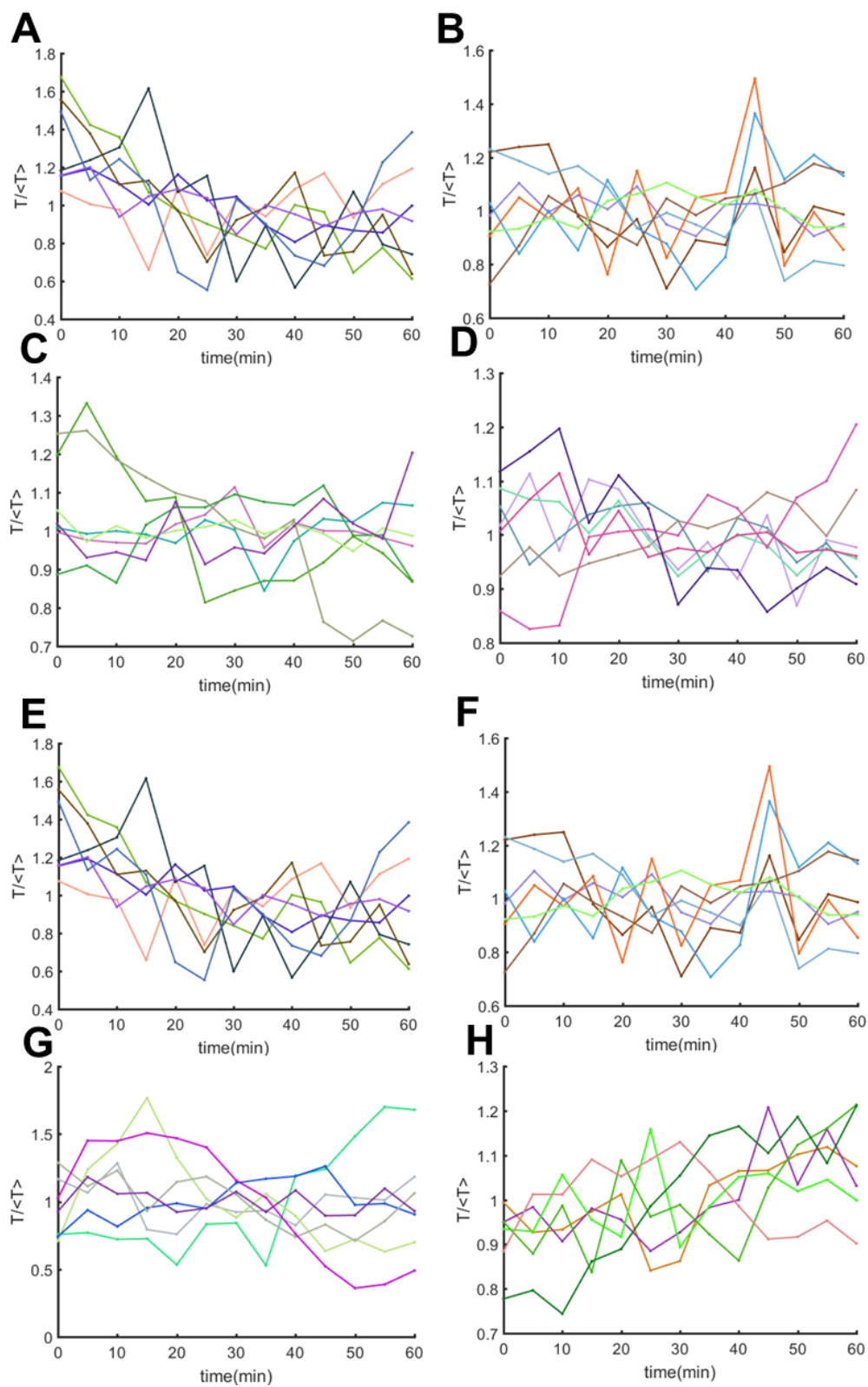
Figure 17: Time-lapses of sum of traction magnitudes (*T*) normalized to the time-averaged *T* (*<T>*) are shown for all AGS cell lines. On the left column (A, C, E, G) shows single cells and on the right column (B, D, F, H) shows 2-4 cell clusters. Cell lines include Mock (A, B), WT E-cad (C, D), extracellular mutant (E, F) and intracellular mutant (G, H) E-cad transfected cells. All graphs show representative samples within that group. Each color corresponds to a different cell/cluster.
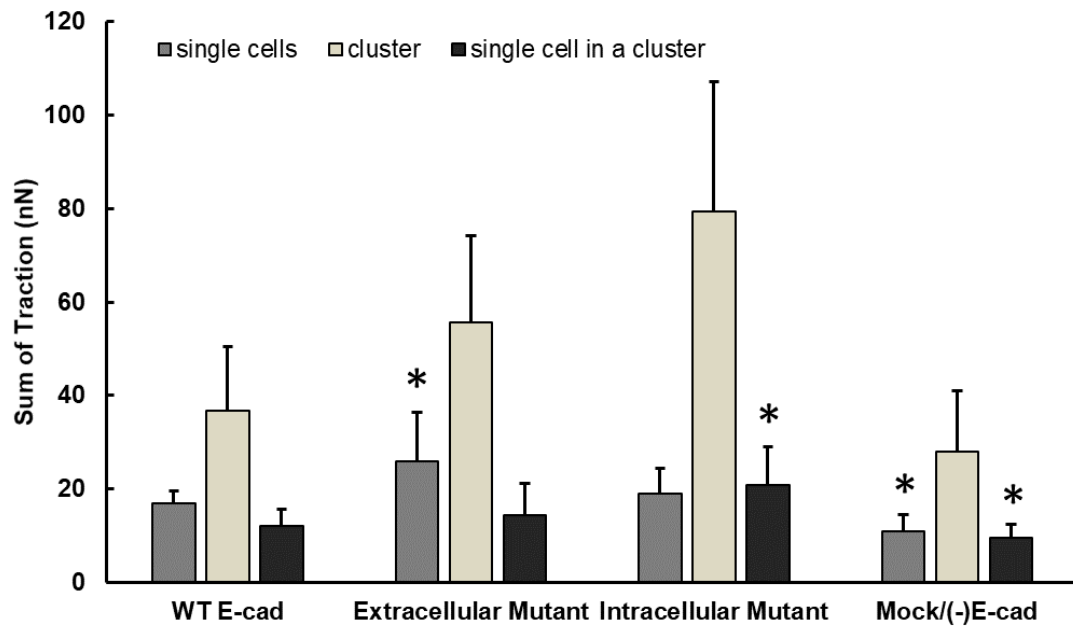
Figure 18: Gastric cancer (AGS) cells transfected with different E-cadherin (E-cad) exhibit different levels of contractility on the same fibronectin and vitronectin (Fn+Vtn) substrate. Time-averaged sum of traction force magnitude ($\langle T \rangle$) for single cells (medium grey), clusters (2-14 cells) (light grey), along with $\langle T \rangle$ per cell in a cluster (dark grey). $\langle T \rangle$ was highest in the cells transfected with an E-cad bearing an extracellular domain point mutation and lowest in the cells transfected with an empty mock vector (no E-cad expression). Extracellular mutant single cells had significantly higher $\langle T \rangle$ than the WT E-cad cells. $\langle T \rangle$ of single Mock cells and $\langle T \rangle$ per cell in a Mock cluster are both significantly lower than the rest of the cell lines. Intracellular mutant showed significantly higher $\langle T \rangle$ per cell in a cluster than the WT E-cad cells. (* Mann-Whitney U test, $p < 0.05$) (Error bars represent median absolute deviations.)
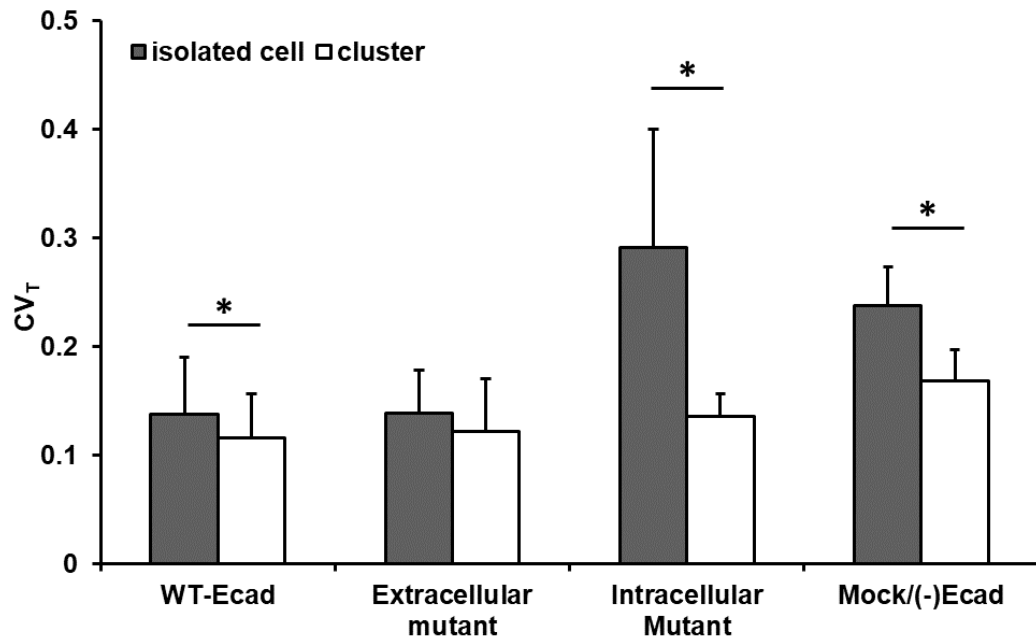
Figure 19: The coefficient of variation of the traction field (CV_T) of single cells are affected by the E-cad transfection; CV_T of clusters are attenuated in some AGS cells lines but not in others. Comparing the CV_T of single cells, intracellular mutant-transfected cells showed significantly higher CV_T in single cells than the rest of WT-Ecad cells and extracellular mutant transfected single cells, while Mock single cells showed significantly lower CV_T than the rest of the single cells ($p < 0.05$ in Mann-Whitney U test, not marked by symbol in graph). For WT E-cad, intracellular mutant, and mock (empty) vector-transfected cells, CV_T was lowered in clusters (2-14 cells). However, for extracellular mutant-transfected cells, CV_T was comparable in single cells and in clusters. (* $p < 0.05$ in Mann-Whitney U Test) (Error bars represent median absolute deviation)
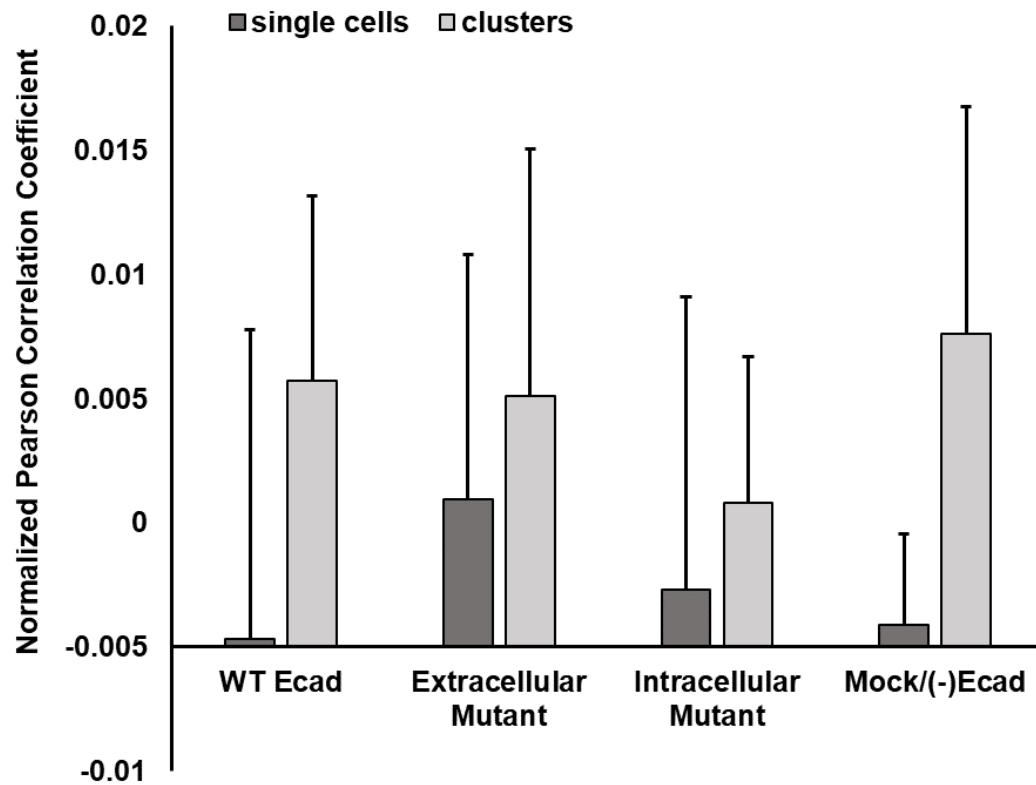
Figure 20: E-cadherin (E-cad) point mutations affect the level of correlation between FA forces in single cells and in multicellular clusters. Normalized Pearson correlation coefficient describes the level of temporal correlation between FA forces. The correlation coefficients of single cells (medium grey) and clusters (light grey) are shown. No significant differences are found between groups. (Error bars represent median absolute deviation)

5.4   Discussions

Results of our measurements indicated that E-cad junctions might play important role in the ability of AGS cells to achieve tensional homeostasis. In particular, we found that the location of the point mutation had different effects on tensional homeostasis, which suggests that different domains of E-cad have different functions in the maintenance of tensional homeostasis. The point mutation in the extracellular domain is located in the EC5 repeat (Figueiredo et al., 2013). Cells bearing the extracellular mutation showed similar levels of CV_T in single cells and in clusters unlike any other cell lines we examined. One possible reason is that the mutation interferes with E-cad homophilic binding to the adjacent cell (Perez & Nelson, 2004). Experiments using a reducing agent dithiothreitol showed that there is at least one disulfide bridge in E-cad that is important to E-cad homophilic binding (Ozawa, Hoschützky, et al., 1990). Evidence from sequence analysis showed that only EC5 had the potential to form disulfide bonds (Boggon et al., 2002). With functional cell-cell junctions in a cluster, cells are able to transfer residual unbalanced tension to neighboring cells. It is possible that the extracellular mutation resulted in malformed E-cad bindings that are thus less effective at or not able to transfer tension between cells at adherens junctions.

The intracellular mutation is located in the binding region of β-catenin (Figueiredo et al., 2013). β-catenin binds the cytoplasmic region of the E-cad and acts as the bridge between E-cad and α-catenin (Ozawa & Kemler, 1992; Ozawa, Ringwald, & Kemler, 1990; Shapiro & Weis, 2009). α-catenin is a well-established mechanosensitive protein. The unfolding of the α-catenin molecule under intracellular tension reveals

cryptic vinculin binding sites (Maki et al., 2016; Yonemura, Wada, Watanabe, Nagafuchi, & Shibata, 2010). Additionally, the binding of vinculin through α-catenin also facilitates the development of the adherens junction and stabilizes it by strengthening the connection to the actin cytoskeleton (Yonemura et al., 2010). As a result, interfering with β-catenin could indirectly interfere with α-catenin function. In our results, the cells transfected with the intracellular mutant version of E-cad exhibited hindered the cell ability to achieve tensional homeostasis in single cells, with significantly higher CV_T compared to all other cell line single cells. One might wonder why the cadherin/catenin complex matters in single cell tensional homeostasis, especially since the transduction of biomechanical signal across catenin is tension-based. In fact, the E-cad/catenin complex has been shown to be under constitutive tension even if it's not engaged in intercellular adhesion (Borghi et al., 2012). Although it is unclear what molecular mechanism happens downstream due to this constitutive tension, Borghi et al. (2012)speculated that it could play a role in the regulation of cortical cytoskeleton activity, which is directly related to tensional homeostasis.

The significance of this aim's finding may go beyond epithelial tensional homeostasis. Cadherin family is expressed widely across cell types, but in different isoforms and at different levels. It is possible that cadherin's role in tensional homeostasis is responsible for or contributes to the cell-type dependency we observed in tensional homeostasis. While E-cad is the main cell-cell adhesion protein in epithelial cells, endothelial cells predominantly express VE-cadherin (Morini Marco F. et al., 2018; Vestweber Dietmar, 2008); fibroblasts express mostly N-cadherin (Matsuyoshi &

Imamura, 1997); and vascular smooth muscle cells has been shown to express N-, R- and T-cadherins (Moiseeva, 2001). Moreover, cadherin expression is known to be altered in some pathology cases. It was found that E-cad was expressed in 96% of atherosclerotic legions, but not in healthy intima of vessels (Bobryshev, Lord, Watanabe, & Ikezawa, 1998). Cadherin switching is also a well-established hall mark of the epithelial to mesenchymal transition that initiates cancer metastasis (Stemmler, 2008; Wheelock, Shintani, Maeda, Fukumoto, & Johnson, 2008). It involves the loss of E-cad expression and the turning on of N-cadherin expression. Interestingly, both atherosclerosis and cancer have been linked to the breakdown of tensional homeostasis. It would be interesting to find out whether that is partially related to the changes in cadherin expression.

Correlation analysis of AGS cell lines showed overall low correlations (compared to single BAECs and BVSMCs in Aim 1, Fig. 16 vs Fig. 20). The correlation coefficients also did not correlate to the level of CV_T very well (Fig. 19 vs Fig. 20). Extracellular mutant clusters showed the highest level of correlation, but only medium values of CV_T. On the other hand, Mock single cells exhibited the highest values of CV_T, but close to zero correlation coefficient. In Aim 1, we found that correlation between FA forces is a contributing factor to cell level fluctuation, but it is not the only one. In AGS cells, it appears that correlation plays a smaller part than other possible contributors (e.g., CV_F, FA stability, heterogeneity of FA forces). This could be due to the epithelial origin of these cells, or their malignant nature.

In conclusion, results from this aim supported our hypothesis that cell-cell

adhesions are important for achieving tensional homeostasis, at least in some cell types.

Through the different effects of E-cad point mutations, our results suggest that the

extracellular and intracellular domains of E-cad are both involved in tensional

homeostasis maintenance, however, they likely play different roles. Since the mutations

used in this aim were related to cases of HDGC, these novel findings may also contribute

to our understanding of gastric cancer pathology.

Chapter 6: THE EFFECTS OF STEADY SHEAR FLOW ON TENSIONAL HOMEOSTASIS

This chapter deals with Specific Aim 3**: To investigate the impact of steady shear flow on endothelial cell tensional homeostasis**.

6.1 Background

Mechanical stresses acting on the endothelium result from the simultaneous action of blood flow and pressure. These stresses activate mechanosensors, signaling pathways, and gene and protein expressions. When these stresses have a clear direction, like in the straight portion of blood vessels, they cause only transient molecular signaling of pro-inflammatory and proliferative pathways, which become downregulated when such directed mechanical stresses are sustained. As a result, vascular homeostasis is maintained through dynamic biochemical signaling changes and cytoskeleton remodeling. In contrast, when mechanical stresses acting on the endothelium have no clear direction, like for example near the branching points and in curved parts of blood vessels, where laminar flow is disturbed, they cause sustained molecular signaling of pro-inflammatory and proliferative pathways. Consequently vascular homeostasis breaks down (Chien, 2007). Disrupted endothelial homeostasis has a direct consequence on endothelial permeability, which is considered an important cause of a number of vascular diseases, such as acute edema, chronic inflammation, hypertension and atherosclerosis (Chien, 2007; Huveneers, Daemen, & Hordijk, 2015).

Here we wanted to investigate whether vascular homeostasis was closely associated with tensional homeostasis in the endothelium. For if it were, one would

expect that directed laminar shear flow applied to a monolayer of endothelial cells would attenuate temporal fluctuations of the traction field.

A few studies have measured traction forces in endothelial cells under different flow regimes. However, their results are often inconclusive or contradictory. Some groups reported a decrease in the traction magnitude (Conway et al., 2013; Steward et al., 2015), while others reported an increase in the traction in response to shear flow (Perrault et al., 2015; Shiu et al., 2004; Ting et al., 2012). Ting and colleagues also reported assembly of adherens junctions under laminar flow, and lowered tractions and disassembly of adherens junctions under a disturbed flow regime (Ting et al., 2012). Most studies report cell alignment with the direction of flow after some period of continuous flow. Some of them report such phenomenon as early as 1 h after the onset of flow (Steward et al., 2015). These studies typically apply a laminar flow that corresponds to shear stress of 10-12 dyn/cm^2 or higher (Barbee et al.,, Mundel, Lal, & Davies, 1995; Conway et al., 2013; Hur et al., 2012; Kohn et al., 2015; Steward et al., 2015; Ting et al., 2012; Tzima et al., 2005). Because of the way the traction experiments were set up, most of previous studies only reported cellular tractions at two time points, before and after the application of flow. While Perrault and colleagues. did look at time-lapsed tractions of the monolayer under flow, their focus was on the short-term responses on the order of tens of minutes to the change in the magnitude of shear flow (Perrault et al., 2015). For example, these investigators changed the magnitude of shear flow five times over 160 min of observation. Shiu *et al.* (2014) measured traction forces 30 min after the onset of flow (from static). On the other hand, Ting *et al.* (2012) exposed monolayers to 14 h of

flow before taking traction measurements.

In this study, we obtained metrics of tensional homeostasis (i.e., the coefficient of variation) in monolayers of endothelial cells exposed to steady shear flow of different magnitudes over the same time regime that we used in our previous aims – namely traction measurements at 5 min intervals over 2 h. For comparison, we also measured tensional homeostasis in isolated endothelial cells under the same flow conditions. The 2 h time frame allowed us to see not just the short-term response to the onset of flow, but also the long-time behavior of the monolayer or single cells after biochemical signaling has adjusted to the sudden onset of the flow. The reason for this is that in real physiological conditions, it is rare for flow conditions to change drastically, like the way we turn on and off artificial flow. For these experiments, we designed a system that would combine traction force measurements using MTM with shear flow measurements in a flow chamber.

6.2   Experimental Design

6.2.1   Design of Flow Chamber MTM

For this aim, we developed a technique to measure traction forces under tunable laminar flow. The technique is based on a modified version of MTM. A 1.0×1.9 cm rectangular glass coverslip is patterned with dot arrays of Alexa488 conjugated Fn dots (2 μm in diameter and 6 μm center-to-center separation) via micro-contact printing (Fig. 21). The pattern is transferred on the top of PAA gel covalently bonded to a 40-mm diameter round glass coverslip. The thickness of the PAA gel is approximately 100 μm.

A parallel plate flow chamber and rubber gasket set (Glycotech) can be vacuum sealed on the glass coverslip, placing the patterned gel inside the flow chamber (Fig. 21). The thickness of the rubber gasket is 254 μm, which makes the resulting chamber height about 154 μm. The inlet and outlet of the flow chamber are connected to a reservoir of cell culture media and a peristaltic pump (Harvard Apparatus). The entire set-up including the media reservoir is then placed inside the environmental chamber where temperature (37ºC), humidity (70%) and CO_2 level (5%) are controlled throughout the experiment.
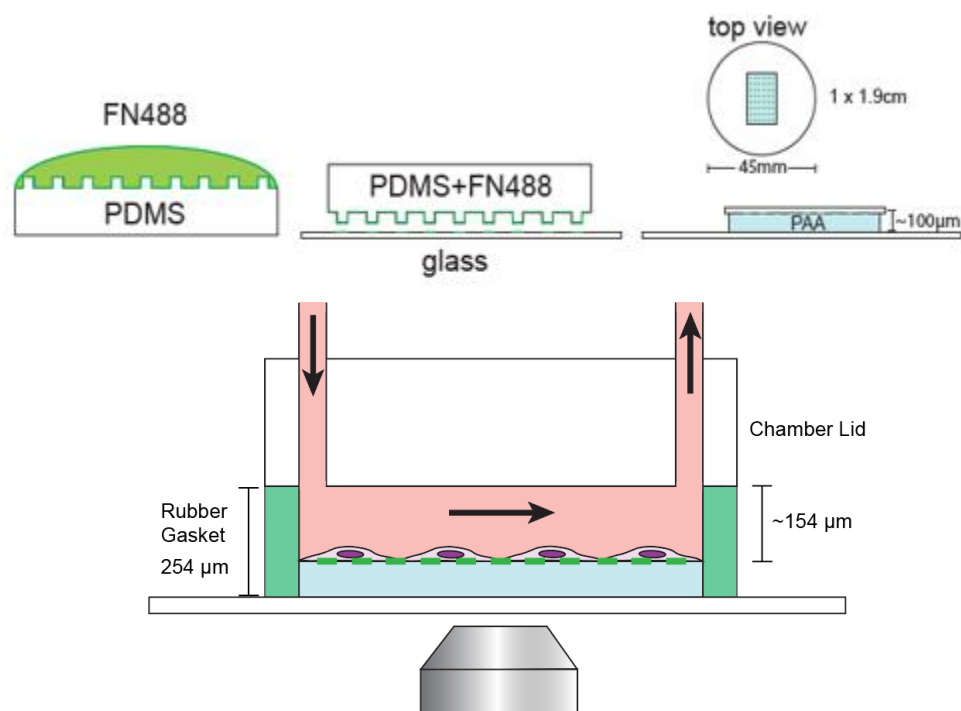
Figure 21: Set-up of flow chamber micropatterning traction microscopy (MTM).
Patterns are made in the same way as ones prepared for conventional MTM (refer back to
Chapter 3), Fn dot patterns are made on rectangular coverslips that are cut to fit the flow
chamber. PAA gel is polymerized with the patterned coverslip on top. Due to surface
tension, the resulting gel is rectangular in shape, even though the sides are not restricted
during polymerization. Final set up of the flow chamber fits on the microscope objective
inside the environmental chamber. Thick black arrows indicate the direction of flow.

6.2.2 *Experiment Procedures*

Primary BAECs under passage 10 are seeded on the patterned PAA gel 18 to 72 h before the experiments. The time after seeding before experiment allows BAECs to grow until areas of monolayers can be found on the gel. There are also isolated single cells that can be found on the same gel. During the experiment, images of both the monolayer and of single cells are taken, as well as the fluorescent Fn at 40× magnification are taken every 5 min, first for 2 h in static cell culture media, followed by 2 h under flow. The velocity of flow is chosen in order to generate laminar flow corresponding to shear stress of either 1 dyn/cm^2 (low), 5 dyn/cm^2 (medium), or 12 dyn/cm^2 (high). For the high shear stress experiments, 10 mg/ml dextran is added to the media to increase viscosity of the media to ~3 cP, which reduces the flow velocity needed to reach the desired shear stress.

To determine statistical significance, we used one-way ANOVA tests. Due to the fact that some groups had a lower sample size ($n = 4$ for high flow group), we could not be sure whether the distribution was normal. One-way ANOVA still assumed normality of the distribution, but has a good tolerance for non-normally distributed data.

It is noteworthy that during traction measurements we could not observe the whole monolayer, but only its part that falls within the field of view of the microscope (216×165 μm).

6.3   Results

Results of our measurements showed that shear flow affected traction field variability, but in a different manner in monolayers than in single cells. A representative image of a section of a monolayer (within a field of view) and the corresponding traction field during shear flow of 1 dyn/cm^2 is shown in Fig. 20A and 20B, respectively. The section of the monolayer is away from the monolayer boundaries and hence no traction forces of high magnitude were observed. With few exceptions, traction forces applied at the dots are homogeneous and of low magnitude (~3 nN).

Time lapses of the sum of magnitudes of traction forces (T) normalized by its time average ($\langle T \rangle$) of single cells (Fig. 23A) and monolayers (Fig. 23B) under static conditions showed that monolayers exhibited much lower temporal fluctuations than single cells. This is consistent with previous observations that the traction field of multicellular clusters exhibit lower temporal fluctuations than isolated cells (Canović et al., 2016).

Time lapses of $T/\langle T \rangle$ of monolayers under static conditions and under shear flow of different magnitudes showed that traction field fluctuations increased with increasing shear flow (Fig. 23B-E, Fig. 25). One reason for this could be that $\langle T \rangle$ increased with increasing flow (Fig. 24). However, only $\langle T \rangle$ obtained at 12 dyn/cm^2 shear stress was significantly higher than $\langle T \rangle$ obtained at 0, 1 and 5 dyn/cm^2 shear stress. Values of CV_T showed a somewhat different trend. There was a significant increase in CV_T in monolayers exposed to 1 dyn/cm^2 and 12 dyn/cm^2 shear stress, and not in monolayers exposed to 5 dyn/cm^2 shear stress relative to CV_T obtained under static (zero shear stress) conditions (Fig. 25). These results, in turn, indicate that an increase in flow-induced shear

stress did not attenuate traction field fluctuations but rather enhanced them, suggesting that the shear stress was detrimental to tensional homeostasis, which was opposite from what we expected. For comparison, we computed CV_T in single cells under static conditions and under shear stress of 1 and 12 dyn/cm^2; we did not observe any significant changes in CV_T among these three groups (Fig. 27). This, in turn, suggests that flow-induced shear stress in the range of 0–12 dyn/cm^2 may have very small effect on tensional homeostasis in single cells. This is not surprising since the net shear force acting on a single cell (calculated as the flow-induced shear stress times the cell projected area) did not exceed an order of 10^{-1} nN for the highest shear stress of 12 dyn/cm^2, which in most cases was below the observable threshold FA force of 0.3 nN. In the case of the monolayers, however, the magnitude of the net shear force was much larger since the surface area of the field of view of a monolayer was much larger than the projected area of single cells and this shear force was comparable with the observable FA traction forces. Interestingly, while CV_T was by a factor of ~4 lower under static conditions and by a factor of ~2 lower at 1 dyn/cm^2 shear stress in monolayers than in single cells, it was nearly the same at 12 dyn/cm^2 shear stress in both monolayers and single cells (Fig. 25 vs. Fig. 27). This is yet another piece of evidence showing that increasing of shear flow enhances traction field fluctuations in monolayers.

6.3.1 Correlation Analysis

We next examined how shear flow affected correlation between traction forces and therefore how it affected CV_T. The correlation analysis revealed that in monolayers the contribution from traction force correlation to CV_T was substantial (Fig. 25). This

correlation increased systematically with increasing flow-induced shear stress (Fig. 26). However, single cells exposed to the same flow range did not show the same increasing trend in CV_T. Instead, the level of fluctuation for cells under no flow, 1 and 12 dyn/cm^2 shear stress were at similar levels (Fig. 27). Importantly, the contribution of force correlation to CV_T was smaller than in monolayers at the same flow conditions (Fig. 27). There was no increase in correlation coefficient either (Fig. 28). Comparing the normalized correlation coefficients, under static and 1 dyn/cm^2 shear stress, single cells showed the same level of correlation between FA forces. Under 12 dyn/cm^2 shear stress, however, single cells showed virtually no correlation (normalized correlation coefficient close to zero) (Fig. 28).
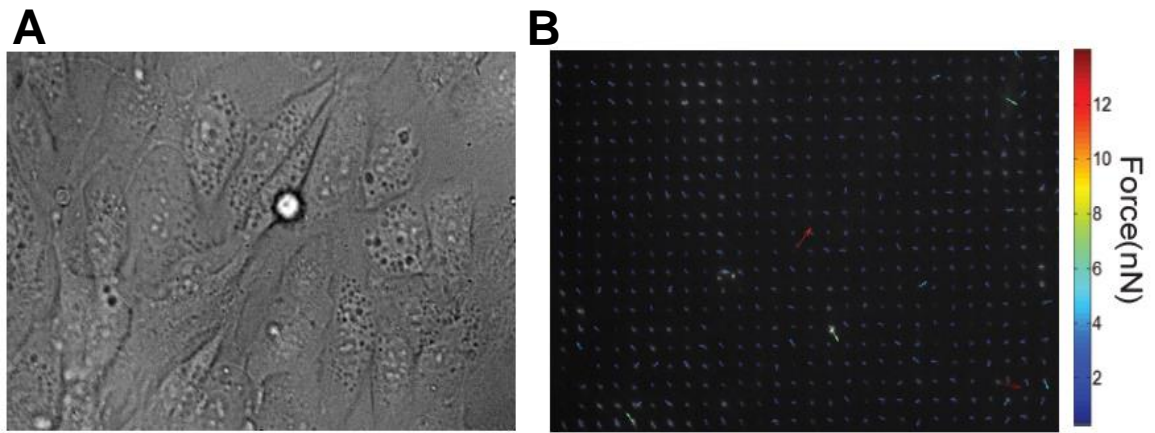
Figure 22: Traction measurements of bovine aortic endothelial cells (BAEC) monolayers under 1 dyn/cm^2 shear stress. We imaged the monolayer (A) and the micropattern protein grid (B) at the same time for traction microscopy. Traction forces (whose direction and magnitude are indicated by arrows) are calculated by MATLAB script based on the material properties of the gel (B).
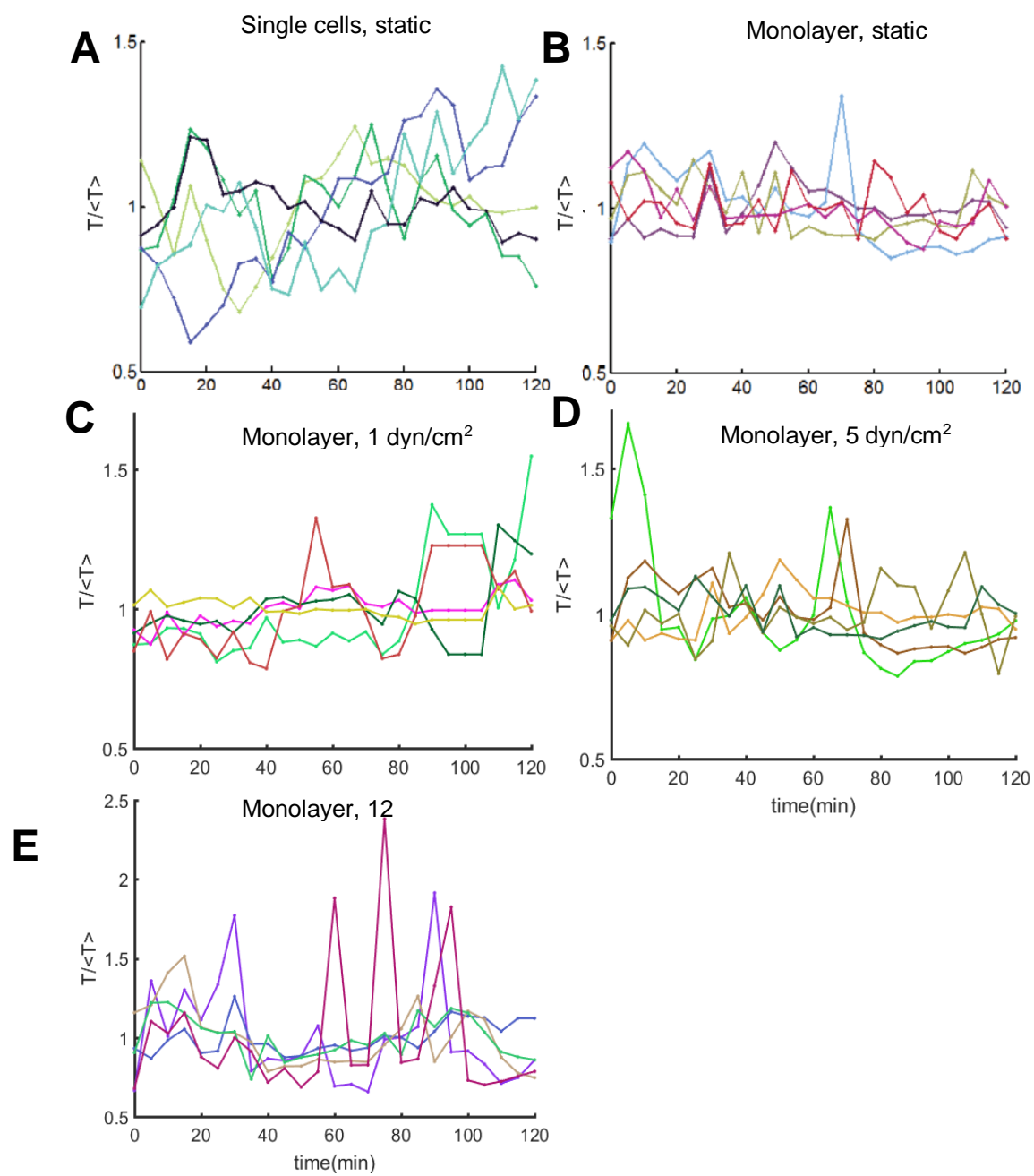
Figure 23: Time lapses of the sum of magnitudes of the traction forces traction (T) normalized by its time-averaged ($\langle T \rangle$) for single cells and monolayers. Temporal fluctuations of the traction field in ingle cells (A) are smaller than in monolayers (B) under no flow regime. Monolayers under 1, 5 and 12 dyn/cm^2 (C-E) showed increasing temporal fluctuations of the traction field with increasing shear stress.
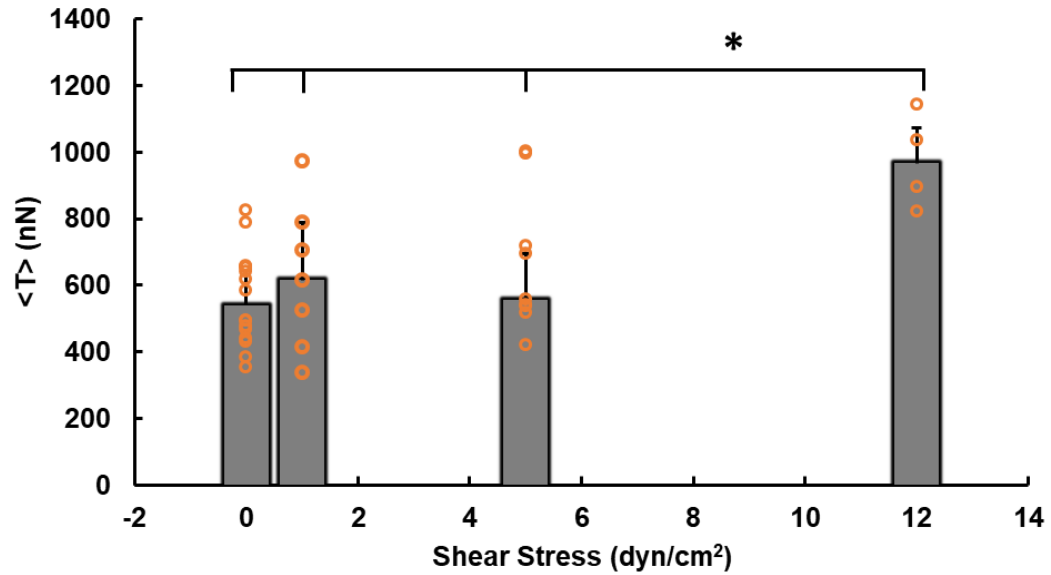
Figure 24: Time-averaged sum of traction ($\langle T \rangle$) plotted with respect to shear stress levels. $\langle T \rangle$ of bovine aortic endothelial cell (BAEC) monolayers under 12 dyn/cm^2 laminar shear stress is significantly higher than the monolayers under no flow, 1 dyn/cm^2 or 5 dyn/cm^2 flows. Significance is defined as $p < 0.05$ in Mann-Whitney U test (*). Each monolayer is plotted as an orange open circle. Grey columns represent the median $\langle T \rangle$ of the group. (Error bars indicate median absolute deviation.)
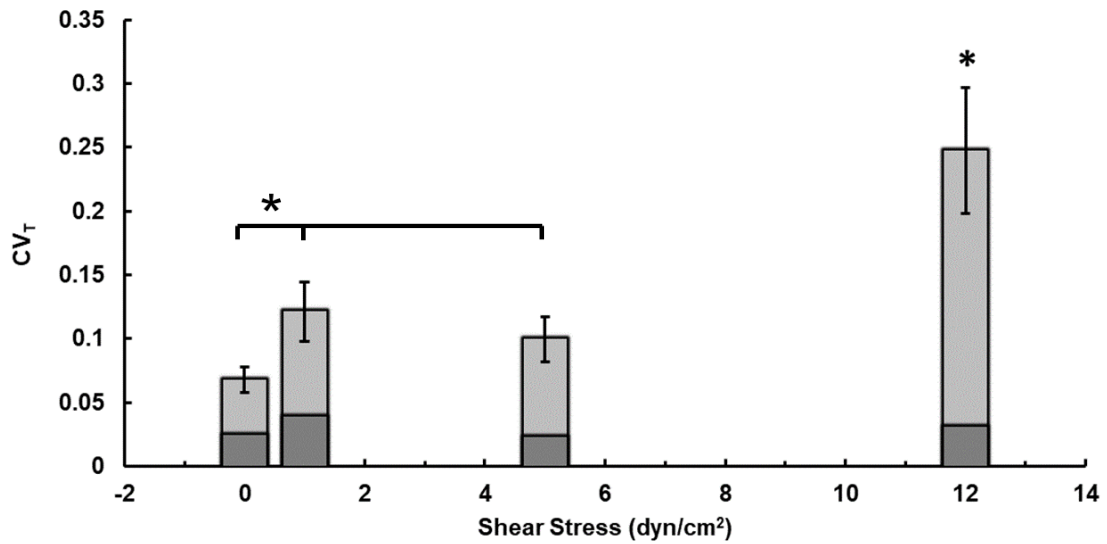
Figure 25: Coefficient of variation of sum of magnitudes of traction forces (CV_T) of monolayers as a function of flow-induced shear stress. Monolayers under static conditions showed lower fluctuations compared to those under 1 dyn/cm^2 and 5 dyn/cm^2 shear stress. Monolayers under 12 dyn/cm^2 shear stress show significantly higher fluctuations than all three other conditions. Significance is defined as $p < 0.05$ in Mann-Whitney U test (*). Light grey bar represents the contribution of correlation between FA forces. Under 12 dyn/cm^2 the contribution of correlation is also higher than the other conditions (not marked on graph). (Error bars indicate median absolute deviations).
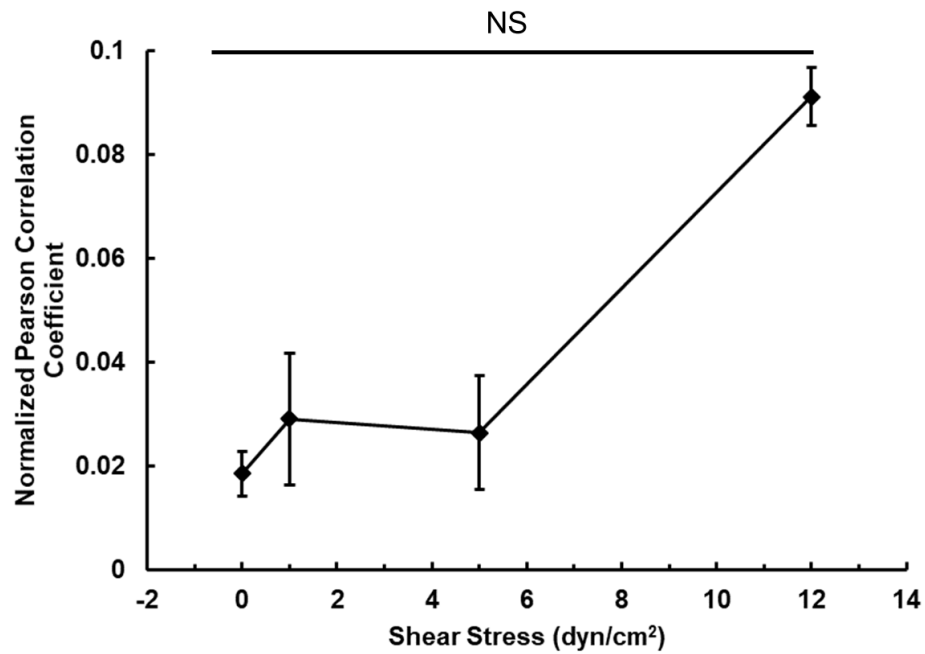
Figure 26: Normalized correlation efficient plotted with respect to shear stress shows an increasing trend of correlation with applied shear stress. Correlation coefficients increase with the magnitude of applied shear stress. No statistical significance was found between groups.
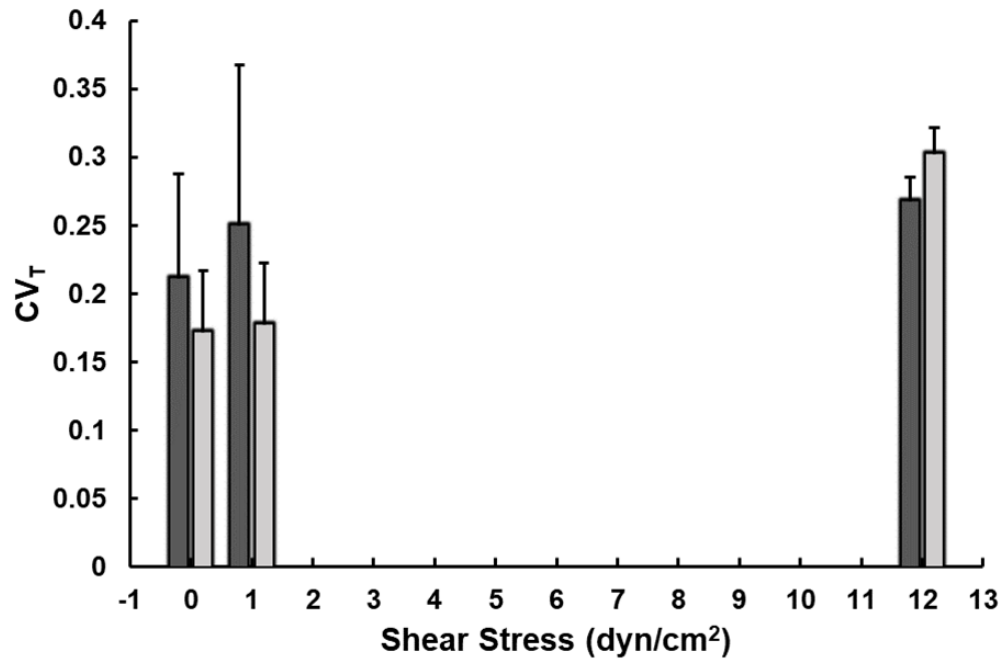
Figure 27: Single cells (BAECs) exhibited similar levels of CV_T under static and flow conditions. The dark grey bars show the experimentally measured CV_T. The light grey bars show the CV_T if the forces were not correlated at all. The contribution from correlation is the different between the two bars. At 12 dyn/cm^2 the contribution of correlation has a negative value. (Error bars represent median absolute deviations.)
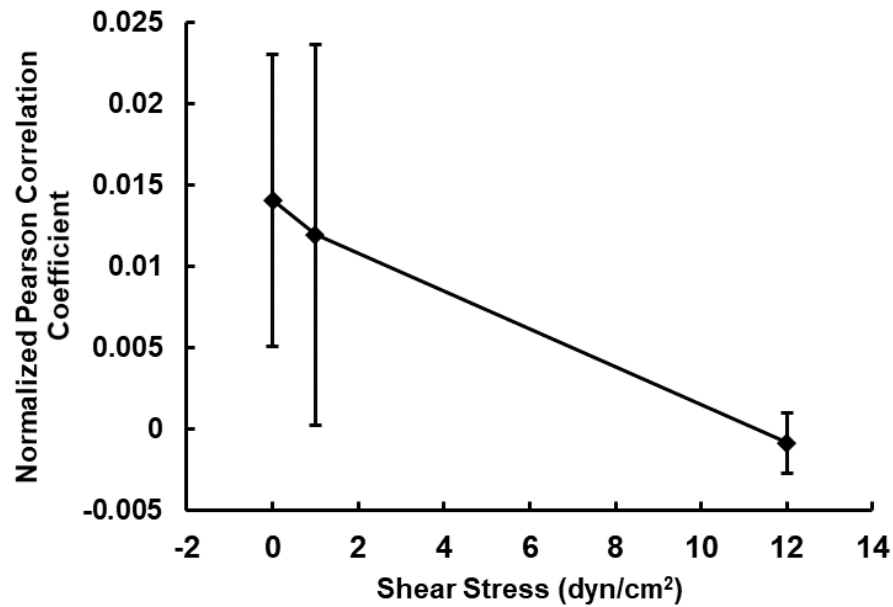
Figure 28: Normalized correlation coefficients of single cells plotted with respect to shear stress show a decreasing trend with increasing applied shear. Under 12 dyn/cm^2 forces within the cells appear close to uncorrelated (correlation coefficient close to zero). There is no significant difference between the correlation coefficients of static and 1 dyn/cm^2 flow cells. (Error bars represent median absolute deviations)

6.4   Discussion

In the landmark paper *Mechanotransduction and Endothelial Cell Homeostasis: Wisdom of the Cell*, Chien raised the idea that laminar flow in its physiological range is essential to vascular homeostasis. Physiological shear stress, along with other mechanical cues (e.g., cyclic circumferential stretch of the endothelium), promote a healthy vascular environment, including downregulation of inflammatory signaling pathways, healthy lipid metabolism and maintains endothelial cells in a quiescent phenotype (Chien, 2007). One major effect that shear stress has on endothelial cells is on cytoskeleton organization. Endothelial cells exposed to sustained shear stress has been shown to align with the direction of flow. Additionally, shear stress has been shown to induce thickening of the stress fiber, a decrease in peak cell height and an increase of cell stiffness. This seems to suggest that shear stress also impacts cytoskeletal tension, which would also affect tensional homeostasis. More recently, Valent and colleagues showed that high fluctuations of traction forces in endothelial cells is correlated to formation of endothelial gaps (Valent et al., 2016). In other words, it appears that tensional homeostasis could be linked with vascular homeostasis and both are affected by shear stress. Our results suggested that shear flow does not promote homeostasis in monolayers. Increase of shear stress lead to a systematic increase in CV_T in monolayers and did not affect CV_T in single cells. These behaviors are paralleled with temporal correlations of traction forces which systematically increase with increasing shear stress in monolayers and decrease in single cells. One reason for this discrepancy between monolayers and single cells could be tied to lack of mechanical equilibrium between traction forces observed in the field of view of

a monolayer, whereas in single cells mechanical equilibrium is maintained all the time.

This can be explained as follows.

At the level of the whole monolayer, basic laws of mechanics demand that

traction forces acting on the monolayer must be balanced at any instant (i.e., the vector

sum of the traction forces must be zero and the sum of their moments must be zero).

However, since we could not observe the entire monolayer, but rather only a section of

the monolayer within the field of view, the traction forces that we observe need not be

balanced. It has been shown previously that in monolayers of epithelial cells traction

forces acting on individual cells are not balanced and that they are balanced on the whole

monolayer level (Trepat et al., 2009). In the case of single cells, we can observe all

traction forces which are balanced at any instant and if they were not, due to experimental

errors, we insure that they are balanced by adjusting force directions and/or magnitudes

according to the procedure described previously (Canović et al., 2014). To quantitate the

extent to which forces acting on the monolayer are out of equilibrium, we used the

approach of Polio et al. (2012). We summed up all traction force vectors acting on a

monolayer within the field of view. If the vector sum (resultant) were not zero, then the

forces were unbalanced. The magnitude of the unbalanced resultant force vector is then

divided by the sum of magnitudes of all force vectors to see whether the resultant is a

small or large fraction of that sum. We also calculated the traction moment matrix by

summing the tensor products of the position vectors of forces and the corresponding

forces. Equilibrium demands that the moment matrix is symmetric, i.e., that $M_{xy} = M_{yx}$.

Thus, if $M_{xy} \neq M_{yx}$, the forces are not balanced. If traction forces within the field of view

were not balanced, then the calculated CV_T is not accurate and may be misleading. Our estimates of the imbalanced traction vector as a fraction of the total sum of forces is on the average ~40% (Fig. 29A), whereas the ratio M_{xy}/M_{yx} ranged between 0.55 to 0.65 (Fig. 29B), indicating that the traction forces in the field of view of a monolayer are far away from equilibrium. Thus, we concluded that values of CV_T as well as the values of the correlation coefficient obtained from the measurements in the monolayers are not accurate. In order to obtain accurate estimates of CV_T for the section of the monolayers within the field of view, we would need to include not only the traction forces but also cell-cell adhesion forces at the boundary of the field of view as well as the shear force. The contribution of the former we cannot estimate by our current technique, whereas the contribution of the latter is small and does not significantly affect findings shown in Fig. 29.

The correlation between traction forces in the monolayer appears to be a major determinant of CV_T (Fig. 25) whereas in single cells the correlation contribution is relatively small (Fig. 27). This is reasonable since forces that we observed in monolayers (within a field of view) are relatively homogeneous (most of them are of approximately same magnitude and same variability, see Fig. 22B), whereas in single cells forces are highly heterogeneous and of different variability, which is known to enhance CV_T (Li et al., 2019).

If we were able to make traction measurements of the entire monolayer, one would expect to see lowered traction field fluctuations under physiological range shear stress. It is interesting to note that single cells did not display lowered fluctuations under

12 dyn/cm^2. One possible reason for this could be associated with the role of cell-cell contact in mechanosensing. Shear flow experiments on endothelial cells showed that VE-cadherin, in combination with VEGFR2 and PECAM-1, are required for cell alignment in the direction of flow (Tzima et al., 2005). Junctional recruitment for vinculin has also been shown to occur specifically through VE-cadherin (Barry, Wang, & Leckband, 2015). To the extent that the directionality of cell alignment is important for homeostasis (Chien, 2007), the mechanotransduction via VE-cadherin may play an important role in tensional homeostasis and vascular homeostasis. It is questionable whether single endothelial cells are able to respond to shear in the way monolayers or clusters of endothelial cells would. Future studies could look into whether multicellularity plays a role in endothelial tensional homeostasis under flow, since single endothelial cells *in vivo* mostly occur after vascular injury.

It is noteworthy that the shear stress range that we used were on the low end of values obtained from vessels *in vivo*. Physiological shear stress measured in arteries ranges from 10-70 dyn/cm^2, whereas shear stress in veins measured lower at 1-6 dyn/cm^2 (Lipowsky, 1995; Malek, Alper, & Izumo, 1999; Paszkowiak & Dardik, 2003). The external shear stress applied by our setup were 1, 5 and 12 dyn/cm^2. Since BAECs are sourced from the aorta of cows, it is possible that those shear stress values are all below the normal physiological shear stress they would experience *in vivo*. However, it is unclear if BAECs *in vitro* require the same magnitude of shear for physiological functions as they do *in vivo*, and it is common for studies to use shear stress of around 12 dyn/cm^2 to represent physiological shear.

In conclusion, results under this aim showed that shear stress affects tensional homeostasis of endothelial monolayers. Based on our observation, how shear stress of different magnitudes affects tensional homeostasis was not always in accordance of their effects on vascular homeostasis. However, the results are inconclusive due to the fact that our experimental setup does not allow inclusion of all traction forces applied to the monolayers. The sections of monolayers being imaged are mechanically imbalanced, which made the CV_T and correlation calculations not representative of the true behavior of the monolayer. To continue investigating tensional homeostasis in endothelial cell monolayers, it would be helpful to use a setup that would allow the application of shear, measurements of traction forces and the inclusion of the entire monolayer in the field of view.
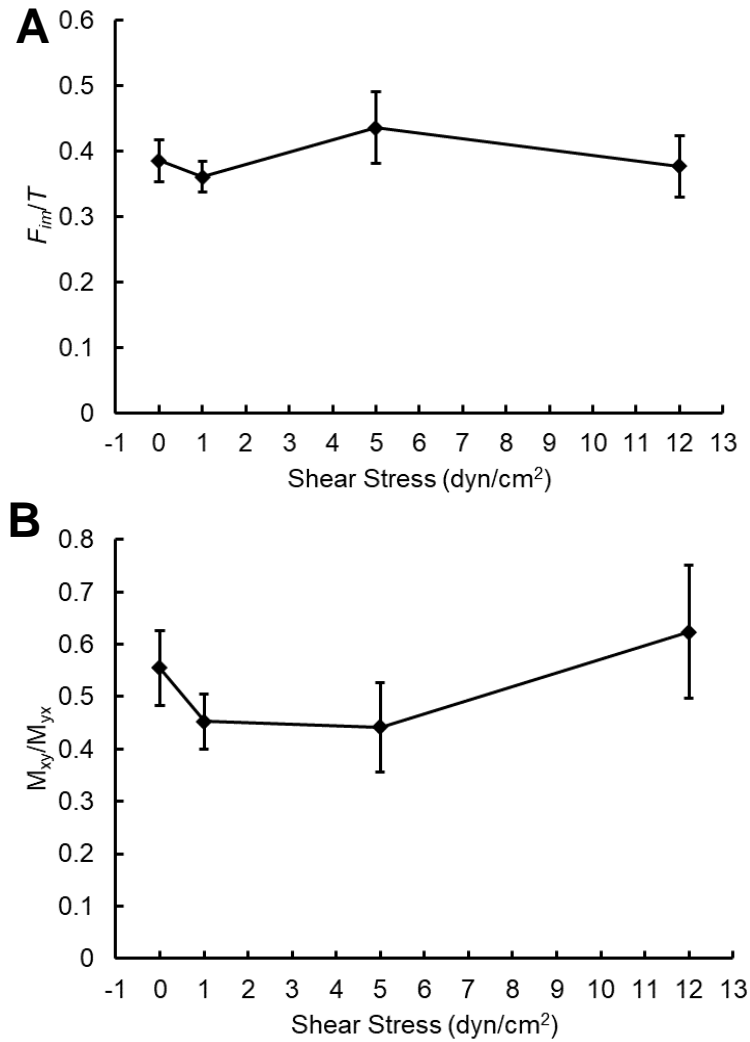
Figure 29: Monolayer sections are not at mechanical equilibrium. Forces in the

monolayer section within field of view is not balanced. The norm of sum of all traction

force vectors (F_{im}) normalized to the sum of all traction force norms (T) has values

around 0.4 for all shear stress conditions (A). Similarly, the moment of x- and y-

component forces (M_{xy}/M_{yx}) has a ratio less than 1, indicating that the measured torque of

the monolayer sections are also not at balance (B).

Chapter 7: CONCLUSION AND FUTURE DIRECTIONS

Since the introduction of the concept of tensional homeostasis around two decades ago (Brown et al. 1998), we have gradually grasped the importance of this phenomenon for normal physiological functions of cells and tissues, and the consequences of its breakdown in some pathological events. We do not yet fully understand exactly how cells maintain tensional homeostasis, nor do we fully understand how it is related to physiological homeostasis of cells and tissues. Past studies commonly used dynamic external perturbation to disturb established homeostasis of cells and/or observe cells during transitional periods (i.e. during spreading, migration etc.). We lack investigations of how cells maintain tensional homeostasis in steady environmental conditions. Not only are the steady conditions (patho)physiologically relevant, they are also ofter the parameters that can be fine-tuned most effectively at tissue-material interfaces. In this thesis, we hypothesized that *cells require specific non-dynamic environmental conditions in order to maintain tensional homeostasis*. We chose three tunable conditions to study; they are substrate stiffness, availability of functional E-cadherin bonds, and shear stress from laminar flow.

7.1   Conclusions

7.1.1   *Aim 1: The Effects of Substrate Stiffness on Traction Dynamics and Tensional Homeostasis*

Aim 1 studied the effect of substrate stiffness on tensional homeostasis of endothelial cells and vascular smooth muscle cells. Stiffness is a commonly examined

environmental parameter in mechanobiology, but rarely has there been a study that looks at temporal traction changes at multiple length scales in the same study. Research carried out in this aim did exactly that. Results revealed that substrate stiffness affects tensional homeostasis at both the whole cell level and at the FA level and that temporal fluctuations of FA forces alone cannot determine cell level traction field temporal fluctuations. This supports the idea that tensional homeostasis is a length-scale-dependent phenomenon (Canović et al., 2016). Additionally, our results confirmed the cell type dependence of tensional homeostasis. Stiffer substrates promoted tensional homeostasis in BAECs but were detrimental to tensional homeostasis in BVSMCs. Through correlations analysis of FA forces, we found that besides the fluctuation of FA forces themselves, the correlation between FA forces is a contributor to cellular traction field fluctuation. Furthermore, the increasing number of FAs with increasing substrate stiffness also contributed to attenuation of the traction field fluctuations.

7.1.2   Aim 2: Role of Cadherin in Tensional Homeostasis

Aim 2 investigated whether the availability of functional E-cadherin bonds affects the tensional homeostasis of epithelial cancer cell lines. We chose AGS cells because 1) they are epithelial in origin and epithelial cells exist in monolayers *in vivo*; 2) epithelial cancer cells naturally express no E-cadherin (Carneiro et al., 2012; Figueiredo et al., 2013), but can be transfected with vectors encoding for variations of healthy and mutated E-cadherins. We found that wild-type E-cadherin cells attenuated traction field fluctuations in single AGS cells and in AGS cell clusters, suggesting that E-cadherin is not only responsible for mechanical linkage between cells, but also may perform a

signaling functions even when it is not engaged in homophilic bonds. Furthermore, results from the cells transfected with E-cadherin with point mutations showed that the effects of mutation are location-dependent. This signals that different domains of the E-cadherin molecule have different functions in the maintenance of tensional homeostasis. Extracellular mutation resulted in no difference between single cells and cluster fluctuations, suggesting that cell-cell adhesion in presence of extracellular mutation on E-cadherin no longer promoted tensional homeostasis. Intracellular mutation resulted in significantly increased fluctuations in single cells, suggesting that the attenuating effect of E-cadherin may be dependent on the intracellular domain particularly. The results of this aim suggested that cell-cell adhesion through wild-type E-cadherin could be a requirement for epithelial tensional homeostasis.

7.1.3   *Aim 3: The Effect of Steady Shear Stress on Tensional Homeostasis*

Aim 3 focused on the effect of laminar flow-induced shear stress on tensional homeostasis in monolayers of endothelial cells. It is known that laminar shear stress of physiological magnitudes promotes vascular homeostasis (Chien, 2007), but it is unclear how tensional homeostasis is affected by shear stress. Results showed that the application of shear stress increased the traction fluctuation of the monolayer sections, especially at 1 dyn/cm^2 and 12 dyn/cm^2 the increase was statistically significant. Further, there was a significantly higher temporal correlation between focal adhesion forces that contributed to high fluctuations. This was an unexpected observation, since 12 dyn/cm^2 shear stress has been shown to promote vascular homeostasis. However, because the observable parts of the monolayer were not in mechanical equilibrium, the measured traction fluctuations

and correlation analysis may not represent the behavior of the monolayer as a whole. Single cells that are mechanically balanced did not display the similar levels of traction fluctuations under static and flow regimes, and did not display the same increase in force correlation.

7.2   Future Directions

From the first observation by Brown and colleagues in the 1990s, the concept of tensional homeostasis has evolved during the three decades of research. The phenomenon of tensional homeostasis stems from the innate variabilities in cytoskeletal tension and the management of it. This variability in tension plays an essential part in fundamental cell behaviors such as stiffness sensing, migration and mitosis. The source of variability could be from a number of processes within the cell, including intracellular calcium (Ca^{2+}) concentrations and the associated activation of myosin light chain kinase, the loss and regain of tension in actin fibers that accompanies their remodeling, and similar dynamics of compressive tension due to remodeling of microtubules. In this project we observed traction forces and their fluctuations as a measurable sign of tension variabilities without investigating the exact source of the variability. A new project in collaboration with the Dr. Allyson Sgro's group will explore the link between tension variability and intracellular Ca^{2+} signaling. It combines fluorescent, live cell Ca^{2+} sensors with micropattern traction microscopy. The results are expected to provide a deeper understanding in the biochemical signaling perspective of tensional homeostasis.

As an extension of this project, future studies can also improve upon the experiment designs of Aim 3. The shear stress experiments under Aim 3 yielded

inconclusive results due to the limitations of the setup. Specifically, we were not able to observe the entire monolayer during the experiment. An island pattern that spatially constrains the size and shape of the monolayer to fit inside the field of view would solve this issue. We have carried out some preliminary studies with confluent bovine aortic endothelial cells on square patterns (Fig. 30). The island pattern still consists of the dot array that is used for micropattern traction microscopy (Fig. 30). Tunable sizes of the islands would allow the formation of clusters/monolayers with cell numbers that range from 2 to 70 or more cells (Fig. 30). Preliminary results on the medium size islands (~11 cells; ~80 FAs) showed similar level of CV_T compared to free-formed clusters with similar number of FAs (data not shown). More studies need to be carried out to compare between cells islands and free-formed clusters of similar cell numbers. For more detailed procedure of island patterning, please refer to Appendix A.1.

Finally, the far-reaching goal of the project was to use cell behavior under these scenarios to learn more about pathology that involves similar environmental alternations. Understanding the mechanical cues that are involved in pathologies is extremely valuable. Most of the times biochemical factors and signaling cascades are the only processes studied in the context of diseases, when in fact we now have an increasing amount of evidence that points to the relevance of forces, stresses and strains in determining disease occurrence and progression. The environmental conditions studied in this thesis project are altered in pathological situations: substrate stiffening is common in vasculature due to aging, as well as tumor environment in cancer; loss or mutation of E-cadherins is another hallmark of caner; and shear stress is often changed in vascular

diseases such as arthrosclerosis. The results of this study emphasize the importance of the mechanical environment of cells and tissue in determining their behavior. Building on that, more specific disease models can be built to better mimic pathological conditions. Aim 2 used mutations found in hereditary diffusive gastric cancer patients, which was a fitting choice to study gastric cancer pathology. Future studies would benefit from using substrate stiffness and protein combinations that are found in the tumor environment or the vascular basement membrane for the purpose of understanding disease situations.
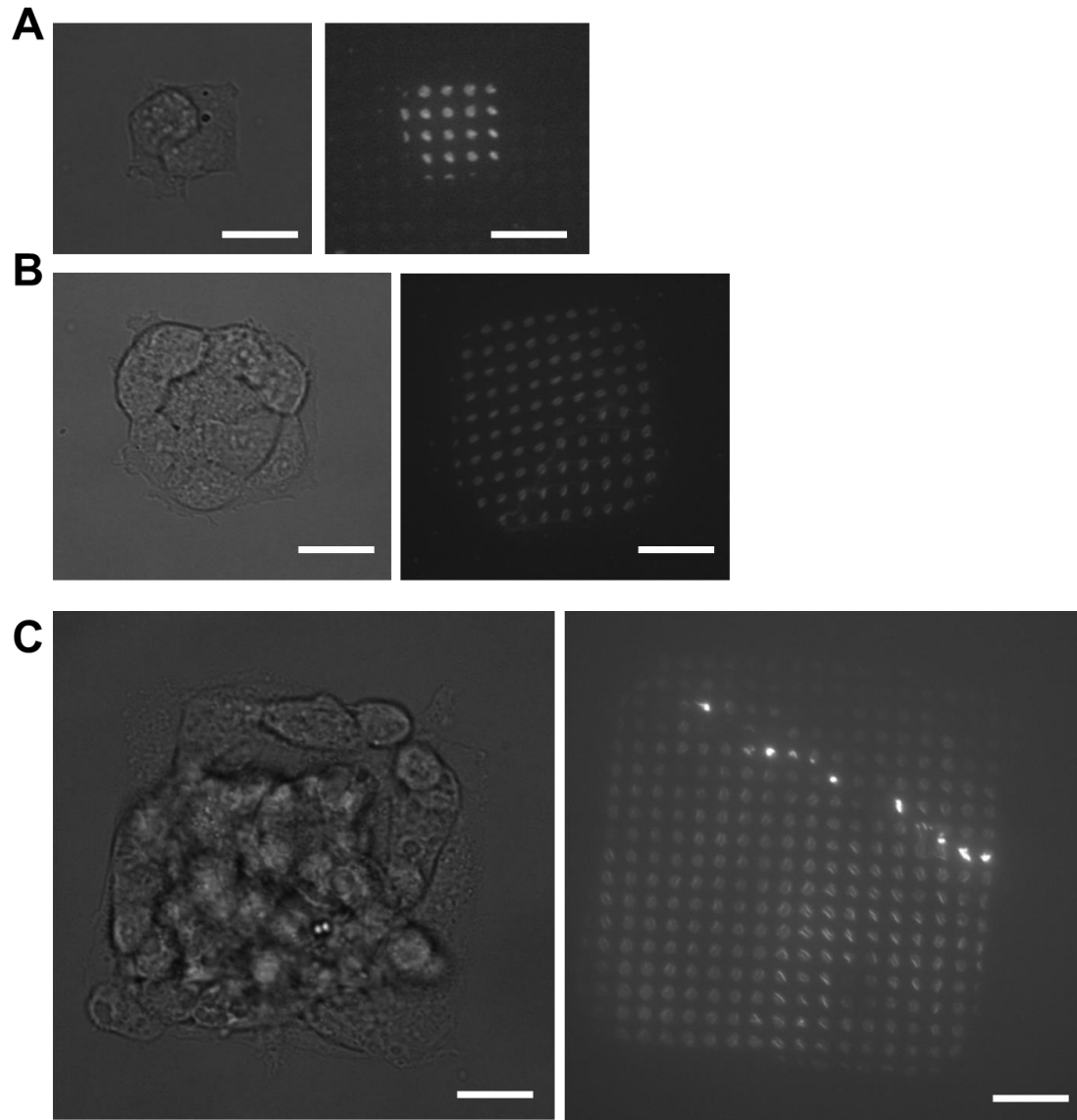
Figure 30: Examples of bovine aortic endothelial cells (BAECs) on island patterns of various sizes. The sizes of the islands are roughly 30 by 30 µm (A), 60 by 60 µm (B) and 120 by 120 µm (C). The number of cells in the pictures are 2, 11 and 68 respectively from panel A to C. Left of each panel show brightfield images of the cells and right panels show the fluorescent fibronectin grid for traction measurements. Scale bar represents 20 µm.

APPENDIX

A.1   Isolation Island Patterning

Island patterns were originally developed by Polio et al (2014). They are used to spatially control the shape and size of cell clusters while providing substrate for traction microscopy at the same time. Similar to the pattern used for normal MTM, the basic pattern for isolation islands is also a Fn dot array pattern, with 2 μm diameter dots, 6 μm center-to-center separation. The difference is that instead of having continuous dot array, the dots form squares of varying sizes. The size of the islands ranges from 5 by 5, 10 by 10 to 20 by 20 dots per side of the square.

Isolation islands are formed using a double removal method (Fig. A1). Compared to the previous method used by Polio et al. (2012), this method reduces the failure rate in generating the dot array pattern using micro-contact printing, thus results in better formed islands of dots in majority of cases. The procedure involves two different silane treated PMS stamps – one with round indents corresponding to the 2 μm dots, another square indents corresponding to the square islands. First, a layer of uniform fluorescent Fn solution is laid down on plasma-cleaned coverslip and incubated for 15 min. Then, the dot removal stamp is used to remove part of the Fn from the coverslip, leaving behind the dot array pattern. Finally, the island removal stamp is applied, leaving behind the island of dots that is required for experiments.
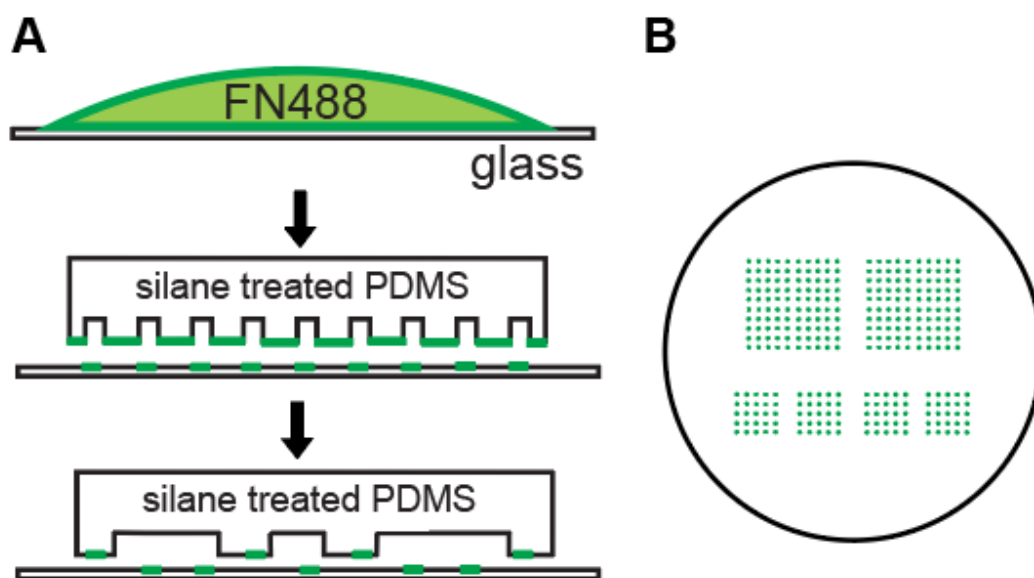
Figure A1: Illustration of the protocol for generating island pattern using a dual removal process. Two silane treated polydimethylsiloxane (PDMS) stamps are used to remove fluorescent fibronectin (Fn) from the coverslip (A). The resulting pattern is dot arrays in the formation of square islands of different sizes (B).

A.2 Dependency of Cellular Traction Fluctuation on FA Number and CV_F

Consider the covariance matrix of a cell/cluster with n FA forces, it can be expressed as follows:

$$\text{COV(T)} = \begin{bmatrix} CV_1^2 \langle F_1 \rangle^2 & \rho(F_1, F_2)CV_1\langle F_1 \rangle CV_2\langle F_2 \rangle & ... & ... \\ \rho(F_2, F_1)CV_2\langle F_2 \rangle CV_1\langle F_1 \rangle & CV_2^2 \langle F_2 \rangle^2 & ... & ... \\ ... & ... & ... & ... \\ ... & ... & ... & CV_n^2\langle F_n \rangle^2 \end{bmatrix} \tag{A1}$$

CV_T can be written as

$$CV_T = \frac{\sqrt{\sum_{i=1}^{n}\sum_{j=1}^{n}\text{COV}_{ij}(T)}}{\sum_{i=1}^{n}\langle F_n \rangle} = \frac{\sqrt{\sum_{i=1}^{n}\sum_{j=1}^{n}\rho(F_i, F_j)CV_i\langle F_i \rangle CV_j\langle F_j \rangle}}{\sum_{i=1}^{n}\langle F_n \rangle} = \frac{\sqrt{\sum_{i,j=1, i\neq j}^{n}\text{COV}_{ij}(T) + \sum_{i=1}^{n}\sigma^2(F_i)}}{\sum_{i=1}^{n}\langle F_n \rangle}$$

$$= \frac{\sqrt{\sum_{i,j=1, i\neq j}^{n}\rho(F_i, F_j)CV_i\langle F_i \rangle CV_j\langle F_j \rangle + \sum_{i=1}^{n}\sigma^2(F_i)}}{\sum_{i=1}^{n}\langle F_n \rangle}. \tag{A2}$$

Based on this expression, the factors that contribute to the CV_T of the cell/cluster include the correlation coefficient ρ, the time-average magnitudes of FA forces $\langle F \rangle$ and the CV of FA forces. Under the three aims, we have evaluated the effects of correlation between FA forces on the experimental CV_T of cells by calculating CV_T with the assumption that all force pairs within the cell is random and not correlated each other at all. It was done by artificially setting the Pearson correlation coefficient of every force pair ($\rho(F_i, F_j)$, where $i \neq j$) to zero (Refer to Chapter 3.6).

From the same expressions, we can make estimations on how the other factors of FA force dynamics affect cellular fluctuation CV_T. Taking an reductive approach, we start by assuming that each force has the same CV_F and $\langle F \rangle$, and all force pairs has the same correlation coefficient of ρ. The resultant expression of CV_T is the following:

$$CV_T = \frac{\sqrt{n!\rho CV_F^2 \langle F \rangle^2 + nCV_F^2 \langle F \rangle^2}}{n\langle F \rangle} = \frac{\sqrt{n!\rho CV_F^2 + nCV_F^2}}{n} = CV_F \frac{\sqrt{n!\rho + n}}{n} \tag{A3}$$

Plotting the experimentally measured CV_T of BAEC single cells on 6.7 kPa gels against the number of FA forces and the average CV_F, we found that CV_T increases with increasing CV_F and increasing number of FA forces (Fig. A2). The relationship between CV_T and average CV_F can be fit to a linear equation with R^2 value of 0.369, which roughly agrees with the simplified prediction of Eq. A3. It makes sense that collectively the fluctuations of FA forces would increase the cellular level traction field fluctuations. However, different from what is described by Eq. A3, CV_T only increased slightly with increasing number of FA forces. This suggests that the estimation from the expression is inaccurate regarding the effect of the number of FA forces, likely due to the assumption of the same CV_F, $\langle F \rangle$, and ρ for all forces and force pairs. The fact is that the effects of number of FA forces cannot be detangled from the effects of the value ρ and the distribution of ρ for all force pairs. Further complicating things, ρ values of force pairs within the same cell/cluster are not independent from each other. To better study the effect of number of FAs and CV_F, future projects can take a computational route by simulating cell/cluster traction fields with existing data, similar to the methods used by Tam *et al.* (2017) and Li *et al.* (2019).
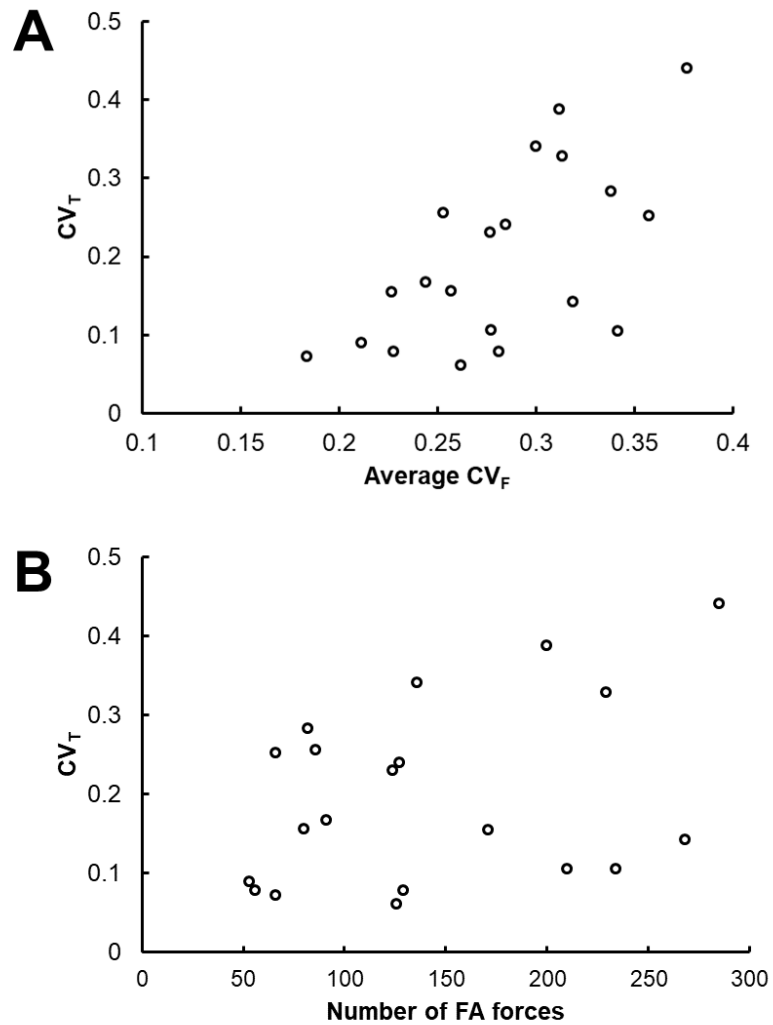
Figure A2: Cellular traction field fluctuation (CV_T) of single BAECs on 6.7 kPa substrates increases with increasing CV_F and remains mostly unchanged with increasing number of FA forces. CV_T of BAECs are plotted against average CV_F (A) and number of FA forces (B). Each cell is represented by an open circle on the graphs.

BIBLIOGRAPHY

Balaban, N. Q., Schwarz, U. S., Riveline, D., Goichberg, P., Tzur, G., Sabanay, I., … Geiger, B. (2001). Force and focal adhesion assembly: A close relationship studied using elastic micropatterned substrates. *Nature Cell Biology*, *3*(5), 466–472. https://doi.org/10.1038/35074532

Barbee, K. A., Mundel, T., Lal, R., & Davies, P. F. (1995). Subcellular distribution of shear stress at the surface of flow-aligned and nonaligned endothelial monolayers. *The American Journal of Physiology*, *268*(4 Pt 2), H1765-1772.

Barry, A. K., Wang, N., & Leckband, D. E. (2015). Local VE-cadherin mechanotransduction triggers long-ranged remodeling of endothelial monolayers. *Journal of Cell Science*, *128*(7), 1341–1351. https://doi.org/10.1242/jcs.159954

Bazzoni, G., & Dejana, E. (2004). Endothelial cell-to-cell junctions: Molecular organization and role in vascular homeostasis. *Physiological Reviews*, *84*(3), 869–901. https://doi.org/10.1152/physrev.00035.2003

Bernard, C., Dastre, A., Vulpian, A. (Alfred), & Bert, P. (1878). *Leçons sur les phénomènes de la vie communs aux animaux et aux végétaux ..* Retrieved from http://archive.org/details/leonssurlesp02bern

Birukova, A. A., Tian, X., Cokic, I., Beckham, Y., Gardel, M. L., & Birukov, K. G. (2013). Endothelial barrier disruption and recovery is controlled by substrate stiffness. *Microvascular Research*, *87*, 50–57. https://doi.org/10.1016/j.mvr.2012.12.006

Bobryshev, Y. V., Lord, R. S., Watanabe, T., & Ikezawa, T. (1998). The cell adhesion molecule E-cadherin is widely expressed in human atherosclerotic lesions. *Cardiovascular Research*, *40*(1), 191–205. https://doi.org/10.1016/s0008-6363(98)00141-2

Boggon, T. J., Murray, J., Chappuis-Flament, S., Wong, E., Gumbiner, B. M., & Shapiro, L. (2002). C-Cadherin Ectodomain Structure and Implications for Cell Adhesion Mechanisms. *Science*, *296*(5571), 1308–1313. https://doi.org/10.1126/science.1071559

Borghi, N., Sorokina, M., Shcherbakova, O. G., Weis, W. I., Pruitt, B. L., Nelson, W. J., & Dunn, A. R. (2012). E-cadherin is under constitutive actomyosin-generated tension that is increased at cell–cell contacts upon externally applied stretch. *Proceedings of the National Academy of Sciences of the United States of America*, *109*(31), 12568–12573. https://doi.org/10.1073/pnas.1204390109

Brown, R. A., Prajapati, R., McGrouther, D. A., Yannas, I. V., & Eastwood, M. (1998). Tensional homeostasis in dermal fibroblasts: Mechanical responses to mechanical loading in three-dimensional substrates. *Journal of Cellular Physiology*, *175*(3), 323–332. https://doi.org/10.1002/(SICI)1097-4652(199806)175:3<323::AID-JCP10>3.0.CO;2-6

Butcher, D. T., Alliston, T., & Weaver, V. M. (2009). A tense situation: Forcing tumour progression. *Nature Reviews Cancer*, *9*(2), 108–122. https://doi.org/10.1038/nrc2544

Butler, J. P., Tolić-Nørrelykke, I. M., Fabry, B., & Fredberg, J. J. (2002). Traction fields, moments, and strain energy that cells exert on their surroundings. *American Journal of Physiology-Cell Physiology*, *282*(3), C595–C605. https://doi.org/10.1152/ajpcell.00270.2001

Byfield, F. J., Reen, R. K., Shentu, T.-P., Levitan, I., & Gooch, K. J. (2009). Endothelial actin and cell stiffness is modulated by substrate stiffness in 2D and 3D. *Journal of Biomechanics*, *42*(8), 1114–1119. https://doi.org/10.1016/j.jbiomech.2009.02.012

Cannon, W. B. (1929). Organization for physiological homeostasis. *Physiological Reviews*, *9*(3), 399–431. https://doi.org/10.1152/physrev.1929.9.3.399

Canović, E. P., Seidl, D. T., Polio, S. R., Oberai, A. A., Barbone, P. E., Stamenović, D., & Smith, M. L. (2014). Biomechanical imaging of cell stiffness and prestress with subcellular resolution. *Biomechanics and Modeling in Mechanobiology*, *13*(3), 665–678. https://doi.org/10.1007/s10237-013-0526-8

Canović, E. P., Zollinger, A. J., Tam, S. N., Smith, M. L., & Stamenović, D. (2016). Tensional homeostasis in endothelial cells is a multicellular phenomenon. *American Journal of Physiology - Cell Physiology*, *311*(3), C528–C535. https://doi.org/10.1152/ajpcell.00037.2016

Carneiro, P., Fernandes, M. S., Figueiredo, J., Caldeira, J., Carvalho, J., Pinheiro, H., … Seruca, R. (2012). E-cadherin dysfunction in gastric cancer – Cellular consequences, clinical applications and open questions. *FEBS Letters*, *586*(18), 2981–2989. https://doi.org/10.1016/j.febslet.2012.07.045

Caveda, L., Martin-Padura, I., Navarro, P., Breviario, F., Corada, M., Gulino, D., … Dejana, E. (1996). Inhibition of cultured cell growth by vascular endothelial cadherin (cadherin-5/VE-cadherin). *The Journal of Clinical Investigation*, *98*(4), 886–893. https://doi.org/10.1172/JCI118870

Chan, A. O. O. (2006). E-cadherin in gastric cancer. *World Journal of Gastroenterology: WJG*, *12*(2), 199–203. https://doi.org/10.3748/wjg.v12.i2.199

Chen, C. S., Tan, J., & Tien, J. (2004). Mechanotransduction at Cell-Matrix and Cell-Cell Contacts. *Annual Review of Biomedical Engineering*, *6*(1), 275–302. https://doi.org/10.1146/annurev.bioeng.6.040803.140040

Chien, S. (2007). Mechanotransduction and endothelial cell homeostasis: The wisdom of the cell. *American Journal of Physiology - Heart and Circulatory Physiology*, *292*(3), H1209–H1224. https://doi.org/10.1152/ajpheart.01047.2006

Civelekoglu-Scholey, G., & Scholey, J. M. (2010). Mitotic force generators and chromosome segregation. *Cellular and Molecular Life Sciences*, *67*(13), 2231–2250. https://doi.org/10.1007/s00018-010-0326-6

Collins, C., Denisin, A. K., Pruitt, B. L., & Nelson, W. J. (2017). Changes in E-cadherin rigidity sensing regulate cell adhesion. *Proceedings of the National Academy of Sciences of the United States of America*, *114*(29), E5835–E5844. https://doi.org/10.1073/pnas.1618676114

Conway, D. E., Breckenridge, M. T., Hinde, E., Gratton, E., Chen, C. S., & Schwartz, M. A. (2013). Fluid Shear Stress on Endothelial Cells Modulates Mechanical Tension across VE-Cadherin and PECAM-1. *Current Biology*, *23*(11), 1024–1030. https://doi.org/10.1016/j.cub.2013.04.049

Davis, M. A., Ireton, R. C., & Reynolds, A. B. (2003). A core function for p120-catenin in cadherin turnover. *The Journal of Cell Biology*, *163*(3), 525–534. https://doi.org/10.1083/jcb.200307111

Dembo, M., & Wang, Y. L. (1999). Stresses at the cell-to-substrate interface during locomotion of fibroblasts. *Biophysical Journal*, *76*(4), 2307–2316.

Doyle, A. D., Carvajal, N., Jin, A., Matsumoto, K., & Yamada, K. M. (2015). Local 3D matrix microenvironment regulates cell migration through spatiotemporal dynamics of contractility-dependent adhesions. *Nature Communications*, *6*, 8720. https://doi.org/10.1038/ncomms9720

Eastwood, M., McGrouther, D. A., & Brown, R. A. (1994). A culture force monitor for measurement of contraction forces generated in human dermal fibroblast cultures: Evidence for cell-matrix mechanical signalling. *Biochimica et Biophysica Acta (BBA) - General Subjects*, *1201*(2), 186–192. https://doi.org/10.1016/0304-4165(94)90040-X

Figueiredo, J., Söderberg, O., Simões-Correia, J., Grannas, K., Suriano, G., & Seruca, R. (2013). The importance of E-cadherin binding partners to evaluate the pathogenicity of E-cadherin missense mutations associated to HDGC. *European Journal of Human Genetics*, *21*(3), 301–309. https://doi.org/10.1038/ejhg.2012.159

Freyman, T. M., Yannas, I. V., Yokoo, R., & Gibson, L. J. (2002). Fibroblast contractile force is independent of the stiffness which resists the contraction. *Experimental Cell Research*, *272*(2), 153–162. https://doi.org/10.1006/excr.2001.5408

Ghibaudo, M., Saez, A., Trichet, L., Xayaphoummine, A., Browaeys, J., Silberzan, P., … Ladoux, B. (2008). Traction forces and rigidity sensing regulate cell functions. *Soft Matter*, *4*(9), 1836–1843. https://doi.org/10.1039/B804103B

Goffin, J. M., Pittet, P., Csucs, G., Lussi, J. W., Meister, J.-J., & Hinz, B. (2006). Focal adhesion size controls tension-dependent recruitment of α-smooth muscle actin to stress fibers. *The Journal of Cell Biology*, *172*(2), 259–268. https://doi.org/10.1083/jcb.200506179

Gomez, G. A., McLachlan, R. W., & Yap, A. S. (2011). Productive tension: Force-sensing and homeostasis of cell–cell junctions. *Trends in Cell Biology*, *21*(9), 499–505. https://doi.org/10.1016/j.tcb.2011.05.006

Guillot, C., & Lecuit, T. (2013). Mechanics of Epithelial Tissue Homeostasis and Morphogenesis. *Science*, *340*(6137), 1185–1189. https://doi.org/10.1126/science.1235249

Hartsock, A., & Nelson, W. J. (2008). Adherens and tight junctions: Structure, function and connections to the actin cytoskeleton. *Biochimica et Biophysica Acta*, *1778*(3), 660–669. https://doi.org/10.1016/j.bbamem.2007.07.012

Humphrey, J. D. (2008a). Mechanisms of Arterial Remodeling in Hypertension: Coupled Roles of Wall Shear and Intramural Stress. *Hypertension*, *52*(2), 195–200. https://doi.org/10.1161/HYPERTENSIONAHA.107.103440

Humphrey, J. D. (2008b). Vascular Adaptation and Mechanical Homeostasis at Tissue, Cellular, and Sub-cellular Levels. *Cell Biochemistry and Biophysics*, *50*(2), 53–78. https://doi.org/10.1007/s12013-007-9002-3

Hur, S. S., Álamo, J. C. del, Park, J. S., Li, Y.-S., Nguyen, H. A., Teng, D., … Chien, S. (2012). Roles of cell confluency and fluid shear in 3-dimensional intracellular forces in endothelial cells. *Proceedings of the National Academy of Sciences of the United States of America*, *109*(28), 11110–11115. https://doi.org/10.1073/pnas.1207326109

Huveneers, S., Daemen, M. J. A. P., & Hordijk, P. L. (2015). Between Rho(k) and a hard place: The relation between vessel wall stiffness, endothelial contractility, and cardiovascular disease. *Circulation Research*, *116*(5), 895–908. https://doi.org/10.1161/CIRCRESAHA.116.305720

Huynh, J., Nishimura, N., Rana, K., Peloquin, J. M., Califano, J. P., Montague, C. R., … Reinhart-King, C. A. (2011). Age-related intimal stiffening enhances endothelial permeability and leukocyte transmigration. *Science Translational Medicine*, *3*(112), 112ra122. https://doi.org/10.1126/scitranslmed.3002761

Ireton, R. C., Davis, M. A., van Hengel, J., Mariner, D. J., Barnes, K., Thoreson, M. A., … Reynolds, A. B. (2002). A novel role for p120 catenin in E-cadherin function. *The Journal of Cell Biology*, *159*(3), 465–476. https://doi.org/10.1083/jcb.200205115

Izquierdo-Álvarez, A., Vargas, D. A., Jorge-Peñas, Á., Subramani, R., Vaeyens, M.-M., & Van Oosterwyck, H. (2019). Spatiotemporal Analyses of Cellular Tractions Describe Subcellular Effect of Substrate Stiffness and Coating. *Annals of Biomedical Engineering*, *47*(2), 624–637. https://doi.org/10.1007/s10439-018-02164-2

Jalali, S., Tafazzoli-Shadpour, M., Haghighipour, N., Omidvar, R., & Safshekan, F. (2015). Regulation of Endothelial Cell Adherence and Elastic Modulus by Substrate Stiffness. *Cell Communication & Adhesion*, *22*(2–6), 79–89. https://doi.org/10.1080/15419061.2016.1265949

Kalaskar, D. M., Downes, J. E., Murray, P., Edgar, D. H., & Williams, R. L. (2013). Characterization of the interface between adsorbed fibronectin and human embryonic stem cells. *Journal of the Royal Society Interface*, *10*(83). https://doi.org/10.1098/rsif.2013.0139

Kohn, J. C., Zhou, D. W., Bordeleau, F., Zhou, A. L., Mason, B. N., Mitchell, M. J., … Reinhart-King, C. A. (2015). Cooperative effects of matrix stiffness and fluid shear stress on endothelial cell behavior. *Biophysical Journal*, *108*(3), 471–478. https://doi.org/10.1016/j.bpj.2014.12.023

Krishnan, R., Canović, E. P., Iordan, A. L., Rajendran, K., Manomohan, G., Pirentis, A. P., … Stamenović, D. (2012). Fluidization, resolidification, and reorientation of the endothelial cell in response to slow tidal stretches. *American Journal of Physiology - Cell Physiology*, *303*(4), C368–C375. https://doi.org/10.1152/ajpcell.00074.2012

Krishnan, R., Klumpers, D. D., Park, C. Y., Rajendran, K., Trepat, X., van Bezu, J., … van Nieuw Amerongen, G. P. (2011). Substrate stiffening promotes endothelial monolayer disruption through enhanced physical forces. *American Journal of Physiology - Cell Physiology*, *300*(1), C146–C154. https://doi.org/10.1152/ajpcell.00195.2010

Levenberg, S., Katz, B. Z., Yamada, K. M., & Geiger, B. (1998). Long-range and selective autoregulation of cell-cell or cell-matrix adhesions by cadherin or integrin ligands. *Journal of Cell Science*, *111 (Pt 3)*, 347–357.

Li, J., Barbone, P. E., Smith, M. L., & Stamenović, D. (2019). Effects of traction force dynamics on tensional homeostasis in multicellular clusters. *Unpublished Manuscript*.

Lipowsky, H. H. (1995). Shear Stress in the Circulation. In J. A. Bevan, G. Kaley, & G. M. Rubanyi (Eds.), *Flow-Dependent Regulation of Vascular Function* (pp. 28–45). https://doi.org/10.1007/978-1-4614-7527-9_2

Macara, I. G., Guyer, R., Richardson, G., Huo, Y., & Ahmed, S. M. (2014). Epithelial homeostasis. *Current Biology: CB*, *24*(17), R815-825. https://doi.org/10.1016/j.cub.2014.06.068

Maki, K., Han, S.-W., Hirano, Y., Yonemura, S., Hakoshima, T., & Adachi, T. (2016). Mechano-adaptive sensory mechanism of α-catenin under tension. *Scientific Reports*, *6*, 24878. https://doi.org/10.1038/srep24878

Malek, A. M., Alper, S. L., & Izumo, S. (1999). Hemodynamic Shear Stress and Its Role in Atherosclerosis. *JAMA: The Journal of the American Medical Association*, *282*(21), 2035–2042. https://doi.org/10.1001/jama.282.21.2035

Maloney, J. M., Walton, E. B., Bruce, C. M., & Van Vliet, K. J. (2008). Influence of finite thickness and stiffness on cellular adhesion-induced deformation of compliant substrata. *Physical Review. E, Statistical, Nonlinear, and Soft Matter Physics*, *78*(4 Pt 1), 041923. https://doi.org/10.1103/PhysRevE.78.041923

Matsuyoshi, N., & Imamura, S. (1997). Multiple Cadherins Are Expressed in Human Fibroblasts. *Biochemical and Biophysical Research Communications*, *235*(2), 355–358. https://doi.org/10.1006/bbrc.1997.6707

Mizutani, T., Haga, H., & Kawabata, K. (2004). Cellular stiffness response to external deformation: Tensional homeostasis in a single fibroblast. *Cell Motility and the Cytoskeleton*, *59*(4), 242–248. https://doi.org/10.1002/cm.20037

Moiseeva, E. P. (2001). Adhesion receptors of vascular smooth muscle cells and their functions. *Cardiovascular Research*, *52*(3), 372–386. https://doi.org/10.1016/S0008-6363(01)00399-6

Morini Marco F., Giampietro Costanza, Corada Monica, Pisati Federica, Lavarone Elisa, Cunha Sara I., … Taddei Andrea. (2018). VE-Cadherin–Mediated Epigenetic

Regulation of Endothelial Gene Expression. *Circulation Research*, *122*(2), 231–245. https://doi.org/10.1161/CIRCRESAHA.117.312392

Mui, K. L., Chen, C. S., & Assoian, R. K. (2016). The mechanical regulation of integrin–cadherin crosstalk organizes cells, signaling and forces. *Journal of Cell Science*, *129*(6), 1093–1100. https://doi.org/10.1242/jcs.183699

Nelson, C. M., & Chen, C. S. (2003). VE-cadherin simultaneously stimulates and inhibits cell proliferation by altering cytoskeletal structure and tension. *Journal of Cell Science*, *116*(17), 3571–3581. https://doi.org/10.1242/jcs.00680

Nelson, C. M., Pirone, D. M., Tan, J. L., & Chen, C. S. (2004). Vascular Endothelial-Cadherin Regulates Cytoskeletal Tension, Cell Spreading, and Focal Adhesions by Stimulating RhoA. *Molecular Biology of the Cell*, *15*(6), 2943–2953. https://doi.org/10.1091/mbc.E03-10-0745

Nollet, F., Kools, P., & van Roy, F. (2000). Phylogenetic analysis of the cadherin superfamily allows identification of six major subfamilies besides several solitary members. *Journal of Molecular Biology*, *299*(3), 551–572. https://doi.org/10.1006/jmbi.2000.3777

Ozawa, M., Hoschützky, H., Herrenknecht, K., & Kemler, R. (1990). A possible new adhesive site in the cell-adhesion molecule uvomorulin. *Mechanisms of Development*, *33*(1), 49–56.

Ozawa, M., & Kemler, R. (1992). Molecular organization of the uvomorulin-catenin complex. *The Journal of Cell Biology*, *116*(4), 989–996. https://doi.org/10.1083/jcb.116.4.989

Ozawa, M., Ringwald, M., & Kemler, R. (1990). Uvomorulin-catenin complex formation is regulated by a specific domain in the cytoplasmic region of the cell adhesion molecule. *Proceedings of the National Academy of Sciences of the United States of America*, *87*(11), 4246–4250. https://doi.org/10.1073/pnas.87.11.4246

Paszek, M. J., Zahir, N., Johnson, K. R., Lakins, J. N., Rozenberg, G. I., Gefen, A., … Weaver, V. M. (2005). Tensional homeostasis and the malignant phenotype. *Cancer Cell*, *8*(3), 241–254. https://doi.org/10.1016/j.ccr.2005.08.010

Paszkowiak, J. J., & Dardik, A. (2003). Arterial wall shear stress: Observations from the bench to the bedside. *Vascular and Endovascular Surgery*, *37*(1), 47–57. https://doi.org/10.1177/153857440303700107

Perez, T. D., & Nelson, W. J. (2004). Cadherin Adhesion: Mechanisms and Molecular Interactions. *Handbook of Experimental Pharmacology*, (165), 3–21. https://doi.org/10.1007/978-3-540-68170-0_1

Perrault, C. M., Brugues, A., Bazellieres, E., Ricco, P., Lacroix, D., & Trepat, X. (2015). Traction Forces of Endothelial Cells under Slow Shear Flow. *Biophysical Journal*, *109*(8), 1533–1536. https://doi.org/10.1016/j.bpj.2015.08.036

Plotnikov, S. V., Pasapera, A. M., Sabass, B., & Waterman, C. M. (2012). Force Fluctuations within Focal Adhesions Mediate ECM-Rigidity Sensing to Guide Directed Cell Migration. *Cell*, *151*(7), 1513–1527. https://doi.org/10.1016/j.cell.2012.11.034

Polio, S. R., Rothenberg, K. E., Stamenović, D., & Smith, M. L. (2012). A micropatterning and image processing approach to simplify measurement of cellular traction forces. *Acta Biomaterialia*, *8*(1), 82–88. https://doi.org/10.1016/j.actbio.2011.08.013

Polio, S.R., Parameswaran, H., Canović, E.P., Gaut, C.M., Aksyonova, D., Stamenović, D., & Smith, M.L. (2014). Topographical control of multiple cell adhesion molecules for traction force microscopy. *Integrative Biology*, *6*(3), 357–365. https://doi.org/10.1039/C3IB40127H

Polio, S. R., Stasiak, S., Krishnan, R., & Parameswaran, H. (2018). Extracellular matrix stiffness regulates force transmission pathways in multicellular ensembles of human airway smooth muscle cells. *BioRxiv*, 402842. https://doi.org/10.1101/402842

Polte, T. R., Eichler, G. S., Wang, N., & Ingber, D. E. (2004). Extracellular matrix controls myosin light chain phosphorylation and cell contractility through modulation of cell shape and cytoskeletal prestress. *American Journal of Physiology. Cell Physiology*, *286*(3), C518-528. https://doi.org/10.1152/ajpcell.00280.2003

Provenzano, P. P., & Keely, P. J. (2011). Mechanical signaling through the cytoskeleton regulates cell proliferation by coordinated focal adhesion and Rho GTPase signaling. *Journal of Cell Science*, *124*(Pt 8), 1195–1205. https://doi.org/10.1242/jcs.067009

Renkawitz, J., & Sixt, M. (2010). Mechanisms of force generation and force transmission during interstitial leukocyte migration. *EMBO Reports*, *11*(10), 744–750. https://doi.org/10.1038/embor.2010.147

Roy, F. van, & Berx, G. (2008). The cell-cell adhesion molecule E-cadherin. *Cellular and Molecular Life Sciences*, *65*(23), 3756–3788. https://doi.org/10.1007/s00018-008-8281-1

Ryan, P. L., Foty, R. A., Kohn, J., & Steinberg, M. S. (2001). Tissue spreading on implantable substrates is a competitive outcome of cell–cell vs. Cell–substratum adhesivity. *Proceedings of the National Academy of Sciences of the United States of America*, *98*(8), 4323–4327. https://doi.org/10.1073/pnas.071615398

Saez, A., Buguin, A., Silberzan, P., & Ladoux, B. (2005). Is the Mechanical Activity of Epithelial Cells Controlled by Deformations or Forces? *Biophysical Journal*, *89*(6), L52–L54. https://doi.org/10.1529/biophysj.105.071217

Sazonova, O. V., Isenberg, B. C., Herrmann, J., Lee, K. L., Purwada, A., Valentine, A. D., … Nugent, M. A. (2015). Extracellular matrix presentation modulates vascular smooth muscle cell mechanotransduction. *Matrix Biology*, *41*, 36–43. https://doi.org/10.1016/j.matbio.2014.11.001

Sazonova, O. V., Lee, K. L., Isenberg, B. C., Rich, C. B., Nugent, M. A., & Wong, J. Y. (2011). Cell-cell interactions mediate the response of vascular smooth muscle cells to substrate stiffness. *Biophysical Journal*, *101*(3), 622–630. https://doi.org/10.1016/j.bpj.2011.06.051

Schwartz, M. A., & DeSimone, D. W. (2008). Cell adhesion receptors in mechanotransduction. *Current Opinion in Cell Biology*, *20*(5), 551–556. https://doi.org/10.1016/j.ceb.2008.05.005

Shapiro, L., & Weis, W. I. (2009). Structure and Biochemistry of Cadherins and Catenins. *Cold Spring Harbor Perspectives in Biology*, *1*(3). https://doi.org/10.1101/cshperspect.a003053

Shiu, Y.-T., Li, S., Marganski, W. A., Usami, S., Schwartz, M. A., Wang, Y.-L., … Chien, S. (2004). Rho mediates the shear-enhancement of endothelial cell migration and traction force generation. *Biophysical Journal*, *86*(4), 2558–2565. https://doi.org/10.1016/S0006-3495(04)74311-8

Smith, M. L., Gourdon, D., Little, W. C., Kubow, K. E., Eguiluz, R. A., Luna-Morris, S., & Vogel, V. (2007). Force-induced unfolding of fibronectin in the extracellular matrix of living cells. *PLoS Biology*, *5*(10), e268. https://doi.org/10.1371/journal.pbio.0050268

Stemmler, M. P. (2008). Cadherins in development and cancer. *Molecular BioSystems*, *4*(8), 835–850. https://doi.org/10.1039/B719215K

Steward, R., Tambe, D., Hardin, C. C., Krishnan, R., & Fredberg, J. J. (2015). Fluid shear, intercellular stress, and endothelial cell alignment. *American Journal of Physiology - Cell Physiology*, ajpcell.00363.2014. https://doi.org/10.1152/ajpcell.00363.2014

Stricker, J., Aratyn-Schaus, Y., Oakes, P. W., & Gardel, M. L. (2011). Spatiotemporal Constraints on the Force-Dependent Growth of Focal Adhesions. *Biophysical Journal*, *100*(12), 2883–2893. https://doi.org/10.1016/j.bpj.2011.05.023

Tam, S. N., Smith, M. L., & Stamenović, D. (2017). Modeling tensional homeostasis in multicellular clusters. *International Journal for Numerical Methods in Biomedical Engineering*, *33*(3), e02801. https://doi.org/10.1002/cnm.2801

Tan, J. L., Tien, J., Pirone, D. M., Gray, D. S., Bhadriraju, K., & Chen, C. S. (2003). Cells lying on a bed of microneedles: An approach to isolate mechanical force. *Proceedings of the National Academy of Sciences of the United States of America*, *100*(4), 1484–1489. https://doi.org/10.1073/pnas.0235407100

Ting, L. H., Jahn, J. R., Jung, J. I., Shuman, B. R., Feghhi, S., Han, S. J., … Sniadecki, N. J. (2012). Flow mechanotransduction regulates traction forces, intercellular forces, and adherens junctions. *American Journal of Physiology - Heart and Circulatory Physiology*, *302*(11), H2220–H2229. https://doi.org/10.1152/ajpheart.00975.2011

Trepat, X., Wasserman, M. R., Angelini, T. E., Millet, E., Weitz, D. A., Butler, J. P., & Fredberg, J. J. (2009). Physical forces during collective cell migration. *Nature Physics*, *5*(6), 426–430. https://doi.org/10.1038/nphys1269

Trichet, L., Le Digabel, J., Hawkins, R. J., Vedula, S. R. K., Gupta, M., Ribrault, C., … Ladoux, B. (2012). Evidence of a large-scale mechanosensing mechanism for cellular adaptation to substrate stiffness. *Proceedings of the National Academy of Sciences of the United States of America*, *109*(18), 6933–6938. https://doi.org/10.1073/pnas.1117810109

Tsai, J., & Kam, L. (2009). Rigidity-dependent cross talk between integrin and cadherin signaling. *Biophysical Journal*, *96*(6), L39-41. https://doi.org/10.1016/j.bpj.2009.01.005

Tzima, E., Irani-Tehrani, M., Kiosses, W. B., Dejana, E., Schultz, D. A., Engelhardt, B., … Schwartz, M. A. (2005). A mechanosensory complex that mediates the endothelial cell response to fluid shear stress. *Nature*, *437*(7057), 426–431. https://doi.org/10.1038/nature03952

Urbano, R. L., Furia, C., Basehore, S., & Clyne, A. M. (2017). Stiff Substrates Increase Inflammation-Induced Endothelial Monolayer Tension and Permeability. *Biophysical Journal*, *113*(3), 645–655. https://doi.org/10.1016/j.bpj.2017.06.033

Valent, E. T., van Nieuw Amerongen, G. P., van Hinsbergh, V. W. M., & Hordijk, P. L. (2016). Traction force dynamics predict gap formation in activated endothelium.

Experimental Cell Research, *347*(1), 161–170. https://doi.org/10.1016/j.yexcr.2016.07.029

Vestweber Dietmar. (2008). VE-Cadherin. *Arteriosclerosis, Thrombosis, and Vascular Biology*, *28*(2), 223–232. https://doi.org/10.1161/ATVBAHA.107.158014

Wang, N., Naruse, K., Stamenović, D., Fredberg, J. J., Mijailovich, S. M., Tolić-Nørrelykke, I. M., … Ingber, D. E. (2001). Mechanical behavior in living cells consistent with the tensegrity model. *Proceedings of the National Academy of Sciences of the United States of America*, *98*(14), 7765–7770. https://doi.org/10.1073/pnas.141199598

Weber, G. F., Bjerke, M. A., & DeSimone, D. W. (2011). Integrins and cadherins join forces to form adhesive networks. *Journal of Cell Science*, *124*(Pt 8), 1183–1193. https://doi.org/10.1242/jcs.064618

Webster, K. D., Ng, W. P., & Fletcher, D. A. (2014). Tensional homeostasis in single fibroblasts. *Biophysical Journal*, *107*(1), 146–155. https://doi.org/10.1016/j.bpj.2014.04.051

Wheelock, M. J., Shintani, Y., Maeda, M., Fukumoto, Y., & Johnson, K. R. (2008). Cadherin switching. *Journal of Cell Science*, *121*(6), 727–735. https://doi.org/10.1242/jcs.000455

Yip, A. K., Iwasaki, K., Ursekar, C., Machiyama, H., Saxena, M., Chen, H., … Sawada, Y. (2013). Cellular response to substrate rigidity is governed by either stress or strain. *Biophysical Journal*, *104*(1), 19–29. https://doi.org/10.1016/j.bpj.2012.11.3805

Yonemura, S., Wada, Y., Watanabe, T., Nagafuchi, A., & Shibata, M. (2010). α-Catenin as a tension transducer that induces adherens junction development. *Nature Cell Biology*, *12*(6), 533–542. https://doi.org/10.1038/ncb2055

Yuan, S. Y., & Rigor, R. R. (2010). *Regulation of Endothelial Barrier Function*. Retrieved from http://www.ncbi.nlm.nih.gov/books/NBK54117/

Zhou, D. W., Lee, T. T., Weng, S., Fu, J., & García, A. J. (2017). Effects of substrate stiffness and actomyosin contractility on coupling between force transmission and vinculin-paxillin recruitment at single focal adhesions. *Molecular Biology of the Cell*, *28*(14), 1901–1911. https://doi.org/10.1091/mbc.E17-02-0116

Zimerman, B., Volberg, T., & Geiger, B. (2004). Early molecular events in the assembly of the focal adhesion-stress fiber complex during fibroblast spreading. *Cell Motility and the Cytoskeleton*, *58*(3), 143–159. https://doi.org/10.1002/cm.20005

Zimmer, S., & Nickenig, G. (2010). Prediction and prevention by progenitors? Stent thrombosis and EPCs. *European Heart Journal*, *31*(21), 2569–2571. https://doi.org/10.1093/eurheartj/ehq217

Zollinger, A. J., Xu, H., Figueiredo, J., Paredes, J., Seruca, R., Stamenović, D., & Smith, M. L. (2018). Dependence of Tensional Homeostasis on Cell Type and on Cell–Cell Interactions. *Cellular and Molecular Bioengineering*, *11*(3), 175–184. https://doi.org/10.1007/s12195-018-0527-x

CURRICULUM VITAE